A Astrophysical Constants and Symbols

Physical Constants

Quantity	Symbol	Value [SI]
Speed of light	c	299 792 458 m s^{-1}
Newtonian gravitational constant	G	$6.6742(10) \times 10^{-11}$ m^3 kg^{-1} s^{-2}
Planck constant	h	$6.6260693(10) \times 10^{-34}$ J s
Reduced Planck constant	$\hbar = h/2\pi$	$1.05457168 \times 10^{-34}$ J s
Planck constant	$\hbar c$	197.326968 MeV fm
Boltzmann constant	k_{B}	1.380658×10^{-23} J/K
Electron mass	m_e	$9.1093897 \times 10^{-31}$ kg
Electron charge	e	$1.60217733 \times 10^{-19}$ C
Proton mass	m_p	$1.67262158 \times 10^{-27}$ kg
Neutron mass	m_n	$1.6749286 \times 10^{-27}$ kg
Unified atomic mass unit	m_u	$1.6605402 \times 10^{-27}$ kg
Radiation constant	$a_{\mathrm{SB}} = \pi^2 k_{\mathrm{B}}^4/15c^3\hbar^3$	7.56×10^{-23} J m^{-3} K^{-4}
Stefan–Boltzmann constant	$\sigma_{\mathrm{SB}} = c a_{\mathrm{SB}}/4$	5.6704×10^{-8} W m^{-2} K^{-4}
Fine structure constant	$\alpha = e^2/4\pi\epsilon_0\hbar c$	1/137.0359895
Classical electron radius	$r_e = e^2/4\pi\epsilon_0 m_e c^2$	$2.81794092 \times 10^{-15}$ m
Thomson cross-section	$\sigma_T = 8\pi r_e^2/3$	$6.65246154 \times 10^{-29}$ m^2
Nuclear radius	$R_0 = 1.2\,A^{1/3}$ fm	1 fm $= 10^{-15}$ m
Nuclear saturation density	n_0	0.1620 fm^{-3}

Astronomical Quantities

Quantity	Symbol	Value [SI]
Astronomical unit	AU	$1.4959787066 \times 10^{11}$ m
Parsec	pc	$3.0856775807 \times 10^{16}$ m
Sidereal year	365.25636042 d	3.1558150×10^{7} s
Solar mass	$M_\odot$	1.98892×10^{30} kg
Solar luminosity	$L_\odot$	3.846×10^{26} W
Solar radius (equatorial)	$R_\odot$	6.961×10^{6} m
Schwarzschild radius of the Sun	$R_S = 2GM_\odot/c^2$	2.95325008 km
Solar system unit of time	$T_\odot = GM_\odot/c^3$	4.92549047 μs
Eddington luminosity	$L_{\mathrm{Ed}} = 4\pi G M m_p c/\sigma_T$	$1.257 \times 10^{31}\ M/M_\odot$ W
Critical magnetic field	$B_{\mathrm{crit}} = m_e^2 c^3/\hbar e$	4.4×10^{9} T
Chandrasekhar mass	$M_{\mathrm{Ch}} = (5.87/\mu^2) M_\odot$	$1.457\,(2/\mu)^2\, M_\odot$
Gravitational wave energy loss	$L_0 = c^5/G$	3.628×10^{52} W
Planck mass	$m_P = \sqrt{\hbar c/G}$	1.22090×10^{19} GeV/c^2
Planck length	$L_P = \sqrt{\hbar G/c^3}$	1.61624×10^{-35} m
Planck time	$t_P = \sqrt{\hbar G/c^5}$	5.39121×10^{-44} s
Planck charge	$q_P = \sqrt{4\pi\epsilon_0 \hbar c}$	1.87554×10^{-18} C
Planck current	$I_P = q_P/t_P$	3.4789×10^{25} A
Planck voltage	$V_P = \hbar/t_P q_P$	1.04295×10^{27} V
Planck impedance	$Z_P = V_P/I_P$	29.9792 Ω

List of Symbols

Physical Variable	Symbol	Typical Unit
Redshift factor	α	Dimensionless
Metric of three-space	γ_{ik}	Dimensionless
Shift vector field	$\boldsymbol{\beta}$	
Exterior curvature	K_{ik}	Square inverse length
Observer (tetrad) field	$\mathbf{e}_a$	Inverse length
One-form basis	Θ^a	Length
Specific angular momentum of black hole	a	Length
Angular momentum of black hole	a_*	Dimensionless
Lagrangian	$\mathcal{L}$	Energy
Lie derivative along X	L_X	Inverse length
Mass of black hole	M_H	Solar mass
Gravitational radius	M	Length
Covariant derivative along X	∇_X	Inverse length
Connection one-forms	$\omega^a{}_b$	Inverse length
Curvature two-forms	$\Omega^a{}_b$	Square inverse length
Grand canonical potential	Ω	Energy
Christoffel symbol	$\Gamma^{\mu}_{\alpha\beta}$	Inverse length
Ricci tensor	R_{ab}	Square inverse length
Einstein tensor	G_{ab}	Square inverse length
Energy–momentum tensor	T^{ab}	Energy density
Faraday tensor	F_{ab}	Electric field
Bardeen (Newtonian) potential	Φ	Dimensionless
Magnetic flux function	Ψ	Magnetic flux
Vector field on manifold	X	Inverse length
Periastron shift of binary orbit	$\dot{\omega}$	Degrees per revolution
Redshift and Doppler amplitude	γ_{RD}	Time
Shapiro range parameter	r	Time
Shapiro inclination parameter	s	Dimensionless
State vector of primitive variables	$\mathbf{P}$	
State vector of conserved variables	$\mathbf{U}$	
Flux vector of conserved variables	$\mathbf{F}$	
Lorentz factor	W	Dimensionless

Abbreviations and Acronyms

Symbol	Meaning
AGN	Active Galactic Nucleus
AMR	Adaptive Mesh Refinement
ASCA	Japanese X-Ray Satellite
BH	Black Hole
CFL	Courant–Friedrichs–Lewy condition
CHANDRA	CHANDRAsekhar X-ray Observatory (NASA)
CHOMBO	Block-Structured Adaptive Mesh Refinement Library
DE200	Development Ephemeris 200
EoS	Equation of State
ESA	European Space Agency
EUVN	EUropean Vlbi Network
GAIA	Satellite named after a Greek Earth Goddess (ESA)
GP-B	Gravity Probe B
GRMHD	General Relativistic MagnetoHydrodynamics
HIPPARCHOS	HIgh Precision PARallax COllecting Satellite
INTEGRAL	INTErnational Gamma-Ray Astrophysics Laboratory
JD	Julian Date
JWST	James Webb Space Telescope (NASA)
LAGEOS	LAser GEOdetic Satellite
LMXB	Low-Mass X-Ray Binary System
MJD	Modified Julian Date
MPI	Message Passing Interface
NS	Neutron Star
PARAMESH	Parallel Adaptive Mesh Refinement
QSO	Quasistellar Object
QSR	Quasistellar Radio Source
ROSITA	ROentgen Survey with an Imaging Telescope Array
RXTE	Rossi X-ray Timing Explorer
SEP	Strong Equivalence Principle
SRMHD	Special Relativistic MagnetoHydrodynamics
VLBA	Very Long Baseline Array (USA)
VLBI	Very Long Baseline Interferometry
VLTI	Very Large Telescopes (ESO)
WD	White Dwarf
WEP	Weak Equivalence Principle
XEUS	X-ray Evolving Universe Spectroscopy Mission (ESA)
XMM–NEWTON	X-ray Multi-Mirror Satellite (ESA)
ZAMO	Zero Angular Momentum Observer

B SLy4 Equation of State for Neutron Star Matter

The equation of state (EoS) of dense neutron star matter is one of the mysteries of these objects. The EoS is a basic input for construction of neutron star models. Its knowledge is needed to calculate various properties of neutron stars. The EoS is predominantly determined by the nuclear (strong) interaction between elementary constituents of dense matter. Even in the neutron star crust, with density below normal nuclear density $\varrho_0 = 2.7 \times 10^{14}$ g cm^{-3} (corresponding to baryon density $n_0 = 0.16$ fm^{-3}), nuclear interactions are responsible for the properties of neutron rich nuclei, crucial for the crust EoS. The knowledge of these interactions is particularly important for the structure of the inner neutron star crust, where nuclei are immersed in a neutron gas, and even more so for the EoS of the liquid core. Nuclear interactions are actually responsible for a dramatic lifting of $M_{\max}$ from 0.7 $M_\odot$, obtained when interactions are switched off, to more realistic values of 1.4 $M_\odot$ as measured in neutron star binary systems.

In the following tables, an equation of state of neutron star matter, describing both the neutron star crust and the liquid core, is given from the paper [136]. It is based on the effective nuclear interaction SLy of the Skyrme type, which is particularly suitable for the application to the calculation of the properties of very neutron rich matter.

Table B.1. Structure and composition of the inner neutron-star crust. For caption, see next table

n_b (fm^{-3})	Z	A	X_n	R_p (fm)	R_n (fm)	R_{cell} (fm)	u (%)
1.2126 E–4	42.198	130.076	0.0000	5.451	5.915	63.503	0.063
1.6241 E–4	42.698	135.750	0.0000	5.518	6.016	58.440	0.084
1.9772 E–4	43.019	139.956	0.0000	5.565	6.089	55.287	0.102
2.0905 E–4	43.106	141.564	0.0000	5.578	6.111	54.470	0.107
2.2059 E–4	43.140	142.161	0.0247	5.585	6.122	54.032	0.110
2.3114 E–4	43.163	142.562	0.0513	5.590	6.128	53.745	0.113
2.6426 E–4	43.215	143.530	0.1299	5.601	6.145	53.020	0.118
3.0533 E–4	43.265	144.490	0.2107	5.612	6.162	52.312	0.123
3.5331 E–4	43.313	145.444	0.2853	5.623	6.179	51.617	0.129
4.0764 E–4	43.359	146.398	0.3512	5.634	6.195	50.937	0.135
4.6800 E–4	43.404	147.351	0.4082	5.645	6.212	50.269	0.142
5.3414 E–4	43.447	148.306	0.4573	5.656	6.228	49.615	0.148
6.0594 E–4	43.490	149.263	0.4994	5.667	6.245	48.974	0.155
7.6608 E–4	43.571	151.184	0.5669	5.690	6.278	47.736	0.169
1.0471 E–3	43.685	154.094	0.6384	5.725	6.328	45.972	0.193
1.2616 E–3	43.755	156.055	0.6727	5.748	6.362	44.847	0.211
1.6246 E–3	43.851	159.030	0.7111	5.784	6.413	43.245	0.239
2.0384 E–3	43.935	162.051	0.7389	5.821	6.465	41.732	0.271
2.6726 E–3	44.030	166.150	0.7652	5.871	6.535	39.835	0.320
3.4064 E–3	44.101	170.333	0.7836	5.923	6.606	38.068	0.377
4.4746 E–3	44.155	175.678	0.7994	5.989	6.698	36.012	0.460
5.7260 E–3	44.164	181.144	0.8099	6.059	6.792	34.122	0.560
7.4963 E–3	44.108	187.838	0.8179	6.146	6.908	32.030	0.706
9.9795 E–3	43.939	195.775	0.8231	6.253	7.048	29.806	0.923
1.2513 E–2	43.691	202.614	0.8250	6.350	7.171	28.060	1.159
1.6547 E–2	43.198	211.641	0.8249	6.488	7.341	25.932	1.566
2.1405 E–2	42.506	220.400	0.8222	6.637	7.516	24.000	2.115
2.4157 E–2	42.089	224.660	0.8200	6.718	7.606	23.106	2.458
2.7894 E–2	41.507	229.922	0.8164	6.825	7.721	22.046	2.967
3.1941 E–2	40.876	235.253	0.8116	6.942	7.840	21.053	3.585
3.6264 E–2	40.219	240.924	0.8055	7.072	7.967	20.128	4.337
3.9888 E–2	39.699	245.999	0.7994	7.187	8.077	19.433	5.058
4.4578 E–2	39.094	253.566	0.7900	7.352	8.231	18.630	6.146
4.8425 E–2	38.686	261.185	0.7806	7.505	8.372	18.038	7.202
5.2327 E–2	38.393	270.963	0.7693	7.685	8.538	17.499	8.470
5.6264 E–2	38.281	283.993	0.7553	7.900	8.737	17.014	10.011
6.0219 E–2	38.458	302.074	0.7381	8.167	8.987	16.598	11.914
6.4183 E–2	39.116	328.489	0.7163	8.513	9.315	16.271	14.323
6.7163 E–2	40.154	357.685	0.6958	8.853	9.642	16.107	16.606
7.0154 E–2	42.051	401.652	0.6699	9.312	10.088	16.058	19.501
7.3174 E–2	45.719	476.253	0.6354	9.990	10.753	16.213	23.393
7.5226 E–2	50.492	566.654	0.6038	10.701	11.456	16.557	26.996
7.5959 E–2	53.162	615.840	0.5898	11.051	11.803	16.772	28.603

Table B.2. Previous table: Structure and composition of the inner neutron-star crust (ground state) calculated within the compressible liquid drop model with SLy effective nucleon–nucleon interaction. X_n is the fraction of nucleons in the neutron gas outside nuclei. Upper part with $X_n = 0$ corresponds to a shell of the outer crust, just above the neutron drip surface in the neutron-star interior, and calculated within the same model. R_p and R_n are the equivalent proton and neutron radii. Wigner–Seitz cell radius and fraction of volume occupied by nuclear matter (equal to that occupied by protons) are denoted by R_{cell} and u, respectively. This table: Equation of state of the inner crust. First line corresponds to the neutron drip point, as calculated within the COMPRESSIBLE LIQUID DROP MODEL. Last line corresponds to the bottom edge of the crust

n_b (fm^{-3})	ϱ (g cm^{-3})	P (erg cm^{-3})	Γ	n_b (fm^{-3})	ϱ (g cm^{-3})	P (erg cm^{-3})	Γ
2.0905 E–4	3.4951 E11	6.2150 E29	1.177	9.9795 E–3	1.6774 E13	3.0720 E31	1.342
2.2059 E–4	3.6883 E11	6.4304 E29	0.527	1.2513 E–2	2.1042 E13	4.1574 E31	1.332
2.3114 E–4	3.8650 E11	6.5813 E29	0.476	1.6547 E–2	2.7844 E13	6.0234 E31	1.322
2.6426 E–4	4.4199 E11	6.9945 E29	0.447	2.1405 E–2	3.6043 E13	8.4613 E31	1.320
3.0533 E–4	5.1080 E11	7.4685 E29	0.466	2.4157 E–2	4.0688 E13	9.9286 E31	1.325
3.5331 E–4	5.9119 E11	8.0149 E29	0.504	2.7894 E–2	4.7001 E13	1.2023 E32	1.338
4.0764 E–4	6.8224 E11	8.6443 E29	0.554	3.1941 E–2	5.3843 E13	1.4430 E32	1.358
4.6800 E–4	7.8339 E11	9.3667 E29	0.610	3.6264 E–2	6.1153 E13	1.7175 E32	1.387
5.3414 E–4	8.9426 E11	1.0191 E30	0.668	3.9888 E–2	6.7284 E13	1.9626 E32	1.416
6.0594 E–4	1.0146 E12	1.1128 E30	0.726	4.4578 E–2	7.5224 E13	2.3024 E32	1.458
7.6608 E–4	1.2831 E12	1.3370 E30	0.840	4.8425 E–2	8.1738 E13	2.6018 E32	1.496
1.0471 E–3	1.7543 E12	1.7792 E30	0.987	5.2327 E–2	8.8350 E13	2.9261 E32	1.536
1.2616 E–3	2.1141 E12	2.1547 E30	1.067	5.6264 E–2	9.5022 E13	3.2756 E32	1.576
1.6246 E–3	2.7232 E12	2.8565 E30	1.160	6.0219 E–2	1.0173 E14	3.6505 E32	1.615
2.0384 E–3	3.4178 E12	3.7461 E30	1.227	6.4183 E–2	1.0845 E14	4.0509 E32	1.650
2.6726 E–3	4.4827 E12	5.2679 E30	1.286	6.7163 E–2	1.1351 E14	4.3681 E32	1.672
3.4064 E–3	5.7153 E12	7.2304 E30	1.322	7.0154 E–2	1.1859 E14	4.6998 E32	1.686
4.4746 E–3	7.5106 E12	1.0405 E31	1.344	7.3174 E–2	1.2372 E14	5.0462 E32	1.685
5.7260 E–3	9.6148 E12	1.4513 E31	1.353	7.5226 E–2	1.2720 E14	5.2856 E32	1.662
7.4963 E–3	1.2593 E13	2.0894 E31	1.351	7.5959 E–2	1.2845 E14	5.3739 E32	1.644

Table B.3. Top: Composition of the liquid core. Fractions of particles are defined as $x_{\rm j} = n_{\rm j}/n_{\rm b}$. Neutron fraction can be calculated using $x_n = 1 - x_p$. Bottom: Equation of state of the liquid neutron star core

$n_{\rm b}$ (fm^{-3})	x_p (%)	x_e (%)	x_μ (%)	$n_{\rm b}$ (fm^{-3})	x_p (%)	x_e (%)	x_μ (%)
0.0771	3.516	3.516	0.000	0.490	7.516	4.960	2.556
0.0800	3.592	3.592	0.000	0.520	7.587	4.954	2.634
0.0850	3.717	3.717	0.000	0.550	7.660	4.952	2.708
0.0900	3.833	3.833	0.000	0.580	7.736	4.955	2.781
0.1000	4.046	4.046	0.000	0.610	7.818	4.964	2.854
0.1100	4.233	4.233	0.000	0.640	7.907	4.979	2.927
0.1200	4.403	4.398	0.005	0.670	8.003	5.001	3.002
0.1300	4.622	4.521	0.101	0.700	8.109	5.030	3.079
0.1600	5.270	4.760	0.510	0.750	8.309	5.094	3.215
0.1900	5.791	4.896	0.895	0.800	8.539	5.178	3.361
0.2200	6.192	4.973	1.219	0.850	8.803	5.284	3.519
0.2500	6.499	5.014	1.485	0.900	9.102	5.410	3.692
0.2800	6.736	5.031	1.705	0.950	9.437	5.557	3.880
0.3100	6.920	5.034	1.887	1.000	9.808	5.726	4.083
0.3400	7.066	5.026	2.040	1.100	10.663	6.124	4.539
0.3700	7.185	5.014	2.170	1.200	11.661	6.602	5.060
0.4000	7.283	4.999	2.283	1.300	12.794	7.151	5.643
0.4300	7.368	4.984	2.383	1.400	14.043	7.762	6.281
0.4600	7.444	4.971	2.473	1.500	15.389	8.424	6.965

$n_{\rm b}$ (fm^{-3})	ϱ (g cm^{-3})	P (erg cm^{-3})	Γ	$n_{\rm b}$ (fm^{-3})	ϱ (g cm^{-3})	P (erg cm^{-3})	Γ
0.0771	1.3038 E14	5.3739 E32	2.159	0.4900	8.8509 E14	1.0315 E35	2.953
0.0800	1.3531 E14	5.8260 E32	2.217	0.5200	9.4695 E14	1.2289 E35	2.943
0.0850	1.4381 E14	6.6828 E32	2.309	0.5500	1.0102 E15	1.4491 E35	2.933
0.0900	1.5232 E14	7.6443 E32	2.394	0.5800	1.0748 E15	1.6930 E35	2.924
0.1000	1.6935 E14	9.9146 E32	2.539	0.6100	1.1408 E15	1.9616 E35	2.916
0.1100	1.8641 E14	1.2701 E33	2.655	0.6400	1.2085 E15	2.2559 E35	2.908
0.1200	2.0350 E14	1.6063 E33	2.708	0.6700	1.2777 E15	2.5769 E35	2.900
0.1300	2.2063 E14	1.9971 E33	2.746	0.7000	1.3486 E15	2.9255 E35	2.893
0.1600	2.7223 E14	3.5927 E33	2.905	0.7500	1.4706 E15	3.5702 E35	2.881
0.1900	3.2424 E14	5.9667 E33	2.990	0.8000	1.5977 E15	4.2981 E35	2.869
0.2200	3.7675 E14	9.2766 E33	3.025	0.8500	1.7302 E15	5.1129 E35	2.858
0.2500	4.2983 E14	1.3668 E34	3.035	0.9000	1.8683 E15	6.0183 E35	2.847
0.2800	4.8358 E14	1.9277 E34	3.032	0.9500	2.0123 E15	7.0176 E35	2.836
0.3100	5.3808 E14	2.6235 E34	3.023	1.0000	2.1624 E15	8.1139 E35	2.824
0.3400	5.9340 E14	3.4670 E34	3.012	1.1000	2.4820 E15	1.0609 E36	2.801
0.3700	6.4963 E14	4.4702 E34	2.999	1.2000	2.8289 E15	1.3524 E36	2.778
0.4000	7.0684 E14	5.6451 E34	2.987	1.3000	3.2048 E15	1.6876 E36	2.754
0.4300	7.6510 E14	7.0033 E34	2.975	1.4000	3.6113 E15	2.0679 E36	2.731
0.4600	8.2450 E14	8.5561 E34	2.964	1.5000	4.0498 E15	2.4947 E36	2.708

C 3+1 Split of Spacetime Curvature

In this appendix we derive the Gauss equation and the Codazzi–Mainardi equations for the 3+1 decomposition of the Riemann curvature.

C.1 Gauss Decomposition

In analogy to the decomposition of the connection form discussed in Sect. 2.8.3 we split the curvature two-form given by the second structure equation

$$\Omega^a{}_b = d\omega^a{}_b + \omega^a{}_c \wedge \omega^c{}_b \,. \tag{C.1}$$

The Gauss decomposition follows from the spatial part of the second structure equation

$$\begin{aligned}
\Omega^i{}_j &= d\omega^i{}_j + \omega^i{}_k \wedge \omega^k{}_j + \omega^i{}_0 \wedge \omega^0{}_j \\
&= d\left[\bar{\omega}^i{}_j(e_k)\bar{\Theta}^k + H^i{}_j\Theta^0\right] + \left(\nabla_i \ln\alpha\Theta^0 - K^i{}_k\Theta^k\right) \wedge \left(\nabla_j \ln\alpha\Theta^0 - K_{jm}\Theta^m\right) \\
&\quad + \left(\bar{\omega}^i{}_k + H^i{}_k\Theta^0\right) \wedge \left(\bar{\omega}^k{}_j + H^k{}_j\Theta^0\right) \\
&= \bar{d}\bar{\omega}^i{}_j + \bar{\omega}^i{}_k \wedge \bar{\omega}^k{}_j \\
&\quad + d(H^i{}_j\Theta^0) - \nabla_i \ln\alpha K_{jm}\,\Theta^0 \wedge \Theta^m + \nabla_j \ln\alpha K^i{}_m\,\Theta^0 \wedge \Theta^m \\
&\quad + K^i{}_m K_{jk}\,\Theta^m \wedge \Theta^k + H^k{}_j\,\omega^i{}_k \wedge \Theta^0 + H^i{}_k\,\Theta^0 \wedge \omega^k{}_j \\
&= \bar{\Omega}^i{}_j + K^i{}_k K_{jm}\,\Theta^k \wedge \Theta^m \\
&\quad - \left[\nabla_i \ln\alpha\, K_{jm} - \nabla_j \ln\alpha\, K^i{}_m\right]\Theta^0 \wedge \Theta^m \\
&\quad + \left[\nabla_k H^i{}_j + \bar{\omega}^i{}_k H^k{}_j - H^i{}_k\bar{\omega}^k{}_j\right] \wedge \Theta^0 \\
&= \bar{\Omega}^i{}_j + K^i{}_k K_{jm}\,\Theta^k \wedge \Theta^m \\
&\quad - \left[\nabla_i(\ln\alpha)\, K_{jm} - \nabla_j(\ln\alpha)\, K^i{}_m + D_m H^i{}_j\right]\Theta^0 \wedge \Theta^m \,.
\end{aligned} \tag{C.2}$$

This shows that we find for the curvature on the three-surface Σ

$$
\begin{aligned}
\Omega^i{}_j|_\Sigma &= [d\omega^i{}_j + \omega^i{}_s \wedge \omega^s{}_j + \omega^i{}_0 \wedge \omega^0{}_j]|_\Sigma \\
&= d\bar{\omega}^i{}_j + \bar{\omega}^i{}_s \wedge \bar{\omega}^s{}_j + \left(-\eta^{im} K_{ms} \bar{\Theta}^s\right) \wedge \left(-K_{jt} \bar{\Theta}^t\right) \\
&= \bar{\Omega}^i{}_j + \left(-K^i{}_s \bar{\Theta}^s\right) \wedge \left(-K_{jt} \bar{\Theta}^t\right) \\
&= \bar{\Omega}^i{}_j + K^i{}_s K_{jt}\, \bar{\Theta}^s \wedge \bar{\Theta}^t\,.
\end{aligned} \tag{C.3}
$$

This Gauss equation expresses the 3D curvature tensor in terms of the projection of the 4D curvature, with extrinsic curvature corrections. In fact, the expressions for the Ricci tensor given in the next section show that the second part of $\Omega^i{}_j$ is not needed for the calculation of the Ricci tensor.

C.2 Codazzi–Mainardi Equations

The Codazzi–Mainardi equation follows from

$$
\begin{aligned}
\Omega^0_{\ i} &= d\omega^0_{\ i} + \omega^0_{\ k} \wedge \omega^k_{\ i} \\
&= d\left[\nabla_i \ln\alpha\, \Theta^0 - K_{ij}\Theta^j\right] + \left[(\nabla_k \ln\alpha)\Theta^0 - K_{kj}\Theta^j\right] \wedge \omega^k_{\ i} \\
&= -\frac{1}{\alpha} d\alpha_{,i} \wedge \Theta^0 - \nabla_k \ln\alpha\, \omega^k_{\ i} \wedge \Theta^0 \\
&\quad -dK_{ij} \wedge \Theta^j - K_{ij}\, d\Theta^j + K_{kj}\, \omega^k_{\ i} \wedge \Theta^j \\
&= \frac{1}{\alpha}\left[d\alpha_{,i} - \alpha_{,k}\omega^k_{\ i}\right] \wedge \Theta^0 - dK_{ij} \wedge \Theta^j + K_{ik}\, \omega^k_{\ a} \wedge \Theta^a + K_{kj}\, \omega^k_{\ i} \wedge \Theta^j \\
&= \frac{1}{\alpha} D(\alpha_{,i}) \wedge \Theta^0 - dK_{ij} \wedge \Theta^j + K_{ij}\, \omega^k_{\ 0} \wedge \Theta^0 \\
&\quad +K_{ik}\, \omega^k_{\ m} \wedge \Theta^m + K_{kj}\, \omega^k_{\ i} \wedge \Theta^j \\
&= \frac{1}{\alpha} D(\alpha_{,i}) \wedge \Theta^0 \\
&\quad -\left[dK_{ij} - K_{ik}\omega^k_{\ j} - K_{kj}\, \omega^k_{\ i}\right] \wedge \Theta^j - K_{ik}\, K^k_{\ m}\Theta^m \wedge \Theta^0\,.
\end{aligned} \tag{C.4}
$$

This decomposition provides then the projection of the 4D curvature $\Omega^0_{\ i}$ known as the Codazzi–Mainardi equation

$$
\Omega^0_{\ i}|_\Sigma = -\bar{D}K_{ij} \wedge \bar{\Theta}^j\,, \tag{C.5}
$$

where $\bar{D}K_{ij} = (D_s K_{ij})\bar{\Theta}^s$.

For the calculation of the Ricci tensor we only need the normal projections

$$
\Omega^i{}_0(e_j, e_0) = \Omega^0_{\ i}(e_j, e_0)\,. \tag{C.6}
$$

From the above we derive for this

$$
\Omega^0_{\ i}(e_j, e_0) = \frac{1}{\alpha} D_j(\alpha_{,i}) + dK_{ij}(e_0) - K_{im}\omega^m_{\ j}(e_0) - K_{kj}\omega^k_{\ i}(e_0) - \mathbf{K}^2_{ij}\,. \tag{C.7}
$$

Remember that

$$dK_{ij}(e_0) = \frac{1}{\alpha}\left(\partial_t - i_\beta \cdot d\right) K_{ij}\,. \tag{C.8}$$

Now we consider the term, following from equation (2.368)

$$\begin{aligned}
(K_\omega)_{ij} &= K_{im}\omega^m{}_j(e_0) + K_{jm}\omega^m{}_i(e_0) \\
&= \frac{1}{\alpha}\,K^m_i\left[\beta_{[m|j]} - c_{[mj]} - \bar\omega_{mj}(\beta)\right] \\
&\quad + \frac{1}{\alpha}\,K^m_j\left[\beta_{[m|i]} - c_{[mi]} - \bar\omega_{mi}(\beta)\right] \\
&= -\frac{1}{\alpha}\left[K_{im}\bar\omega^m{}_j(\beta) + K_{jm}\bar\omega^m{}_i(\beta)\right] \\
&\quad + \frac{1}{2\alpha}\left[K^m_i\beta_{m|j} - K^m_i\beta_{j|m} + K^m_j\beta_{m|i} - K^m_j\beta_{i|m}\right. \\
&\quad \left. - K^m_i c_{mj} + K^m_i c_{jm} - K^m_j c_{mi} + K^m_j c_{im}\right] \\
&= -\frac{1}{\alpha}\left[K_{im}\bar\omega^m{}_j(\beta) + K_{jm}\bar\omega^m{}_i(\beta)\right] \\
&\quad + \frac{1}{2\alpha}\left[-K^m_i\left(\beta_{m|j} + \beta_{j|m} - (c_{mj} + c_{jm})\right) - 2K^m_i c_{mj}\right. \\
&\qquad - K^m_j\left(\beta_{m|i} + \beta_{i|m} - (c_{mi} + c_{im})\right) - 2K^m_j c_{im} \\
&\qquad \left. + 2K^m_i\beta_{m|j} + 2K^m_j\beta_{m|i}\right]\,.
\end{aligned} \tag{C.9}$$

In this expression, all other terms including c_{im} cancel out. Using the definition of the extrinsic curvature K_{ij}, equation (2.367), we find

$$\begin{aligned}
(K_\omega)_{ij} &= -K_{im}K^m_j - K^m_j K_{mi} + \frac{1}{\alpha}\,K_{im}\beta^m{}_{|j} + \frac{1}{\alpha}\,K_{jm}\beta^m{}_{|i} \\
&\quad - \frac{1}{\alpha}\left[K_{im}\bar\omega^m{}_j(\beta) + K_{jm}\bar\omega^m{}_i(\beta)\right] \\
&= -K_{im}K^m_j - K^m_j K_{mi} + \frac{1}{\alpha}\,K_{im}\beta^m{}_{,j} + \frac{1}{\alpha}\,K_{jm}\beta^m{}_{,i}\,.
\end{aligned} \tag{C.10}$$

Together with the expression for the Lie derivative of the extrinsic curvature

$$\mathcal{L}_\beta K_{ij} = \beta^m K_{ij,m} + K_{im}\beta^m{}_{,j} + K_{mj}\beta^m{}_{,i} \tag{C.11}$$

we found for the curvature component

$$\begin{aligned}
\Omega^0{}_i(e_j, e_0) &= \frac{1}{\alpha}D_j(\alpha_{,i}) + \frac{1}{\alpha}(\partial_t - \mathcal{L}_\beta)K_{ij} \\
&\quad + K_{im}K^m_j + K_{jm}K^m_i - \mathbf{K}^2_{ij} \\
&= \frac{1}{\alpha}D_j(\alpha_{,i}) + \frac{1}{\alpha}(\partial_t - \mathcal{L}_\beta)K_{ij} + K_{jm}K^m_i\,.
\end{aligned} \tag{C.12}$$

D 3+1 Split of Rotating Neutron Star Geometry

D.1 The 3+1 Split of the Connection

We will apply Cartan's methods to calculate the curvature tensor for rotating spacetimes with respect to Bardeen observers. In a first step we calculate the exterior derivatives for the fundamental one-forms (7.16) (A, $B = 2, 3$)

$$\begin{aligned} d\Theta^A &= \sum_B \exp(\mu_A)\, \mu_{A,B}\, dx^B \wedge dx^A + \exp(\mu_A)\mu_{A,\phi}\, d\phi \wedge dx^B \\ &= \exp(-\mu_B)\mu_{A,B}\, \Theta^B \wedge \Theta^A\,. \end{aligned} \tag{D.1}$$

Similarly, we find

$$d\Theta^1 = \sum_A \exp(-\mu_A)\, \psi_{,A}\, \Theta^A \wedge \Theta^1 - \sum_A \exp(\psi - \nu - \mu_A)\omega_{,A}\, \Theta^A \wedge \Theta^0\,, \tag{D.2}$$

as well as

$$d\Theta^0 = \sum_A \exp(-\mu_A)\, \nu_{,A}\, \Theta^A \wedge \Theta^0\,. \tag{D.3}$$

Here we used the inversion

$$d\phi = \exp(-\psi)\Theta^1 + \exp(\psi - \nu)\omega\Theta^0\,. \tag{D.4}$$

Comparing this with Cartan's first structure equations

$$d\Theta^0 = -\sum_A \omega^0{}_A \wedge \Theta^A - \omega^0{}_1 \wedge \Theta^1 \tag{D.5}$$

$$d\Theta^1 = -\sum_A \omega^1{}_A \wedge \Theta^A - \omega^1{}_0 \wedge \Theta^0 \tag{D.6}$$

and

$$d\Theta^A = -\sum_B \omega^A{}_B \wedge \Theta^B - \omega^A{}_1 \wedge \Theta^1 - \omega^A{}_0 \wedge \Theta^0\,, \tag{D.7}$$

we conclude for axisymmetric connections

$$\omega^1{}_A = -\omega^A_1 = \exp(-\mu_A)\psi_{,A}\,\Theta^1 - \exp(-\psi)\mu_{,A}\Theta^A \tag{D.8}$$

$$\omega^A_B = -\omega^B_A = \exp(-\mu_B)\mu_{A,B}\,\Theta^A - \exp(-\mu_A)\mu_{B,A}\,\Theta^B\,. \tag{D.9}$$

The following ansatz solves the structure equations for the six connection forms of the Lorentz connection for axisymmetric and stationary spacetimes ($\omega^0_i = \omega^i{}_0$, $\omega^i{}_j = -\omega^j{}_i$)

$$\omega^0{}_1 = -\frac{1}{2}\exp(\psi - \nu - \mu_2)\,\omega_{,2}\Theta^2 - \frac{1}{2}\exp(\psi - \nu - \mu_3)\omega_{,3}\Theta^3 \tag{D.10}$$

$$\omega^0{}_2 = \exp(-\mu_2)\,\nu_{,2}\,\Theta^0 - \frac{1}{2}\exp(\psi - \nu - \mu_2)\,\omega_{,2}\,\Theta^1 \tag{D.11}$$

$$\omega^0{}_3 = \exp(-\mu_3)\,\nu_{,3}\,\Theta^0 - \frac{1}{2}\exp(\psi - \nu - \mu_3)\,\omega_{,3}\,\Theta^1 \tag{D.12}$$

$$\omega^1{}_2 = \exp(-\mu_2)\,\psi_{,2}\,\Theta^1 + \frac{1}{2}\exp(\psi - \nu - \mu_2)\,\omega_{,2}\,\Theta^0 \tag{D.13}$$

$$\omega^1{}_3 = \exp(-\mu_3)\,\psi_{,3}\,\Theta^1 + \frac{1}{2}\exp(\psi - \nu - \mu_3)\,\omega_{,3}\,\Theta^0 \tag{D.14}$$

$$\omega^2{}_3 = \exp(-\mu_3)\mu_{2,3}\,\Theta^2 - \exp(-\mu_2)\mu_{3,2}\,\Theta^3\,. \tag{D.15}$$

These relations can be contracted in a way which shows the features of the general decomposition found in Sect. 2.8

$$\omega^0{}_A = \nabla_A \ln(\alpha)\,\Theta^0 - K_{A1}\Theta^1 \tag{D.16}$$

$$\omega^1{}_A = (\nabla_A\psi)\,\Theta^1 + \frac{1}{2\alpha}\,(R\nabla_A\omega)\,\Theta^0 = \bar{\omega}^1{}_A + \frac{1}{2\alpha}\,(R\nabla_A\omega)\,\Theta^0 \tag{D.17}$$

$$\omega^2{}_3 = (\nabla_3\mu_2)\,\Theta^2 - (\nabla_2\mu_3)\Theta^3 = \bar{\omega}^2{}_3\,, \tag{D.18}$$

where K_{ij} is the extrinsic curvature (remember that $c_{ij} \equiv 0$ in a stationary spacetime), given in orthonormal basis,

$$K_{\hat{i}\hat{j}} = \frac{1}{2\alpha}\,(\beta_{i;j} + \beta_{j;i})\,. \tag{D.19}$$

With the definition of the covariant derivative for $\boldsymbol{\beta} = (-\omega\exp\Psi, 0, 0)$

$$\beta_{i;j} = e_j(\boldsymbol{\beta}) - \omega^m_i(e_j)\beta_m \tag{D.20}$$

we obtain the following form for the extrinsic curvature

$$K_{\hat{i}\hat{j}} = -\frac{R}{2\alpha}\begin{pmatrix} 0 & \nabla_2\omega & \nabla_3\omega \\ \nabla_2\omega & 0 & 0 \\ \nabla_3\omega & 0 & 0 \end{pmatrix}, \tag{D.21}$$

which shows that $\mathrm{Tr}(\mathbf{K}) = 0$. $\nabla_A\alpha = e^\mu_A\partial_\mu\alpha$ denotes the derivative along the meridional vector field $\mathbf{e}_A$ and $R = \exp(\psi)$ is the cylindrical radius.

The expressions for the connection one-forms are just a special case of the general 3+1 split derived in Sect. 2.8

$$\omega^0{}_i = (\nabla_i \ln \alpha)\, \Theta^0 - K_{ij}\, \Theta^j \tag{D.22}$$
$$\omega^i{}_j = \bar{\omega}^i{}_j + H^i{}_j\, \Theta^0\,, \tag{D.23}$$

where the matrix **H** is antisymmetric (for stationary spacetimes)

$$H_{ij} = \frac{1}{\alpha}\beta_{[i|j]}\,. \tag{D.24}$$

$\boldsymbol{\beta}$ is often called the vector potential of the gravitomagnetic field and the antisymmetric matrix **H** defines then the gravitomagnetic field itself, quite in analogy to the magnetic field in electrodynamics. All components of the connection therefore have a quite clear physical or geometrical interpretation.

D.2 The Curvature of Time Slices

For the calculation of the Ricci tensor of the hypersurface we need the curvature of the meridional plane

$$\bar{\Omega}^2{}_3 = d\bar{\omega}^2{}_3 + \bar{\omega}^2{}_1 \wedge \bar{\omega}^1{}_3 \tag{D.25}$$

and the curvature of the other 3D directions

$$\bar{\Omega}^1{}_A = d\bar{\omega}^1{}_A + \bar{\omega}^1{}_B \wedge \bar{\omega}^B{}_A\,. \tag{D.26}$$

For this purpose we define two poloidal vectors ($A = 2, 3$)

$$Q_A \equiv \exp(-\mu_A)\omega_{,A}\,, \qquad \Psi_A \equiv \exp(-\mu_A)\psi_{,A} = \nabla_A \psi\,. \tag{D.27}$$

In terms of these quantities we can write for any function $F\left(x^2, x^3\right)$

$$\begin{aligned} d(F\bar{\Theta}^1) &= \sum_A \exp(-\psi - \mu_A)\,(F \exp\psi)_{,A}\, \bar{\Theta}^A \wedge \bar{\Theta}^1 \\ &= \sum_A \frac{1}{R}\nabla_A[RF]\, \bar{\Theta}^A \wedge \bar{\Theta}^1 \end{aligned} \tag{D.28}$$

$$\begin{aligned} d(F\bar{\Theta}^A) &= \sum_B \exp(-\mu_A - \mu_B)(\exp\mu_A F)_{,B}\, \bar{\Theta}^B \wedge \bar{\Theta}^A \\ &= \sum_B \exp(-\mu_A)\nabla_B[\exp(\mu_A)F]\, \bar{\Theta}^B \wedge \bar{\Theta}^A\,. \end{aligned} \tag{D.29}$$

So we need the exterior derivatives of $\omega^1{}_2$, $\omega^1{}_3$ and of $\omega^2{}_3$. Using this rule in conjunction with the above connection form we obtain

$$
\begin{aligned}
d\bar{\omega}^1{}_2 + \bar{\omega}^1{}_3 \wedge \bar{\omega}^3{}_2 = {} & \frac{1}{R}\nabla_A[R\Psi_2]\,\bar{\Theta}^A \wedge \bar{\Theta}^1 \\
& -\Psi_3\nabla_3\mu_2\,\bar{\Theta}^1 \wedge \bar{\Theta}^2 + \Psi_3\nabla_2\mu_3\,\bar{\Theta}^1 \wedge \bar{\Theta}^3 && \text{(D.30)} \\
d\bar{\omega}^1{}_3 + \bar{\omega}^1{}_2 \wedge \bar{\omega}^2{}_3 = {} & \frac{1}{R}\nabla_A[R\Psi_3]\,\bar{\Theta}^A \wedge \bar{\Theta}^1 \\
& +\Psi_2\nabla_3\mu_2\,\bar{\Theta}^1 \wedge \bar{\Theta}^2 - \Psi_2\nabla_2\mu_3\,\bar{\Theta}^1 \wedge \bar{\Theta}^3 && \text{(D.31)} \\
d\bar{\omega}^2{}_3 + \bar{\omega}^2{}_1 \wedge \bar{\omega}^1{}_3 = {} & -\big[\exp(-\mu_2)\,\nabla_3[\exp(\mu_2)\nabla_3\mu_2] \\
& + \exp(-\mu_3)\,\nabla_2[\exp(\mu_3)\nabla_2\mu_3]\big]\,\bar{\Theta}^2 \wedge \bar{\Theta}^3\,. && \text{(D.32)}
\end{aligned}
$$

With these expressions the curvature of the hypersurfaces can be written in closed form

$$
\begin{aligned}
\bar{\Omega}^1{}_2 = {} & -\left[\frac{1}{R}\nabla_2[R\Psi_2] + \Psi_3[\nabla_3\mu_2]\right]\bar{\Theta}^1 \wedge \bar{\Theta}^2 \\
& + \left[-\frac{1}{R}\nabla_3[R\Psi_2] + \Psi_3[\nabla_2\mu_3]\right]\bar{\Theta}^1 \wedge \bar{\Theta}^3 && \text{(D.33)} \\
\bar{\Omega}^1{}_3 = {} & -\left[\frac{1}{R}\nabla_3[R\Psi_3] + \Psi_2[\nabla_2\mu_3]\right]\bar{\Theta}^1 \wedge \bar{\Theta}^3 \\
& + \left[-\frac{1}{R}\nabla_2[R\Psi_3] + \Psi_2[\nabla_3\mu_2]\right]\bar{\Theta}^1 \wedge \bar{\Theta}^2 && \text{(D.34)} \\
\bar{\Omega}^2{}_3 = {} & -\Big[\exp(-\mu_2)\nabla_3[\exp(\mu_2)\nabla_3\mu_2] \\
& + \exp(-\mu_3)\nabla_2[\exp(\mu_3)\nabla_2\mu_3]\Big]\,\bar{\Theta}^2 \wedge \bar{\Theta}^3\,. && \text{(D.35)}
\end{aligned}
$$

The curvature tensor of a three-surface has nine independent components and satisfies in our case $R_{1213} = R_{1312}$ and $R_{1223} = 0 = R_{1323}$.

With these expression we can calculate the six components of the Ricci tensor of the hypersurface, $\bar{R}_{ij} = \bar{\Omega}^m_i(e_m, e_j)$,

$$
\begin{aligned}
\bar{R}_{11} = {} & \bar{\Omega}^2{}_1(e_2, e_1) + \bar{\Omega}^3{}_1(e_3, e_1) = \bar{\Omega}^1{}_2(e_1, e_2) + \bar{\Omega}^1{}_3(e_1, e_3) = \\
= {} & -\frac{1}{R}\nabla_2[R\Psi_2] - \Psi_3[\nabla_3\mu_2] - \frac{1}{R}\nabla_3[R\Psi_3] - \Psi_2[\nabla_2\mu_3] && \text{(D.36)} \\
\bar{R}_{22} = {} & \bar{\Omega}^1{}_2(e_1, e_2) + \bar{\Omega}^3{}_2(e_3, e_2) \\
= {} & -\frac{1}{R}\nabla_2[R\Psi_2] - \Psi_3[\nabla_3\mu_2] - \exp(-\mu_2)\nabla_3[\exp(\mu_2)\nabla_3\mu_2] \\
& - \exp(-\mu_3)\nabla_2[\exp(\mu_3)\nabla_2\mu_3] && \text{(D.37)} \\
\bar{R}_{33} = {} & \bar{\Omega}^1{}_3(e_1, e_3) + \bar{\Omega}^2{}_3(e_2, e_3) \\
= {} & -\frac{1}{R}\nabla_3[R\Psi_3] - \Psi_2[\nabla_2\mu_3] - \exp(-\mu_2)\nabla_3[\exp(\mu_2)\nabla_3\mu_2] \\
& - \exp(-\mu_3)\nabla_2[\exp(\mu_3)\nabla_2\mu_3] && \text{(D.38)} \\
\bar{R}_{12} = {} & \bar{\Omega}^2{}_1(e_2, e_2) + \bar{\Omega}^3{}_1(e_3, e_2) = 0 && \text{(D.39)}
\end{aligned}
$$

$$\bar{R}_{13} = \bar{\Omega}^2{}_1(e_2, e_3) + \bar{\Omega}^3{}_1(e_3, e_3) = 0 \tag{D.40}$$

$$\bar{R}_{23} = \bar{\Omega}^1{}_2(e_1, e_3) + \bar{\Omega}^3{}_2(e_3, e_3) = -\frac{1}{R}\nabla_3[R\Psi_2] + \Psi_3[\nabla_2\mu_3]\,. \tag{D.41}$$

By summation we get the Ricci scalar on the hypersurface

$$\begin{aligned}
\bar{R} &= \bar{R}_{11} + \bar{R}_{22} + \bar{R}_{33} \\
&= -2\left[\frac{1}{R}\nabla_2[R\Psi_2] + \Psi_3(\nabla_3\mu_2) + \frac{1}{R}\nabla_3[R\Psi_3] + \Psi_2(\nabla_2\mu_3)\right] \\
&\quad -2\exp(-\mu_2)\nabla_3[\exp(\mu_2)\nabla_3\mu_2] - 2\exp(-\mu_3)\nabla_2[\exp(\mu_3)\nabla_2\mu_3] \\
&= -2\left[\frac{1}{R}\nabla_2[R\Psi_2] + \Psi_3(\nabla_3\mu_2) + \frac{1}{R}\nabla_3[R\Psi_3] + \Psi_2(\nabla_2\mu_3)\right] \\
&\quad -2\Delta(\mu_2, \mu_3)\,,
\end{aligned} \tag{D.42}$$

where we have defined the second-order elliptic operator

$$\begin{aligned}
\Delta(\mu_2, \mu_3) = {} & \exp(-\mu_2)\nabla_3[\exp(\mu_2)(\nabla_3\mu_2)] \\
& + \exp(-\mu_3)\nabla_2[\exp(\mu_3)(\nabla_2\mu_3)]\,.
\end{aligned} \tag{D.43}$$

E Equations of GRMHD

E.1 Electromagnetic Fields

A complete description of the electromagnetic field is provided by the Faraday tensor $F^{\mu\nu}$, which is related to the electric and magnetic field, E^μ and B^μ, measured by an observer with four-velocity O

$$F^{\mu\nu} = O^\mu E^\nu - O^\nu U^\mu + O_\varrho \eta^{\varrho\mu\nu\sigma} B_\sigma \,. \tag{E.1}$$

Both, electric and magnetic fields are orthogonal to O and are recovered from the Faraday tensor by means of the following relations

$$E^\mu = F^{\mu\nu} O_\nu \tag{E.2}$$

and

$$B^\mu = \frac{1}{2} \eta^{\mu\nu\varrho\sigma} O_\nu F_{\varrho\sigma} = O_\nu * F^{\nu\mu} \,. \tag{E.3}$$

The dual of the electromagnetic tensor is defined as

$$*F^{\mu\nu} = \frac{1}{2}\, \eta^{\mu\nu\varrho\sigma} F_{\varrho\sigma} \,, \tag{E.4}$$

or expressed as

$$*F^{\mu\nu} = O^\mu B^\nu - O^\nu B^\mu + \eta^{\mu\nu\varrho\sigma} O_\varrho E_\sigma \,. \tag{E.5}$$

$\eta^{\mu\nu\varrho\sigma} = [\mu\nu\varrho\sigma]/\sqrt{-g}$ is the total antisymmetric tensor related to the volume element (see Sect. 2.3).

We now decompose the Faraday tensor into electric and magnetic components measured by Eulerian observers **n** by means of

$$E^\mu = F^{\mu\nu} n_\nu \,, \quad B^\mu = - * F^{\mu\nu} n_\nu \,. \tag{E.6}$$

Both fields are purely spatial, $E^\mu n_\mu = 0 = B^\mu n_\mu$. This is equivalent to decompose the Faraday tensor into

$$\boxed{F^{\mu\nu} = n^\mu E^\nu - n^\nu F^\mu + n_\varrho \eta^{\varrho\mu\nu\sigma} B_\sigma \,.} \tag{E.7}$$

This electromagnetic part simplifies if we adopt the ideal MHD approximation: the electric field as measured in the plasma frame vanishes due to the high conductivity of the plasma. In SRMHD this is the famous relation $\mathbf{E} + \mathbf{v} \times \mathbf{B} = 0$. The covariant expression for this condition is (Ohm's law)

$$U^\mu F_{\mu\nu} = 0 \,. \tag{E.8}$$

But even in GR, we may still define magnetic fields as measured in plasma frame

$$b^\mu = -\frac{1}{2}\eta^{\mu\nu\varrho\sigma} U_\nu F_{\varrho\sigma} \,. \tag{E.9}$$

In the case of ideal MHD, this relation can easily be inverted to give

$$F^{\mu\nu} = U_\varrho \eta^{\varrho\mu\nu\sigma} b_\sigma \,. \tag{E.10}$$

Taking the dual, we obtain

$$*F^{\mu\nu} = b^\mu U^\nu - b^\nu U^\mu \,. \tag{E.11}$$

The magnetic field b^μ only lives in three-space, since $U_\mu b^\mu = 0$. Inserting this into the expression (10.160) yields the energy–momentum tensor of the electromagnetic part in terms of the comoving magnetic field

$$T^{\mu\nu}_{\rm (ED)} = \frac{b^2}{4\pi} U^\mu U^\nu + \frac{b^2}{8\pi} g^{\mu\nu} - \frac{1}{4\pi} b^\mu b^\nu \,. \tag{E.12}$$

This expression is very similar to the classical EM tensor except for the contribution to the energy density. In summary, we have found the stress–energy tensor for a plasma

$$\boxed{T^{\mu\nu} = \left(\varrho_0 + \epsilon + P + \frac{b^2}{4\pi}\right) U^\mu U^\nu + \left(P + \frac{b^2}{8\pi}\right) g^{\mu\nu} - \frac{1}{4\pi} b^\mu b^\nu \,.} \tag{E.13}$$

This is the stress–energy tensor which we need for the equations of motion.

We may find the relations between magnetic fields in the plasma frame and the observer's frame by defining a projection operator $P_{\mu\nu} = g_{\mu\nu} + U_\mu U_\nu$. Since b^μ is orthogonal to U^μ, we find $P^\mu_\nu b^\nu = b^\mu$. It follows therefore from the definition of B^μ that

$$P^\mu_\nu B^\nu = P^\mu_\nu n_\varrho (b^\varrho U^\nu - b^\nu U^\varrho) = -n_\varrho U^\varrho b^\mu \,. \tag{E.14}$$

Hence we have

$$\boxed{b^\mu = -\frac{P^\mu_\nu B^\nu}{n_\nu U^\nu} \,.} \tag{E.15}$$

We can now evaluate the time and spatial components

$$b^t = U_i B^i/\alpha = \frac{W(\mathbf{v}\cdot\mathbf{B})}{\alpha} \tag{E.16}$$

$$b^i = \frac{B^i/\alpha + b^t U^i}{U^t} = \frac{B^i + W^2(\mathbf{v}\cdot\mathbf{B})v^i}{W}\,, \tag{E.17}$$

where $U^t = W/\alpha$. Finally, the modulus of the plasma magnetic field can be written as

$$b^2 = \frac{B^2 + \alpha^2 (b^t)^2}{W^2} = \frac{B^2 + W^2(\mathbf{v}\cdot\mathbf{B})^2}{W^2}\,, \tag{E.18}$$

where $B^2 = B_i B^i$.

Maxwell's equations follow from the homogeneous equations

$$\nabla_\nu * F^{\mu\nu} = 0 = \frac{1}{\sqrt{-g}}\,\partial_\nu[\sqrt{-g}\, * F^{\mu\nu}]\,, \tag{E.19}$$

where $\sqrt{-g} = \alpha\sqrt{\gamma}$. The time component gives the divergence condition

$$\boxed{\frac{1}{\sqrt{\gamma}}\,\partial_i[\sqrt{\gamma}\, B^i] = 0\,.} \tag{E.20}$$

The spatial components give the induction equation in conservative form

$$\frac{1}{\sqrt{-g}}\partial_t[\sqrt{\gamma}\, B^i] + \frac{1}{\sqrt{-g}}\partial_j\left[\sqrt{-g}\,\left(U^j b^i - U^i b^j\right)\right] = 0\,. \tag{E.21}$$

On the other hand we also find

$$U^j b^i - U^i b^j = V^j B^i - V^i B^j\,, \tag{E.22}$$

where $V^i = v^i - \beta^i/\alpha$. The induction equation can therefore be written in the form

$$\boxed{\frac{1}{\sqrt{-g}}\partial_t[\sqrt{\gamma}\, B^i] + \frac{1}{\sqrt{-g}}\partial_j\left[\sqrt{-g}\,\left(V^j B^i - V^i B^j\right)\right] = 0\,.} \tag{E.23}$$

This form of the induction equation is equivalent to the conservative formulation of the Newtonian MHD.

E.2 Conservative Formulation of GRMHD

Similar to the approach chosen to model pure hydrodynamical flows in Sect. 3.1, we shortly discuss the time evolution of magnetohydrodynamic fields based on a conservative schemes. Baryon number conservation gives

$$\frac{1}{\sqrt{-g}}\partial_t\left[\sqrt{\gamma}D\right]+\frac{1}{\sqrt{-g}}\partial_j\left[\sqrt{-g}DV^j\right]=0\,, \tag{E.24}$$

where $D=\varrho_0\,\alpha U^t=\varrho_0 W$ is a relativistic mass density. Similar to the hydro case, we introduce the momentum fluxes measured by Eulerian observers

$$S_i=-n_\mu T^\mu_{\ i}=\alpha T^t_{\ i}=[\varrho_0 h+b^2/4\pi]W^2\,v_i-\alpha b^t b_i/4\pi\,, \tag{E.25}$$

as well as the total energy density

$$\tau=n_\mu n_\nu T^{\mu\nu}-D=\alpha^2 T^{tt}-D=\varrho h_* W^2-P_T-\alpha^2(b^t)^2-D\,, \tag{E.26}$$

where $P_T=P+b^2/8\pi$ is the total pressure in the plasma and $h_*=h+b^2/4\pi\varrho_0$ the total enthalpy. The system is completed by means of an equation of state in the form of $P=(\Gamma-1)\varrho_0 e$.

The spatial components of the energy–momentum conservation provide momentum conservation

$$\frac{1}{\sqrt{-g}}\partial_t[\sqrt{\gamma}S_i]+\frac{1}{\sqrt{-g}}\partial_j[\sqrt{-g}T^j_{\ i}]=T^{\mu\nu}\left(\frac{\partial g_{\nu i}}{\partial x^\mu}-\Gamma^\sigma_{\ \nu\mu}g_{\sigma i}\right)\,, \tag{E.27}$$

and the time-component gives the energy equation

$$\begin{aligned}\frac{1}{\sqrt{-g}}\partial_t[\sqrt{\gamma}\tau]&+\frac{1}{\sqrt{-g}}\partial_j[\sqrt{-g}(\alpha T^{tj}-DV^j)]\\&=\alpha\left(T^{\mu t}\frac{\partial\log\alpha}{\partial x^\mu}-T^{\mu\nu}\Gamma^t_{\ \nu\mu}\right)\,.\end{aligned} \tag{E.28}$$

The GRMHD equations have therefore the form of a hyperbolic system, similar to (3.32),

$$\boxed{\frac{1}{\sqrt{-g}}\left(\frac{\partial[\sqrt{\gamma}\mathbf{U}]}{\partial t}+\frac{\partial[\sqrt{-g}\mathbf{F}^i]}{\partial x^i}\right)=\mathcal{S}\,,} \tag{E.29}$$

which are obtained by combining the plasma equations with the induction equation (E.23). The state vector of GRMHD now consists of eight variables

$$\mathbf{U}=(D,S_i,\tau,B^i)^T\,, \tag{E.30}$$

explicitly given by the vector in the state space

$$\mathbf{U}=\begin{pmatrix}D\\S_1\\S_2\\S_3\\\tau\\B^1\\B^2\\B^3\end{pmatrix}=\begin{pmatrix}\varrho_0 W\\(\varrho_0 h+b^2/4\pi)W^2 v_1-\alpha b^t b_1/4\pi\\(\varrho_0 h+b^2/4\pi)W^2 v_2-\alpha b^t b_2/4\pi\\(\varrho_0 h+b^2/4\pi)W^2 v_3-\alpha b^t b_3/4\pi\\(\varrho_0 h+b^2/4\pi)W^2-P_T-\alpha^2(b^t)^2/4\pi-D\\B^1\\B^2\\B^3\end{pmatrix}\,. \tag{E.31}$$

The corresponding fluxes $\mathbf{F}$ are now given by

$$\mathbf{F}^i = \begin{pmatrix} DV^i \\ S_1 V^i - b_1 B^i/4\pi W + P_T \delta^i_1 \\ S_2 V^i - b_2 B^i/4\pi W + P_T \delta^i_2 \\ S_3 V^i - b_3 B^i/4\pi W + P_T \delta^i_3 \\ \tau V^i + P_T v^i - \alpha b^t B^i/W \\ B^1 V^i - B^i V^1 \\ B^2 V^i - B^i V^2 \\ B^3 V^i - B^i V^3 \end{pmatrix} , \tag{E.32}$$

where $V^i \equiv v^i - \beta^i/\alpha$. The energy–momentum tensor in the sources $\mathcal{S}$ now includes both parts, plasma and electromagnetic fields

$$\mathcal{S} = \begin{pmatrix} 0 \\ T^{\mu\nu}\partial_\mu g_{\nu 1} - \Gamma^\varrho_{\nu\mu} g_{\varrho 1} \\ T^{\mu\nu}\partial_\mu g_{\nu 2} - \Gamma^\varrho_{\nu\mu} g_{\varrho 2} \\ T^{\mu\nu}\partial_\mu g_{\nu 3} - \Gamma^\varrho_{\nu\mu} g_{\varrho 3} \\ \alpha(T^{\mu t}\partial_\mu \alpha - T^{\mu\nu}\Gamma^t_{\nu\mu}) \\ 0 \\ 0 \\ 0 \end{pmatrix} . \tag{E.33}$$

E.3 Numerical Schemes

Recovery of Primitive Variables

Conservative MHD schemes require methods to transform between conserved variables $\mathbf{U}$ and primitive variables $\mathbf{P}$. The time integration of GRMHD determines the three-momenta

$$S_i = (\varrho_0 h + b^2/4\pi) W^2 v_i - \alpha b^t b_i/4\pi , \tag{E.34}$$

the mass-density D and the energy τ. The associated four-momentum vector defined as

$$P_\mu = -n_\nu T^\nu_{\ \mu} = \alpha T^t_{\ \mu} \tag{E.35}$$

has then the following form

$$P_\mu = W(\varrho_0 h + b^2/4\pi) U_\mu - (P + b^2/8\pi) n_\mu - \alpha b^t b_\mu/4\pi . \tag{E.36}$$

It is useful to remember the two relations

$$b^2 = \frac{1}{W^2}\left(\mathbf{B}^2 + (U_\mu B^\mu)^2\right) , \quad n_\nu B^\nu = -U_\mu B^\mu . \tag{E.37}$$

Noble et al. [311] discuss the mathematical properties of the inverse transformation and present six numerical methods for performing the inversion. Comparisons between the methods are made using a survey over phase space, a two-dimensional explosion problem, and a general relativistic MHD accretion disk simulation.

In the first method, we solve two algebraic equations simultaneously for $H = W^2 h\varrho_0$ and $\mathbf{v}^2$. The momentum vector can be written, using $\mathbf{B} \to \mathbf{B}/\sqrt{4\pi}$, and the relation (E.42) in the following form

$$\mathbf{S} = (H + \mathbf{B}^2)\,\mathbf{v} - \frac{(\mathbf{S}\cdot\mathbf{B})}{H}\,\mathbf{B} \tag{E.38}$$

and the energy as

$$\tau = \frac{\mathbf{B}^2}{2}(1+\mathbf{v}^2) + \frac{\mathbf{S}\cdot\mathbf{B}}{2H} + H - D - P(e,\varrho_0)\,. \tag{E.39}$$

The first equation can be solved to get $\mathbf{v}^2$ as an explicit function of H

$$\mathbf{v}^2(H) = \frac{\mathbf{S}^2 H^2 + (\mathbf{S}\cdot\mathbf{B})^2(\mathbf{B}^2 + 2H)}{(\mathbf{B}^2 + H)^2 H^2}\,. \tag{E.40}$$

The energy equation provides then a second relation if we adopt a simple EoS

$$\tau = \frac{\mathbf{B}^2}{2}(1+\mathbf{v}^2) + \frac{\mathbf{S}\cdot\mathbf{B}}{2H} + H - D - \left(\frac{\Gamma - 1}{\Gamma}\left[(1-\mathbf{v}^2)H - \varrho_0\right]\right)\,. \tag{E.41}$$

The final step is to find $\mathbf{v}$ by using $\mathbf{S}$. Starting with the expressions for b^t, b^i and b^2 in the definition of $\mathbf{S}$ one finds

$$\boxed{\mathbf{S} = (H + \mathbf{B}^2)\,\mathbf{v} - (\mathbf{v}\cdot\mathbf{B})\,\mathbf{B}\,.} \tag{E.42}$$

This shows that the relativistic momentum flow $\mathbf{S}$ has, besides kinematic factors, two relativistic corrections, the magnetic energy density $\mathbf{B}^2/4\pi$ and a Poynting contribution $\propto \mathbf{v}\cdot\mathbf{B}$. Since $\mathbf{v}\cdot\mathbf{B} = (\mathbf{S}\cdot\mathbf{B})/H$, we can use this to solve for the velocity field in terms of conserved variables

$$\boxed{\mathbf{v} = \frac{1}{H + \mathbf{B}^2}\left[\mathbf{S} + \frac{(\mathbf{S}\cdot\mathbf{B})}{H}\,\mathbf{B}\right]\,.} \tag{E.43}$$

Koide et al. [231] have proposed an alternative procedure to solve a combined system for the variables $x = W - 1$ and $y = W(\mathbf{v}\cdot\mathbf{B})$ which is given as

$$\begin{aligned} x(x+2)\left[\Gamma R x^2 + (2\Gamma R - d)x + \Gamma R - d + e + \frac{\Gamma}{2}y^2\right] & \qquad\qquad (E.44)\\ = (\Gamma x^2 + 2\Gamma x + 1)^2\left[f^2(x+1)^2 + 2\sigma y + 2\sigma x y + g^2 y^2\right] & \end{aligned}$$

$$\begin{aligned} \left[\Gamma(R - g^2)x^2 + (2\Gamma R - 2\Gamma g^2 - d)x + \Gamma R - d + e - g^2 + \frac{\Gamma}{2}y^2\right] y & \\ = \sigma(x+1)(\Gamma x^2 + 2\Gamma x + 1)\,, & \qquad\qquad (E.45) \end{aligned}$$

where $R = D + \tau$, $d = (\Gamma - 1)D$, $e = (1 - \Gamma/2)\mathbf{B}^2/4\pi$, and $\sigma = \mathbf{B} \cdot \mathbf{S}$. These algebraic equations are solved at each grid point using a two-variable Newton–Raphson iteration method. The primitive variables are then reconstructed from x, y, D, $\mathbf{S}$, τ, and $\mathbf{B}$ with the following expressions

$$W = 1 + x \tag{E.46}$$

$$P = \frac{(\Gamma - 1)\left[\tau - xD - (2 - 1/W^2)\mathbf{B}^2/8\pi + (y/W)^2/2\right]}{Wx(x+2) + 1} \tag{E.47}$$

$$\mathbf{v} = \frac{\mathbf{S} + (y/W)\mathbf{B}}{D + \left[\tau + P + \mathbf{B}^2/2W^2 + (y/W)^2/2\right]} . \tag{E.48}$$

On Numerical Implementations

There are many possible ways to numerically integrate the GRMHD equations. As in the Newtonian case, nonconservative schemes enjoyed wide use in the astrophysical community (e.g. ZEUS3D and NIRVANA2). They permit the integration of the internal energy density ϵ rather than the total energy equation. This is advantageous in regions of a plasma flow where the internal energy is small compared to the total energy, which is in fact the common situation in nonrelativistic astrophysics. De Villiers and Hawley [133] have developed a nonconservative scheme of GRMHD following a ZEUS-like approach. Modern approaches to solve GRMHD are however based on the above conservative formulation. This guarantees a true momentum and energy conservation.

Since we update $\mathbf{U}$ rather than $\mathbf{P}$, we must solve at the end of each timestep for $\mathbf{P}(\mathbf{U})$. This can be done in various ways. The simplest approach is to use Newton–Raphson routines with the value of $\mathbf{P}$ given by the previous time-step as an initial guess. Here, only five equations need to be solved, since B^i are analytically given. The Newton–Raphson procedure requires an expensive evaluation of the Jacobian $\partial\mathbf{U}/\partial\mathbf{P}$ and is in general limited in accuracy, i.e. it is a source of numerical noise. The evaluation of $\mathbf{P}(\mathbf{U})$ is at the heart of each numerical procedure for solving SRMHD or GRMHD. This procedure must be robust and CPU friendly.

A further important step is the evaluation of the fluxes $\mathbf{F}$. Gammie et al. [166] use a MUSCL type scheme with HLL fluxes (Harten et al. [194]). The fluxes are defined at zone faces. A slope-limited linear extrapolation from the zone center gives the values $\mathbf{P}_R$ and $\mathbf{P}_L$ for the primitive variables at the right and left sides of each zone interface. From $\mathbf{P}_R$ and $\mathbf{P}_L$ one calculates the maximum right- and leftgoing wave speeds and the fluxes $\mathbf{F}_R = \mathbf{F}(\mathbf{P}_R)$ and $\mathbf{F}_L = \mathbf{F}(\mathbf{P}_L)$. In the PPM reconstruction scheme, a quartic polynomial interpolation is used to obtain the primitive variables to the left and right of the grid cell interface. The relativistic version of the PPM algorithm can be found in Marti and Müller [271].

The exact solution of the Riemann problem in special relativistic magnetohydrodynamics (SRMHD) is discussed in [172]. Both initial states leading to a set of only three waves analogous to the ones in relativistic hydrodynamics, as well as generic initial states leading to the full set of seven MHD waves are considered. Because of its generality, the solution presented could serve as an important test for numerical codes solving the MHD equations in relativistic regimes.

Time-Stepping Procedure

To advance time-steps, the higher order algorithms discussed in Sect. 3.1 can be applied. They are not repeated here.

Constrained Transport

Shock-capturing schemes do not guarantee $\nabla \cdot \mathbf{B} = 0$ for all time-steps. Some constrained transport schemes are needed to maintain $\nabla \cdot \mathbf{B} = 0$. Procedures of this type are discussed by Toth [398]. The flux-interpolated constrained transport (flux-CT) scheme introduced by Toth [398] is quite favorable for coding. In this algorithm, the numerical flux of the induction equation computed at each point is replaced with a linear combination of the numerical fluxes computed at each point and neighboring points. This procedure does not require a staggered mesh.

F Solutions

Problems in Chapter 2

2.1 The exterior derivative of $\omega = *A$ is an n-form, given by

$$\begin{aligned}(d\omega)_{ai_1\cdots i_{n-1}} &= (d * A)_{ai_1\cdots i_{n-1}} \\ &= n\nabla_{[a}(A^b\eta_{bi_1\cdots i_{n-1}]}) \\ &= n\,\eta_{b[i_1\cdots i_{n-1}}\nabla_{a]}A^b\,. \end{aligned} \tag{F.1}$$

Since

$$d\omega = f\,\eta = *f\,, \tag{F.2}$$

with its dual

$$f = (-1)^s **f = (-1)^s\ *d\omega\,, \tag{F.3}$$

we obtain in our case

$$\begin{aligned}*d\omega &= *d*A \\ &= \frac{1}{n!}\,\eta^{ai_1\cdots i_{n-1}}(\eta_{b[i_1\cdots i_{n-1}}\nabla_{a]}A^b) \\ &= \frac{1}{(n-1)!}(-1)^s\,(n-1)!\,\delta^a_b\,\nabla_a A^b \\ &= (-1)^s\,\nabla_a A^a\,. \end{aligned} \tag{F.4}$$

From the definition of the Levi-Civita tensor we obtain

$$d\omega = (\nabla_a A^a)\sqrt{|g|}\,d^n x\,. \tag{F.5}$$

2.3 See [2].

2.4 For this, see classical textbooks on general relativity; see also Sect. 6.4.3.

Problems in Chapter 3

3.1 For the solution of this problem we use the covariant expression (3.32) and calculate the Christoffel symbols for the various coordinate systems. In cylindrical coordinates (r, ϕ, z), the equations of special relativistic hydrodynamics (3.11) are given by

$$\frac{\partial D}{\partial t} + \frac{1}{r}\frac{\partial (rDv_r)}{\partial r} + \frac{1}{r}\frac{\partial (Dv_\phi)}{\partial \phi} + \frac{\partial (Dv_z)}{\partial z} = 0 \tag{F.6}$$

$$\frac{\partial S_r}{\partial t} + \frac{1}{r}\frac{\partial [r(S_r v_r + P)]}{\partial r} + \frac{1}{r}\frac{\partial (S_r v_\phi)}{\partial \phi} + \frac{\partial (S_r v_z)}{\partial z} = \frac{P}{r} + \frac{\varrho_0 h W^2 v_\phi^2}{r} \tag{F.7}$$

$$\frac{\partial S_\phi}{\partial t} + \frac{1}{r}\frac{\partial (rS_\phi v_r)}{\partial r} + \frac{1}{r}\frac{\partial (S_\phi v_\phi + P)}{\partial \phi} + \frac{\partial (S_\phi v_z)}{\partial z} = -\frac{\varrho_0 h W^2 v_r v_\phi}{r} \tag{F.8}$$

$$\frac{\partial S_z}{\partial t} + \frac{1}{r}\frac{\partial (rS_z v_r)}{\partial r} + \frac{1}{r}\frac{\partial (S_z v_\phi)}{\partial \phi} + \frac{\partial (S_z v_z + P)}{\partial z} = 0 \tag{F.9}$$

$$\frac{\partial \tau}{\partial t} + \frac{1}{r}\frac{\partial [r(S_r - Dv_r)]}{\partial r} + \frac{1}{r}\frac{\partial (S_\phi - Dv_\phi)}{\partial \phi} + \frac{\partial (S_z - Dv_z)}{\partial z} = 0\,. \tag{F.10}$$

The discretized equation for cylindrical coordinates is given as

$$\frac{d\mathbf{U}_{i,j,k}}{dt} = -\frac{r_{i+1/2}\mathbf{F}^r_{i+1/2,j,k} - r_{i-1/2}\mathbf{F}^r_{i-1/2,j,k}}{r_i \Delta r} - \frac{\mathbf{F}^\phi_{i,j+1/2,k} - \mathbf{F}^\phi_{i,j-1/2,k}}{r_i \Delta \phi} - \frac{\mathbf{F}^z_{i,j,k+1/2} - \mathbf{F}^z_{i,j,k-1/2}}{\Delta z} + S_{i,j,k}\,, \tag{F.11}$$

3.2 In spherical coordinates (r, θ, ϕ), the equations of special relativistic hydrodynamics (3.11) are given by

$$\frac{\partial D}{\partial t} + \frac{1}{r^2}\frac{\partial (r^2 Dv_r)}{\partial r} + \frac{1}{r\sin\theta}\frac{\partial (\sin\theta D v_\theta)}{\partial \theta} + \frac{1}{r\sin\theta}\frac{\partial (Dv_\phi)}{\partial \phi} = 0 \tag{F.12}$$

$$\frac{\partial S_r}{\partial t} + \frac{1}{r^2}\frac{\partial [r^2(S_r v_r + P)]}{\partial r} + \frac{1}{r\sin\theta}\frac{\partial (\sin\theta S_r v_\theta)}{\partial \theta} + \frac{1}{r\sin\theta}\frac{\partial (S_r v_\phi)}{\partial \phi} = \frac{2P}{r} + \frac{\varrho_0 h W^2 (v_\theta^2 + v_\phi^2)}{r} \tag{F.13}$$

$$\frac{\partial S_\theta}{\partial t} + \frac{1}{r^2}\frac{\partial (r^2 S_\theta v_r)}{\partial r} + \frac{1}{r\sin\theta}\frac{\partial [\sin\theta(S_\theta v_\theta + P)]}{\partial \theta} + \frac{1}{r\sin\theta}\frac{\partial (S_\theta v_\phi)}{\partial \phi} = \frac{P\cot\theta}{r} - \frac{\varrho_0 h W^2 (v_\phi^2 \cot\theta - v_r v_\theta)}{r} \tag{F.14}$$

$$\frac{\partial S_\phi}{\partial t} + \frac{1}{r^2}\frac{\partial (r^2 S_\phi v_r)}{\partial r} + \frac{1}{r\sin\theta}\frac{\partial(\sin\theta S_\phi v_\theta)}{\partial\theta} + \frac{1}{r\sin\theta}\frac{\partial(S_\phi v_\phi + P)}{\partial\phi}$$
$$= -\frac{\varrho_0 h W^2 v_\phi (v_r + v_\theta\cot\theta)}{r} \tag{F.15}$$

$$\frac{\partial\tau}{\partial t} + \frac{1}{r^2}\frac{\partial[r^2(S_r - Dv_r)]}{\partial r} + \frac{1}{r\sin\theta}\frac{\partial[\sin\theta(S_\theta - Dv_\theta)]}{\partial\theta}$$
$$+\frac{1}{r\sin\theta}\frac{\partial(S_\phi - Dv_\phi)}{\partial\phi} = 0\,. \tag{F.16}$$

The discretized equation for spherical coordinates is given as

$$\begin{aligned}\frac{d\mathbf{U}_{i,j,k}}{dt} = & -\frac{r^2_{i+1/2}\mathbf{F}^r_{i+1/2,j,k} - r^2_{i-1/2}\mathbf{F}^r_{i-1/2,j,k}}{r_i^2\Delta r} \\ & -\frac{\sin\theta_{j+1/2}\mathbf{F}^\theta_{i,j+1/2,k} - \sin\theta_{j-1/2}\mathbf{F}^\theta_{i,j-1/2,k}}{r_i\sin\theta_j\Delta\theta} \\ & -\frac{\mathbf{F}^\phi_{i,j,k+1/2} - \mathbf{F}^\phi_{i,j,k-1/2}}{r_i\sin\theta_j\Delta\phi} + S_{i,j,k}\,.\end{aligned} \tag{F.17}$$

3.3 Spherically symmetric motion of gas with velocity $\beta = v/c$ corresponds to four-velocity $u^\alpha = (W, W\beta, 0, 0)$ in spherical coordinates ($c = 1$). Rest-mass conservation gives

$$\frac{1}{r^2}\frac{d}{dt}\left(r^2\varrho W\right) + W\varrho\,\frac{\partial\beta}{\partial r} = 0\,, \tag{F.18}$$

where d/dt is the convective derivative defined by $\frac{d}{dt} \equiv \frac{\partial}{\partial t} + \beta\frac{\partial}{\partial r}$. Similarly, $\nabla_\mu T_\alpha{}^\mu = 0$ yields

$$\frac{1}{r^2}\frac{d}{dt}\left(r^2 Whu_\alpha\right) + Whu_\alpha\frac{\partial\beta}{\partial r} + \partial_\alpha p = 0\,, \tag{F.19}$$

where $h = e + p$. This gives two independent equations ($\alpha = 0, 1$). Choose $\nabla_\mu T_1{}^\mu = 0$ as one equation, and the projection $u^\alpha\nabla_\mu T_\alpha{}^\mu = 0$ as the other. Show that conservation of momentum and energy may be expressed by

$$\frac{1}{r^2}\frac{d}{dt}\left(r^2W^2h\beta\right) = -\frac{\partial p}{\partial r} - W^2h\beta\frac{\partial\beta}{\partial r} \tag{F.20}$$
$$\frac{1}{r^2}\frac{d}{dt}\left(r^2Wh\right) = W\,\frac{dp}{dt} - Wh\,\frac{\partial\beta}{\partial r}\,. \tag{F.21}$$

Apply equations (F.18) and (F.20) to the blast (the gas between FS and RS), and make the approximation $\partial\beta/\partial r = 0$, i.e.

$$W(t, r) = \Gamma(t)\,, \qquad r_r < r < r_f\,, \tag{F.22}$$

where $r_r(t)$ and $r_f(t)$ are the instantaneous radii of RS and FS, respectively. Then integration of equations (F.18) and (F.20) over r between RS and FS (at t = const) yields

$$\frac{\Gamma}{r^2}\frac{d}{dr}\left(r^2\,\Sigma\,\Gamma\right) = \varrho_r(\beta-\beta_r)\Gamma^2 + \frac{1}{4}\varrho_f \tag{F.23}$$

$$\frac{1}{r^2}\frac{d}{dr}\left(r^2 H\Gamma^2\right) = h_r\,(\beta-\beta_r)\Gamma^2 + p_r \tag{F.24}$$

$$\frac{\Gamma}{r^2}\frac{d}{dr}\left(r^2 H\,\Gamma\right) = \Gamma^2\frac{dP}{dr} + (h_r - p_r)(\beta-\beta_r)\Gamma^2 + \frac{3}{4}\,p_f\,, \tag{F.25}$$

where $\Sigma \equiv \int_{r_r}^{r_f}\varrho\,dr$, $H \equiv \int_{r_r}^{r_f} h\,dr$, and $P \equiv \int_{r_r}^{r_f} p\,dr$. In the derivation of these equations we used the identity for a function $f(t,r)$ and $F(t) = \int_{r_r}^{r_f} f(t,r)\,dr$,

$$\int_{r_r(t)}^{r_f(t)}\frac{df}{dt}\,dr = \frac{dF}{dt} - f_f(\beta_f-\beta) - f_r(\beta-\beta_r)\,. \tag{F.26}$$

Here $f_f(t) \equiv f(t, r_f[t])$ and $f_r(t) \equiv f(t, r_r[t])$; $\beta_r = dr_r/dt$ and $\beta_f = dr_f/dt$ are the velocities of RS and FS in the lab frame. The relativistic blast is a very thin shell, $r_f - r_r \sim r/\Gamma^2 \ll r$, and we used $r_f \approx r_r \approx r$ when calculating the integrals. In the integrated equations we took into account that $\Gamma \gg 1$. Then the jump conditions at the FS give $\beta_f - \beta = 1/4\Gamma^2$ and $h_f = 4p_f \gg \varrho_f$. The convective derivative d/dt has been replaced by $\beta\,d/dr \approx d/dr$ and $\Gamma^2\beta$ by Γ^2 in the second equation.

Problems in Chapter 4

4.1 The perturbed orbital equation can be written as

$$\begin{aligned}\frac{d^2u_1}{d\phi^2} + u_1 &= \frac{3G^2M^2}{L^2}\,(1+e\,\cos\phi)^2\\ &= \frac{3G^2M^2}{L^2}\,\left[(1+e^2/2) + 2e\,\cos\phi + (e^2/2)\cos 2\phi\right]\,.\end{aligned} \tag{F.27}$$

This equation can be solved by means of the identity

$$\frac{d^2}{d\phi^2}(\phi\,\cos\phi) + \phi\,\sin\phi = 2\cos\phi\,. \tag{F.28}$$

A solution to the perturbed equation is then given by

$$u_1 = \frac{3G^2M^2}{L^2}\left[1 + e^2/2 + e\phi\,\sin\phi - \frac{e^2}{6}\cos 2\phi\right]. \tag{F.29}$$

The first term is simply a constant offset, and the third term oscillates around zero. The second term represents a secular perturbation which accumulates over the orbits. The full solution can therefore be written as

$$u = 1 + e\cos\phi + \frac{3G^2M^2e}{L^2}\,\phi\,\sin\phi\,. \tag{F.30}$$

This expression can be rewritten as an equation for an ellipse with an angular period deviating from 2π

$$u = 1 + e\cos[(1 - \Delta)\phi]\,, \tag{F.31}$$

where we have defined

$$\Delta = \frac{3G^2M^2}{L^2}\,. \tag{F.32}$$

We have therefore found that a planet suffers a perihelion advance each orbit by an angle

$$\Delta\phi = 2\pi\Delta = \frac{6\pi G^2M^2}{L^2}\,. \tag{F.33}$$

4.2 The Christoffel symbols for Schwarzschild are

$$\begin{array}{lll} \Gamma^t_{tr} = \frac{GM}{r(r-2GM)} & \Gamma^r_{tt} = \frac{GM}{r^3}(r-2GM) & \Gamma^r_{rr} = -\frac{GM}{r(r-2GM)} \\ \Gamma^\theta_{r\theta} = \frac{1}{r} & \Gamma^r_{\theta\theta} = -(r-2GM) & \Gamma^\phi_{r\phi} = \frac{1}{r} \\ \Gamma^r_{\phi\phi} = -(r-2GM)\sin^2\theta & \Gamma^\theta_{\phi\phi} = -\sin\theta\,\cos\theta & \Gamma^\phi_{\theta\phi} = \frac{\cos\theta}{\sin\theta}\,. \end{array} \tag{F.34}$$

The geodesics equations give then the following relations

$$\frac{d^2t}{d\lambda^2} + \frac{2GM}{r(r-2GM)}\frac{dt}{d\lambda}\frac{dr}{d\lambda} = 0 \tag{F.35}$$

$$\begin{aligned} \frac{d^2r}{d\lambda^2} + \frac{GM}{r^3}(r-2GM)\left(\frac{dt}{d\lambda}\right)^2 - \frac{GM}{r(r-2GM)}\left(\frac{dr}{d\lambda}\right)^2 & \\ -(r-2GM)\left[\left(\frac{d\theta}{d\lambda}\right)^2 + \sin^2\theta\left(\frac{d\phi}{d\lambda}\right)^2\right] &= 0 \end{aligned} \tag{F.36}$$

$$\frac{d^2\theta}{d\lambda^2} + \frac{2}{r}\frac{dr}{d\lambda}\frac{d\theta}{d\lambda} - \sin\theta\,\cos\theta\left(\frac{d\phi}{d\lambda}\right)^2 = 0 \tag{F.37}$$

$$\frac{d^2\phi}{d\lambda^2} + \frac{2}{r}\frac{dr}{d\lambda}\frac{d\phi}{d\lambda} + 2\frac{\cos\theta}{\sin\theta}\frac{d\theta}{d\lambda}\frac{d\phi}{d\lambda} = 0\,. \tag{F.38}$$

The third equation shows that a particle with initially $\dot{\theta} = 0$ in the equatorial plane will stay in the equatorial plane.

Problems in Chapter 6

6.1 Particle density, energy density and pressure are given for an ideal Fermi gas

$$n = \frac{8\pi}{(2\pi\hbar)^3}\int_0^{p_F} p^2\,dp \tag{F.39}$$

$$\varrho = \frac{8\pi}{(2\pi\hbar)^3}\int_0^{p_F} \sqrt{p^2+m^2}\,p^2\,dp \tag{F.40}$$

$$P = \frac{1}{3}\frac{8\pi}{(2\pi\hbar)^3}\int_0^{p_F} \frac{p^2}{\sqrt{p^2+m^2}}\,p^2\,dp\,. \tag{F.41}$$

Chemical equilibrium between protons, neutrons and electrons requires for the chemical potentials

$$\mu_n = \mu_p + \mu_e\,, \tag{F.42}$$

where

$$\mu = \epsilon_F = \sqrt{p_F^2 + m^2} = \sqrt{\Lambda^2 n^{2/3} + m^2} \tag{F.43}$$

with the definition $\Lambda = (3\pi^2\hbar)^{1/3}$. From the chemical equilibrium we obtain

$$\frac{n_p}{n_n} = \frac{1}{8}\left[\frac{1 + \frac{2(m_n^2 - m_p^2 - m_e^2)}{\Lambda^2 n_n^{2/3}} + \frac{(m_n^2 - m_p^2)^2 - 2m_e^2(m_n^2 + m_p^2) + 4m_e^4}{\Lambda^4 n_n^{4/3}}}{1 + m_n^2/\Lambda^2 n_n^{4/3}}\right]^{3/2}. \tag{F.44}$$

With the mass difference $Q = m_n - m_p$, and since $Q \ll m_n$ and $m_e \ll m_n$, we can simplify the expression

$$\frac{n_p}{n_n} = \frac{1}{8}\left[\frac{1 + (4Q/m_n)(\varrho_0/m_n n_n)^{2/3} + 4[(Q^2 - m_e^2)/m_n^2](\varrho_0/m_n n_n)^{4/3}}{1 + (\varrho_0/m_n n_n)^{2/3}}\right]^{3/2} \tag{F.45}$$

where the density $\varrho_0 = m_n^4/\Lambda^3 = 6.11 \times 10^{15}$ g/cm^3 is a characteristic density. For the Fermi momentum of the electrons one obtains

$$\begin{aligned} p_{F,e}^2 &= \Lambda^2 n_e^{2/3} = m_n^2 (m_n n_n/\varrho_0)^{2/3} (n_p/n_n)^{2/3} \\ &= \frac{(m_n^2/4)(m_n n_n/\varrho_0)^{4/3} + Q m_n (m_n n_n/\varrho_0)^{2/3} + Q^2 - m_e^2}{1 + (m_n n_n/\varrho_0)^{2/3}}\,. \end{aligned} \tag{F.46}$$

Since the maximal momentum of the electron in the classical neutron decay is $p_{\max} = \sqrt{Q^2 - m_e^2} = 1.19$ MeV, in neutron stars we have generally $p_{F,e} \gg p_{\max}$.

For small neutron densities n_n, the proton–neutron ratio decreases with increasing number density, until it reaches a minimum at the density

$$\varrho_{\min} \simeq \varrho_0 \left(\frac{4(Q^2 - m_e^2)}{m_n^2}\right)^{3/4} = 1.28 \times 10^{-4}\,\varrho_0 = 7.8 \times 10^{11}\,\text{g cm}^{-3}\,. \tag{F.47}$$

Beyond this density, n_p/n_n increases and goes asymptotically to the value of 1/8. At nuclear densities, one finds typical values of $n_p/n_n \simeq 0.01$ and $p_{F,e} \simeq 100$ MeV. For much higher densities, muons are created, since $p_{F,e} > 105$ MeV.

6.2 The maximal mass of a neutron star consisting of noninteracting neutrons is $M_{\max} = 0.71\,M_\odot$ with a central density $\varrho_c = 4 \times 10^{15}$ g/cm^3 and a radius $R = 9.6$ km.

6.3 Solvers for the TOV equations can easily be found on the web.

6.6 From the expressions for the Kepler problem one obtains for the time derivative $\dot{\phi}$, which follows from the angular momentum

$$L = \frac{M_1 M_2}{M_1 + M_2}\, r^2 \dot{\phi} \tag{F.48}$$

and hence together with the expression for L

$$\dot{\phi} = \frac{(M_1 + M_2)\, a\sqrt{1 - e^2}}{r^2} \,. \tag{F.49}$$

In addition, the expression for r implies therefore

$$\dot{r} = e\, \sin\phi \sqrt{\frac{M_1 + M_2}{a(1 - e^2)}} \,. \tag{F.50}$$

With these relations one can derive the first and second time derivatives of the moments of inertia

$$I_{xx} = M_1 x_1^2 + M_2 x_2^2 = \frac{M_1 M_2}{M_1 + M_2}\, r^2 \cos^2\phi \tag{F.51}$$

$$I_{yy} = \frac{M_1 M_2}{M_1 + M_2}\, r^2 \sin^2\phi \tag{F.52}$$

$$I_{xy} = \frac{M_1 M_2}{M_1 + M_2}\, r^2 \sin\phi\cos\phi \tag{F.53}$$

$$I = I_{xx} + I_{yy} = \frac{M_1 M_2}{M_1 + M_2}\, r^2 \,. \tag{F.54}$$

the following expressions

$$\dot{I}_{xx} = -\frac{2M_1 M_2}{\sqrt{(M_1 + M_2)a(1 - e^2)}}\, r\cos\phi\sin\phi \tag{F.55}$$

$$\ddot{I}_{xx} = -\frac{2M_1 M_2}{a(1 - e^2)}\, (\cos 2\phi + e\cos^3\phi) \tag{F.56}$$

$$\dot{I}_{yy} = \frac{2M_1 M_2}{\sqrt{(M_1 + M_2)a(1 - e^2)}}\, r\,(sin\phi\cos\phi + e\sin\phi) \tag{F.57}$$

$$\ddot{I}_{yy} = \frac{2M_1 M_2}{a(1 - e^2)}\, (\cos 2\phi + e\cos\phi + e\cos^3\phi + e^2) \tag{F.58}$$

$$\dot{I}_{xy} = \frac{2M_1 M_2}{\sqrt{(M_1 + M_2)a(1 - e^2)}}\, r\,(\cos^2\phi - \sin^2\phi + e\cos\phi) \tag{F.59}$$

$$\ddot{I}_{xy} = -\frac{2M_1 M_2}{a(1 - e^2)}\, (\sin 2\phi + e\sin\phi + e\sin\phi\cos^2\phi) \,. \tag{F.60}$$

From here we get the third time derivatives

$$\dddot{I}_{xx} = \frac{2M_1M_2}{a(1-e^2)}\,(2\sin 2\phi + 3e\cos^2\phi\sin\phi)\,\dot{\phi} \tag{F.61}$$

$$\dddot{I}_{yy} = -\frac{2M_1M_2}{a(1-e^2)}\,(2\sin 2\phi + e\sin\phi + 3e\cos^2\phi\sin\phi)\,\dot{\phi} \tag{F.62}$$

$$\dddot{I}_{xy} = -\frac{2M_1M_2}{a(1-e^2)}\,(2\cos 2\phi - e\cos\phi + 3e\cos^3\phi)\,\dot{\phi} \tag{F.63}$$

$$\dddot{I} = -\frac{2M_1M_2}{a(1-e^2)}\,e\sin\phi\,\dot{\phi}\,. \tag{F.64}$$

These quantities determine the energy loss

$$-\frac{dE}{dt} = \frac{1}{5}\left[\dddot{I}_{ik}\dddot{I}_{ik} - \frac{1}{3}(\dddot{I})^2\right] = \frac{1}{5}\left[(\dddot{I}_{xx})^2 + (\dddot{I}_{yy})^2 + 2(\dddot{I}_{xy})^2 - \frac{1}{3}(\dddot{I})^2\right]. \tag{F.65}$$

6.9 The Crab Nebula is a unique cosmic lab with an extremely broad spectrum of nonthermal radiation (radio and optical emission is strongly polarized). The spectrum extends through 20 decades in frequency space, ranging from radio wavelengths to gamma-ray emission. It is commonly assumed that the synchrotron nebula is powered by electrons and positrons generated by the central pulsar and terminated by a standing reverse shock at a distance of about 0.1 pc from the pulsar (Fig. 1.8). A discussion of the global spectrum of the Crab Nebula (Fig. F.1) can be found in Aharonian and Atoyan [24] and Aharonian et al. [25].

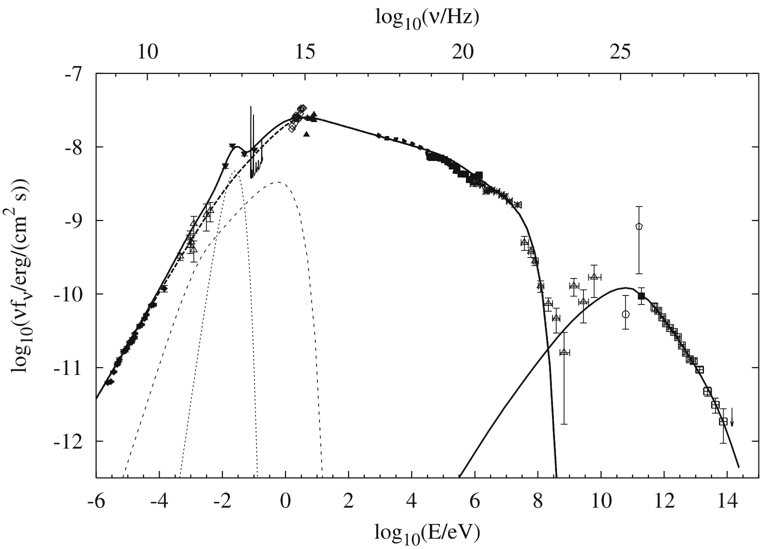

Fig. F.1. Energy spectrum of the Crab Nebula compiled from the literature. The *solid* and *dashed curves* correspond to synchrotron and inverse Compton emission, respectively. Figure adapted from [25]

6.10 We start with the Boltzmann equation for massless particles (photons or neutrinos)

$$p^\alpha \frac{\partial f}{\partial x^\alpha} + \Gamma^\alpha_{\beta\gamma} p^\beta p^\gamma \frac{\partial f}{\partial p^\alpha} = \left(\frac{df}{d\tau}\right)_{\text{coll}} , \tag{F.66}$$

where f is the invariant neutrino (photon) distribution function, p^α the neutrino four-momentum and Γ the Christoffel symbols for the metric of a neutron star. Since the collision term is only known in a comoving frame, we transform to comoving momenta p^α

$$p^a e^\alpha_a \frac{\partial f}{\partial x^\alpha} + e^\alpha_a \omega^a{}_{bc}\, p^b p^c \frac{\partial f}{\partial p^\alpha} = \left(\frac{df}{d\tau}\right)_{\text{coll}} , \tag{F.67}$$

with basis vectors $\mathbf{e}_a$ for the comoving observer. The connection coefficients are those derived in Sect. 4.2

$$\omega^1{}_{00} = \exp(-\lambda)\,(\partial_r \Phi) \tag{F.68}$$

$$\omega^1{}_{22} = -\frac{\exp(-\lambda)}{r} = \omega^1{}_{33} = -\omega^2{}_{21} = -\omega^3{}_{31} \tag{F.69}$$

$$\omega^2{}_{33} = -\frac{\cot\theta}{r} = -\omega^3{}_{32} \,. \tag{F.70}$$

The neutrino four-momentum can be parametrized by

$$p^a = \hat{E}\left(1, \mu, \sqrt{1-\mu^2}\cos\chi, \sqrt{1-\mu^2}\sin\chi\right), \tag{F.71}$$

where μ is the cosine of the angle between the neutrino momentum and the radial direction, $\hat{E}$ is the neutrino energy in the comoving frame. With these quantities, the Boltzmann equation is simply given by

$$\begin{aligned} \hat{E} e^t_0 \frac{\partial f}{\partial t} + \hat{E} e^r_1 \frac{\partial f}{\partial r} - \hat{E}\mu e^t_0 \frac{\partial f}{\partial r} \hat{E}^2 \mu \omega^1{}_{00} \frac{\partial f}{\partial \hat{E}} & \\ - \hat{E}(1-\mu^2)(\omega^1{}_{00} + \omega^1{}_{22}) \frac{\partial f}{\partial \mu} = \left(\frac{df}{d\tau}\right)_{\text{coll}} & . \end{aligned} \tag{F.72}$$

As with photon distributions, one defines the nth moments

$$M_n = \frac{1}{2}\int_{-1}^{1} d\mu\, \mu^n\, f\,, \quad Q_n = \frac{1}{2}\int_{-1}^{1} d\mu\, \mu^n \left(\frac{df}{d\tau}\right)_{\text{coll}} . \tag{F.73}$$

They satisfy the following evolution equations

$$\begin{aligned} \hat{E}\left(e^t_0 \frac{\partial M_0}{\partial t} + e^r_1 \frac{\partial M_1}{\partial r}\right) & -\hat{E}^2\, \omega^2{}_{00} \frac{\partial M_1}{\partial \hat{E}} \\ & -2\hat{E}(\omega^1{}_{00} + \omega^1{}_{22})\, M_1 = Q_0 \end{aligned} \tag{F.74}$$

$$\begin{aligned} \hat{E}\left(e^t_0 \frac{\partial M_1}{\partial t} + e^r_1 \frac{\partial M_2}{\partial r}\right) & -\hat{E}^2\, \omega^2{}_{00} \frac{\partial M_2}{\partial \hat{E}} \\ & +\hat{E}(\omega^1{}_{00} + \omega^1{}_{22})\,(M_0 - 3M_2) = Q_1 \,. \end{aligned} \tag{F.75}$$

We now introduce the number density N_ν, the number flux F_ν and the number source term S_N, together with the mean neutrino energy density J_ν, energy flux H_ν, pressure P_ν and energy source term S_E by means of the definitions

$$N_\nu = \frac{1}{2\pi^2}\int_0^\infty M_0 \hat{E}^2\, d\hat{E} \tag{F.76}$$

$$F_\nu = \frac{1}{2\pi^2}\int_0^\infty M_1 \hat{E}^2\, d\hat{E} \tag{F.77}$$

$$S_N = \frac{1}{2\pi^2}\int_0^\infty Q_0 \hat{E}\, d\hat{E} \tag{F.78}$$

$$J_\nu = \frac{1}{2\pi^2}\int_0^\infty M_0 \hat{E}^3\, d\hat{E} \tag{F.79}$$

$$H_\nu = \frac{1}{2\pi^2}\int_0^\infty M_1 \hat{E}^3\, d\hat{E} \tag{F.80}$$

$$P_\nu = \frac{1}{2\pi^2}\int_0^\infty M_2 \hat{E}^3\, d\hat{E} \tag{F.81}$$

$$S_E = \frac{1}{2\pi^2}\int_0^\infty Q_0 \hat{E}^2\, d\hat{E}\,. \tag{F.82}$$

After integration over the neutrino energy and by using the continuity equation, one recovers the neutrino (photon) transport equations

$$\frac{\partial[N_\nu/n_B]}{\partial t} + \frac{\partial[4\pi r^2 \exp\Phi\, F_\nu]}{\partial r} = \exp\Phi\,\frac{S_N}{n_B} \tag{F.83}$$

$$\begin{aligned}\frac{\partial[J_\nu/n_B]}{\partial t} &+ P_\nu\,\frac{\partial[1/n_B]}{\partial t}\\ &+ \exp(-\Phi)\,\frac{\partial[4\pi r^2 \exp(2\Phi)\, H_\nu]}{\partial r} = \exp\Phi\,\frac{S_E}{n_B}\,.\end{aligned} \tag{F.84}$$

The flux of energy $L(r)$ per unit time through a spherical shell at distance r from the center is proportional to the gradient of the temperature

$$L(r) = -4\pi r^2 \kappa(r)\,\frac{\partial[\exp(\Phi) T]}{\partial r}\,\exp(-\Phi)\sqrt{1-\frac{2m(r)}{r}}\,, \tag{F.85}$$

where the factor $\exp(-\Phi)\sqrt{1-2m(r)/r}$ corresponds to the relativistic correction of the time-scale (redshift) and the shell thickness. For this purpose, it is useful to introduce the shell volume $A(r)$ defined by

$$\frac{\partial A}{\partial r} = \frac{4\pi r^2 n}{\sqrt{1-2m(r)/r}}\,, \tag{F.86}$$

where $n(r)$ is the baryon number density. With this shell variable, one can write the energy balance and the thermal energy transport as

$$\frac{\partial}{\partial A}[L(A)\exp(2\Phi)] = -\frac{1}{n}\left[\epsilon_\nu \exp(2\Phi) + c_V \frac{\partial[T\exp\Phi]}{\partial t}\right] \tag{F.87}$$

$$\frac{\partial}{\partial A}[T(A)\exp(\Phi)] = -\frac{3\kappa\varrho}{4acT^3}\frac{L\exp\Phi}{4\pi r^2}\,. \tag{F.88}$$

These equations are supplemented by the stellar structure equations for the mass distribution $m(A)$ and the potential $\Phi(A)$

$$\frac{\partial m}{\partial A} = \frac{\varrho}{n}\sqrt{1-\frac{2m(A)}{r}} \tag{F.89}$$

$$\frac{\partial \Phi}{\partial A} = \frac{4\pi r^3 P + m(A)}{4\pi r^2 n}\frac{1}{\sqrt{1-2m(A)/r}}\,. \tag{F.90}$$

The pressure profile follows from the hydrodynamical equilibrium (see Sect. 2.7)

$$\frac{\partial P}{\partial A} = -(\varrho + P)\frac{\partial \Phi}{\partial A}\,. \tag{F.91}$$

6.11 For systems consisting of a radio pulsar and a white dwarf, it is extremely difficult to measure the periastron advance, since these systems are highly circular. Then also time dilation and gravitational redshift are difficult to measure. The only relativistic effect, which can be used, is the Shapiro time delay. If the range and shape of the Shapiro delay can be measured, this gives the mass M_c of the companion (WD) and the inclination $\sin i$. Together with the mass function, this provides an accurate measurement of the neutron star mass in such systems. With this method, the two post-Keplerian parameters have been measured for the millisecond pulsar PSR J1909–3744 ($P = 2.95$ ms, $P_b = 1.533449$ d, projected semimajor axis $a\sin i = 1.89799$ lt-s) [216]: (i) the range parameter $r = GM_c/c^3 = (1.004 \pm 0.011)$ μs and (ii) the shape parameter $s = \sin i = 0.99822 \pm 0.00011$. This gives the mass of the white dwarf $M_c = (0.2038 \pm 0.0022)\,M_\odot$ and the orbital inclination $i = (86.58 \pm 0.11)$ degrees. Therefore, we get the neutron star mass $M_n = (1.438 \pm 0.024)\,M_\odot$.

The eccentricity of the system is extremely low, $e = 1.35 \times 10^{-7}$. This corresponds to $\dot\omega$ predicted by GR in the range of 0.14 deg yr^{-1}. Since this mass of the neutron star in a recycled system is only slightly higher than the masses observed for other systems, it appears that the production of a millisecond pulsar is possible with the accretion of less than 0.2 $M_\odot$. Most of the mass would be lost from the system.

Problems in Chapter 7

7.1 Since $\sqrt{\gamma} = \exp(\psi + \mu_2 + \mu_3)$, we find

$$
\begin{aligned}
\alpha\,\mathrm{Div}\left[\frac{\nabla\psi}{\alpha}\right] &= \frac{1}{\sqrt{\gamma}}\left\{\partial_A\left[\frac{\sqrt{\gamma}}{\alpha}g^{AB}\partial_B\psi\right]\right\} \\
&= \frac{\alpha}{\sqrt{\gamma}}\left\{\frac{\exp\mu_3}{\alpha}\,\partial_2[\exp(\psi-\mu_2)\partial_2\psi] + \frac{\exp\mu_2}{\alpha}\,\partial_3[\exp(\psi-\mu_3)\partial_3\psi]\right. \\
&\quad + \frac{\exp(\psi-\mu_2)}{\alpha}\,(\partial_2\psi)\exp\mu_3(\partial_2\mu_3) \\
&\quad + \frac{\exp(\psi-\mu_3)}{\alpha}\,(\partial_3\psi)\exp\mu_2(\partial_3\mu_2) \\
&\quad - \frac{\exp(\psi-\mu_2+\mu_3)}{\alpha^2}\,(\partial_2\psi)(\partial_2\alpha) \\
&\quad \left. - \frac{\exp(\psi-\mu_3+\mu_2)}{\alpha^2}\,(\partial_3\psi)(\partial_3\alpha)\right\} \\
&= \frac{1}{R}\nabla_A[R\Psi_A] + \Psi_3\nabla_3\mu_2 + \Psi_2\nabla_2\mu_3 - \frac{1}{\alpha}(\nabla_A\Psi)(\nabla_A\alpha)\,. \qquad \text{(F.92)}
\end{aligned}
$$

7.2 The components of the Riemann tensor in the orthonormal frame follow from the curvature two-form

$$
\Omega^a{}_b = \frac{1}{2}R^a{}_{bcd}\,\Theta^c\wedge\Theta^d\,, \qquad \text{(F.93)}
$$

with the following expressions

$$
\begin{aligned}
R_{1010} &= -\Psi_2(\nabla_2\nu) - \Psi_3(\nabla_3\nu) - \frac{1}{4}\frac{R^2}{\alpha^2}(\nabla\omega\cdot\nabla\omega) && \text{(F.94)}\\
R_{2020} &= -\frac{1}{\alpha}\nabla_2(\nabla_2\alpha) - (\nabla_3\nu)(\nabla_3\mu_2) + \frac{3}{4}\frac{R^2}{\alpha^2}(\nabla_2\omega)^2 && \text{(F.95)}\\
R_{3030} &= -\frac{1}{\alpha}\nabla_3(\nabla_3\alpha) - (\nabla_2\nu)(\nabla_2\mu_3) + \frac{3}{4}\frac{R^2}{\alpha^2}(\nabla_3\omega)^2 && \text{(F.96)}\\
R_{3020} &= -\frac{1}{\alpha}\nabla_3(\nabla_2\alpha) + (\nabla_3\nu)(\nabla_2\mu_3) + \frac{3}{4}\frac{R^2}{\alpha^2}(\nabla_3\omega)(\nabla_2\omega) && \text{(F.97)}\\
R_{1212} &= \frac{1}{R}\,\nabla_2(R\Psi_2) + \Psi_3(\nabla_3\mu_2) + \frac{1}{4}\,\frac{R^2}{\alpha^2}(\nabla_2\omega)^2 && \text{(F.98)}\\
R_{1313} &= \frac{1}{R}\,\nabla_3(R\Psi_3) + \Psi_2(\nabla_2\mu_3) + \frac{1}{4}\,\frac{R^2}{\alpha^2}(\nabla_3\omega)^2 && \text{(F.99)}\\
R_{2323} &= \exp(-\mu_2)\nabla_3[\exp(\mu_2)\nabla_3\mu_2] \\
&\quad + \exp(-\mu_3)\nabla_2[\exp(\mu_3)\nabla_2\mu_3] = \Delta(\mu_2,\mu_3) && \text{(F.100)}\\
R_{1213} &= \frac{1}{R}\,\nabla_3(R\Psi_2) - \Psi_3(\nabla_2\mu_3) + \frac{1}{4}\,\frac{R^2}{\alpha^2}(\nabla_2\omega)(\nabla_3\omega) && \text{(F.101)}
\end{aligned}
$$

$$R_{1023} = -\frac{1}{2}\exp(-\mu_3)/\alpha)\nabla_2[(R\exp(\mu_3)\nabla_3\omega] + \frac{1}{2}\exp(-\mu_2)\nabla_3[(R\exp(\mu_2)/\alpha)\nabla_2\omega] \quad (F.102)$$

$$R_{2012} = \frac{R}{\alpha}(\nabla_2\omega)(\Psi_2 - \nabla_2\nu/2) + \frac{1}{2\alpha}\nabla_2[R\nabla_2\omega] + \frac{R}{2\alpha}(\nabla_3\omega)(\nabla_3\mu_2) \quad (F.103)$$

$$R_{2013} = \frac{1}{2\alpha}\nabla_2[R\nabla_3\omega] + \frac{R}{2\alpha}(\nabla_2\omega)[2\Psi_3 - \nabla_3\mu_2 - \nabla_3\nu] \quad (F.104)$$

$$R_{3013} = \frac{1}{2\alpha}\nabla_3[R\nabla_3\omega] + \frac{R}{\alpha}(\nabla_3\omega)[\Psi_3 - \nabla_3\nu/2] + \frac{R}{2\alpha}(\nabla_2\omega)(\nabla_2\mu_3)\,. \quad (F.105)$$

The following components vanish identically

$$R_{1012} = 0 = R_{1013} = R_{1002} = R_{1003} = R_{2023} = R_{3023} = R_{1223} = R_{1323}\,. \quad (F.106)$$

From these curvature, you can directly obtain the Ricci tensors.

7.4 For the calculation of the hydrodynamical equilibrium in the metric field of a rotating star

$$P_{,A} + \frac{P}{\sqrt{-g}}\,\partial_A\left[\sqrt{-g}\right] = T^{BC}\,\partial_B(g_{CA}) - T^{\mu\nu}\,\Gamma^B_{\mu\nu}\,g_{BA}\,, \quad (F.107)$$

we need the Christoffel symbols ($A = 2, 3$)

$$\Gamma^A_{00} = -\frac{1}{2}\exp(-2\mu)\partial_A[\omega^2\exp 2\Psi - \alpha^2] \quad (F.108)$$

$$\Gamma^A_{11} = -(\partial_A\Psi)\exp(2\Psi - 2\mu)\,, \qquad \Gamma^A_{22} = \partial_A\mu \quad (F.109)$$

$$\Gamma^A_{01} = \frac{1}{2}\exp(-2\mu)\partial_A(\omega\exp\Psi)\,, \qquad \Gamma^A_{33} = -\partial_A\mu\,. \quad (F.110)$$

By inserting these relations into the above equation, we obtain

$$\begin{aligned} P_{,A} = -P\Big[&\partial_A\nu + \partial_A\Psi + \frac{1}{2}\exp(-2\nu)\partial_A(\omega^2\exp 2\Psi - \exp 2\nu) \\ &- \omega\partial_A(\omega\exp 2\Psi) - \exp 2\Psi(\exp -2\Psi - \omega^2\exp -2\nu)\Big] \\ &-(\varrho + P)(u^t)^2\Big[-\frac{1}{2}\exp(-2\nu)\partial_A(\omega^2\exp 2\Psi - \exp 2\nu) \\ &+ \Omega\partial_A(\omega\exp 2\Psi) - \Omega^2\exp 2\Psi\partial_A\Psi\Big] \end{aligned}$$

$$
\begin{aligned}
&= -(\varrho + P)\partial_A \ln\alpha \\
&\quad -(\varrho + P)(u^t)^2 \exp 2\Psi \left[(\omega - \Omega)^2 \partial_A \nu - (\omega - \Omega)\partial_A \omega \right. \\
&\quad\quad \left. -(\omega - \Omega)^2 \partial_A \Psi\right] .
\end{aligned} \tag{F.111}
$$

In the last bracket we add and subtract the term $(\omega - \Omega)\partial_A \Omega$

$$
\begin{aligned}
P_{,A} &= -(\varrho + P)\partial_A \ln\alpha \\
&\quad -(\varrho + P)\frac{\gamma^2}{\alpha^2} \exp 2\Psi \left[(\omega - \Omega)^2 \partial_A \nu - (\omega - \Omega)\partial_A(\omega - \Omega)\right. \\
&\quad \left. -(\omega - \Omega)^2 \partial_A \Psi - (\omega - \Omega)\partial_A \Omega\right] \\
&= -(\varrho + P)\partial_A \ln\alpha \\
&\quad +\frac{1}{2}(\varrho + P)\frac{\gamma^2}{\alpha^2} \exp 2\nu\, \partial_A[\exp(2\Psi - 2\nu)(\omega - \Omega)^2] \\
&\quad +(\varrho + P)\frac{\gamma^2}{\alpha^2} \exp 2\Psi(\omega - \Omega)\partial_A \Omega .
\end{aligned} \tag{F.112}
$$

Since the three-velocity is given by

$$
V^2 = \exp(2\Psi - 2\nu)(\omega - \Omega)^2 \tag{F.113}
$$

with the Lorentz factor $\gamma = 1/\sqrt{1 - V^2}$ and $u^t = \gamma/\alpha$, we obtain

$$
\begin{aligned}
P_{,A} &= -(\varrho + P)\partial_A \ln\alpha \\
&\quad +\frac{1}{2}(\varrho + P)\gamma^2\, \partial_A[V^2 - 1] \\
&\quad +(\varrho + P)(u^t)^2 \exp 2\Psi(\omega - \Omega)\partial_A \Omega .
\end{aligned} \tag{F.114}
$$

Now, we use the identity

$$
(u^t)^2 \exp 2\Psi(\omega - \Omega) = -u^t\,[g_{01}u^t + g_{11}u^1] = -u^t u_\phi . \tag{F.115}
$$

With this, the equilibrium condition can be written as

$$
P_{,A} = (\varrho + P)\left[\partial_A \ln\left(\frac{\gamma}{\alpha}\right) - u^t u_\phi\, \partial_A \Omega\right]. \tag{F.116}
$$

Problems in Chapter 8

8.1 From the discussion in Sect. 4.4, we get the two expressions for bound orbits

$$
\tau = \frac{1}{L}\int \frac{d\phi}{u^2} = \frac{1}{L}\int \frac{d\phi}{d\chi}\,\frac{d\chi}{u^2} \tag{F.117}
$$

and

$$t = \frac{E}{L}\int \frac{d\phi}{d\chi}\,\frac{d\chi}{u^2(1-2Mu)}\,. \tag{F.118}$$

Using the explicit solution, we can bring this to the form

$$\tau = \frac{l^{3/2}}{\sqrt{M}}\sqrt{1-\mu(3+e^2)}\int_\chi^\pi \frac{d\chi}{(1+e\cos\chi)^2\sqrt{1-2\mu(3+e\cos\chi)}} \tag{F.119}$$

and

$$t = \frac{l^{3/2}}{\sqrt{M}}\sqrt{(2\mu-1)^2-4\mu^2e^2} \tag{F.120}$$
$$\times\int_\chi^\pi \frac{d\chi}{(1+e\cos\chi)^2\sqrt{1-2\mu(3+e\cos\chi)}\sqrt{1-2\mu(1+e\cos\chi)}}\,.$$

With the definition of the Newtonian period

$$P = \sqrt{\frac{4\pi^2 l^3}{(1-e^2)^3 GM}}\,, \tag{F.121}$$

the factors in front of the integrals can be written as

$$\frac{1}{2\pi}P\,(1-e^2)^{3/2}\sqrt{1-\mu(3+e^2)} \tag{F.122}$$

and

$$\frac{1}{2\pi}P\,(1-e^2)^{3/2}\sqrt{(2\mu-1)^2-4\mu^2e^2}\,. \tag{F.123}$$

In the case $e=0$, the orbit is a circle with radius r_c given by

$$r_c = l\,,\qquad \mu = M/r_c\,. \tag{F.124}$$

Angular momentum L and energy E of the orbit are related to the parameter l and e given by

$$L^2 = \frac{Mr_c}{1-3M/r_c}\,,\qquad \frac{E^2}{L^2} = \frac{(1-2M/r_c)^2}{Mr_c}\,. \tag{F.125}$$

The first equation gives a quadratic equation for the radius

$$r_c^2 - L^2 r_c/M + 3L^2 = 0 \tag{F.126}$$

with the solutions

$$r_c = \frac{L^2}{2M}\left[1\pm\sqrt{1-12M^2/L^2}\right]. \tag{F.127}$$

Therefore, no circular orbit is possible for $L/M < 2\sqrt{3}$, and for the minimum allowed value of L/M we find

$$r_c = 6M\,, \quad E^2 = 8/9\,, \quad L/M = 2\sqrt{3}\,. \tag{F.128}$$

The larger of the roots locates the minimum of the effective potential curve, while the smaller root locates the maximum in the effective potential. Therefore, the circular orbit with the larger radius will be stable, the orbit of the smaller radius unstable.

The periods for one complete revolution of these circular orbits, measured in proper time and coordinate time t, are

$$\tau_{\rm period} = P\sqrt{\frac{1-3\mu}{1-6\mu}} \tag{F.129}$$

and

$$t_{\rm period} = \frac{P}{\sqrt{1-6\mu}}\,. \tag{F.130}$$

Note that $t_{\rm period} \to \infty$ for $r_c \to 6M$.

8.2 In cosmology, dark energy is a hypothetical form of energy which permeates all of space and has strong negative pressure. According to the theory of relativity, the effect of such a negative pressure is qualitatively similar to a force acting in opposition to gravity at large scales. Invoking such an effect is currently the most popular method for explaining the observations of an accelerating Universe as well as accounting for a significant portion of the missing mass in the Universe.

Two proposed forms for dark energy are the cosmological constant Λ, a constant energy density filling space homogeneously, and quintessence, a dynamic field whose energy density can vary in time and space. Distinguishing between the alternatives requires high-precision measurements of the expansion of the Universe to understand how the speed of the expansion changes over time. The rate of expansion is parameterized by the cosmological equation of state. Measuring the equation of state of dark energy is one of the biggest efforts in observational cosmology today. Other ideas for dark energy have come from string theory, brane cosmology and the holographic principle.

8.3 The Riemann tensors for spherically symmetric spacetimes can be found in Sect. 4.2.1.

8.4 For this purpose, we define two new potentials

$$X = \chi + \omega = \frac{\sqrt{\Delta} + a\delta}{[r^2 + a^2 + a\sqrt{\Delta\delta}]\sqrt{\delta}} \tag{F.131}$$

$$Y = \chi - \omega = \frac{\sqrt{\Delta} - a\delta}{[r^2 + a^2 - a\sqrt{\Delta\delta}]\sqrt{\delta}}\,. \tag{F.132}$$

The equations

$$-\frac{\mu}{\delta}(\mu_2+\mu_3)_{,2}+\frac{r-M}{\varDelta}(\mu_2+\mu_3)_{,3}=\frac{2}{(X+Y)^2}(X_{,2}Y_{,3}+Y_{,2}X_{,3}) \tag{F.133}$$

and

$$\begin{aligned}&2(r-M)\frac{\partial}{\partial r}(\mu_2+\mu_3)\ +2\mu\frac{\partial}{\partial\mu}(\mu_2+\mu_3)\\ &=\frac{4}{(X+Y)^2}(\varDelta X_{,2}Y_{,2}-\delta X_{,3}Y_{,3})\ -3\frac{M^2-a^2}{\varDelta}-\frac{1}{\delta}\,.\end{aligned} \tag{F.134}$$

Making use of the solutions for X and Y with their derivatives, one obtains after some calculations the two equations

$$-\frac{\mu}{\delta}(\mu_2+\mu_3)_{,2}+\frac{r-M}{\varDelta}(\mu_2+\mu_3)_{,3}=\frac{\mu}{\varrho^2\varDelta\delta}\left[(r-M)(\varrho^2+2a^2\delta)-2r\varDelta\right] \tag{F.135}$$

and

$$(r-M)\frac{\partial}{\partial r}(\mu_2+\mu_3)+\mu\frac{\partial}{\partial\mu}(\mu_2+\mu_3)=2-\frac{(r-M)^2}{\varDelta}-2\frac{rM}{\varrho^2}\,. \tag{F.136}$$

These two equations are solved by means of the ansatz

$$\boxed{\exp(\mu_2+\mu_3)=\frac{\varrho^2}{\sqrt{\varDelta}}\,.} \tag{F.137}$$

The solutions for the two meridional metric functions are therefore

$$\boxed{\exp(2\mu_2)=\varrho^2/\varDelta\,,\quad \exp(2\mu_3)=\varrho^2\,.} \tag{F.138}$$

8.7 The Riemann tensors for the Kerr solution obey the following symmetries

$$R_{1213}=R_{0302}\,,\quad R_{1330}=R_{1202}\,,\quad R_{0202}=-R_{1313} \tag{F.139}$$

$$R_{0303}=-R_{1212}\,,\quad R_{2323}=-R_{0101}=R_{0202}+R_{0303}\,. \tag{F.140}$$

A straightforward calculation gives the following tetrad components

$$R_{0101}=-R_{2323}=-\frac{Mr}{\varrho^6}(r^2-3a^2\cos^2\theta) \tag{F.141}$$

$$\begin{aligned}R_{0202}&=-R_{1313}\\ &=\frac{Mr}{\Sigma^2\varrho^6}(r^2-3a^2\cos^2\theta)\,[2(r^2+a^2)^2+a^2\varDelta\sin^2\theta]\end{aligned} \tag{F.142}$$

$$\begin{aligned}R_{0303}&=-R_{1212}\\ &=-\frac{Mr}{\Sigma^2\varrho^6}(r^2-3a^2\cos^2\theta)\,[(r^2+a^2)^2+2a^2\varDelta\sin^2\theta]\end{aligned} \tag{F.143}$$

$$R_{0123} = \frac{aM\cos\theta}{\varrho^6}\,(3r^2 - a^2\cos^2\theta) \tag{F.144}$$

$$R_{0213} = \frac{aM\cos\theta}{\Sigma^2\varrho^6}\,(3r^2 - a^2\cos^2\theta)[2(r^2+a^2)^2 + a^2\Delta\sin^2\theta] \tag{F.145}$$

$$R_{0312} = \frac{aM\cos\theta}{\Sigma^2\varrho^6}\,(3r^2 - a^2\cos^2\theta)[(r^2+a^2)^2 + 2a^2\Delta\sin^2\theta] \tag{F.146}$$

$$\begin{aligned} R_{0302} &= R_{1213} \\ &= -\frac{aM\cos\theta}{\Sigma^2\varrho^6}\,(3r^2 - a^2\cos^2\theta)\,3a\sqrt{\Delta}(r^2+a^2)\sin\theta \end{aligned} \tag{F.147}$$

$$\begin{aligned} R_{0212} &= R_{1330} \\ &= -\frac{Mr\cos\theta}{\Sigma^2\varrho^6}\,(r^2 - 3a^2\cos^2\theta)\,3a\sqrt{\Delta}(r^2+a^2)\sin\theta\,. \end{aligned} \tag{F.148}$$

These components become singular only for $\theta = \pi/2$ and $r = 0$. This is the ring singularity for the Kerr solution.

8.8 Ray-tracers are suitably developed by applying object-oriented methods (C++ classes).

8.9 The equations of motion in the gravitational field of a gravastar can be solved by

$$\frac{dt}{ds} = E\left(\frac{1}{f} - \frac{f\widetilde{\omega}^2}{\varrho^2}\right) + L\,\frac{f\widetilde{\omega}}{\varrho^2} \tag{F.149}$$

$$\frac{d\phi}{ds} = -E\,\frac{f\widetilde{\omega}}{\varrho^2} + L\,\frac{f}{\varrho^2} \tag{F.150}$$

For motion in the equatorial plane we have

$$\left(\frac{dr}{ds}\right)^2\,\frac{\exp(2\gamma)}{f} = \frac{E^2}{f} - \frac{f}{\varrho^2}(L - \widetilde{\omega}E)^2 \equiv V(\varrho) \tag{F.151}$$

which defines an effective potential $V(\varrho)$. Circular orbits follow from the condition $V = 0 = dV/d\varrho$ which determine the energy and angular momentum

$$E = \frac{\sqrt{f}}{\sqrt{1 - f^2x^2/\varrho^2}} \tag{F.152}$$

$$L = E(p + \widetilde{\omega}) \tag{F.153}$$

with the definitions

$$p = \varrho^2\left(-l + \sqrt{l^2 + m - m^2\varrho^2}\right)/n \tag{F.154}$$

$$l = f\dot{\widetilde{\omega}} \tag{F.155}$$

$$m = \dot{f}/f \tag{F.156}$$

$$n = f - \varrho^2\dot{f} \tag{F.157}$$

$$\dot{f} \equiv df/d\varrho^2 \tag{F.158}$$

The innermost stable circular orbit (ISCO) follows from $d^2V/d\varrho^2 = 0$.

Problems in Chapter 9

9.1 The spin evolution of black holes is discussed in [299].

9.2 The evolution of a massive black hole pair is first given by the action of dynamical friction by a uniform background of light stars with isotropic velocity distribution. These black holes form a bounded pair (binary), and the binding energy of the binary increases over time through dynamical friction. If the dynamical friction remains effective until the separation of the two black holes in the binary becomes small enough for the gravitational radiation to shrink the separation further, the two black holes will merge. Such mergings of two massive black holes would emit strong gravitational wave which will be observable through space-based gravitational wave detectors such as LISA. For more details, see [290]

9.3 If the stellar population of the bulge contains black holes formed in the final core collapse of ordinary stars with $M \geq 30M_\odot$, then about 25,000 stellar mass black holes should have migrated by dynamical friction into the central parsec of the Milky Way, forming a black hole cluster around the central supermassive black hole. These black holes can be captured by the central black hole when they randomly reach a highly eccentric orbit due to relaxation, either by direct capture (when their Newtonian peribothron is less than four Schwarzschild radii), or after losing orbital energy through gravitational waves. The overall depletion timescale is $\sim$ 30 Gyr, so most of the 25,000 black holes remain in the central cluster today. The presence of this black hole cluster would have several observable consequences. First, the low-mass, old stellar population should have been expelled from the region occupied by the black hole cluster due to relaxation, implying a core in the profile of solar-mass red giants with a radius of $\sim$ 2 pc (i.e. $1'$). The observed central density cusp (which has a core radius of only a few arcseconds) should be composed primarily of young ($\leq$ 1 Gyr) stars. Second, flares from stars being captured by supermassive black holes in other galaxies should be rarer than usually expected because the older stars will have been expelled from the central regions by the black hole clusters of those galaxies. Third, the young ($\leq$ 2 Gyr) stars found at distances $\sim$ 3–10 pc from the Galactic center should be preferentially on highly eccentric orbits. Fourth, if future high-resolution K-band images reveal sources microlensed by the Milky Way's central black hole, then the cluster black holes could give rise to secondary ("planet-like") perturbations on the main event. For more details, see [298].

During five years of Chandra observations, Muno et al. [306] have identified seven X-ray transients located within 23 pc of Sgr A*. These sources each vary in luminosity by more than a factor of 10 and have peak X-ray luminosities greater than 5×10^{33} ergs s^{-1}, which strongly suggests that they are accreting black holes or neutron stars. The peak luminosities of the transients are intermediate between those typically considered outburst and quiescence for X-ray binaries. Remarkably, four of these transients lie within only 1 pc of Sgr A*. This implies that, compared to the numbers of similar systems located between 1 and 23 pc, transients are overabundant by a factor of > 20 per unit stellar mass within 1 pc of Sgr A*. It is likely that the excess transient X-ray sources are low-mass X-ray binaries that were produced, as in the cores of globular clusters, by three-body interactions between binary star systems and either black holes or neutron stars that have been concentrated in the central parsec through dynamical friction. Alternatively, they could be high-mass X-ray binaries that formed among the young stars that are present in the central parsec.

9.6 The light cylinder surfaces are given by the solution of the equation

$$(\Omega_F - \omega)^2 \varpi_L^2 = c^2 \alpha^2 \tag{F.159}$$

for given $\Omega_F = b\Omega_H$ with $b \leq 1$. With the expressions for $\alpha(r,\theta)$, $\omega(r,\theta)$ and $\widetilde{\omega}(r,\theta)$ this can be transformed to an implicit equation for $r_L = r_L(\theta)$.

9.7 The general expression for the redshifted energy flux $\mathbf{S}_E$ and the angular momentum flux about the axis of rotation $\mathbf{S}_L$ are given by the energy–momentum tensor

$$\begin{aligned}
\mathbf{S}_E &= \frac{1}{4\pi}\left[\alpha(\mathbf{E}\times\mathbf{B}) - \omega(\mathbf{E}\cdot\mathbf{m})\mathbf{E} - \omega(\mathbf{B}\cdot\mathbf{m})\mathbf{B} + \frac{1}{2}\omega(\mathbf{E}^2+\mathbf{B}^2)\mathbf{m}\right],\\
\mathbf{S}_L &= \frac{1}{4\pi}\left[-(\mathbf{E}\cdot\mathbf{m})\mathbf{E} - (\mathbf{B}\cdot\mathbf{m})\mathbf{B} + \frac{1}{2}(\mathbf{E}^2+\mathbf{B}^2)\mathbf{m}\right].
\end{aligned} \tag{F.160}$$

Since the toroidal component of the fluxes are irrelevant, we only need to consider the poloidal components

$$\begin{aligned}
\mathbf{S}_L^p &= -\frac{\varpi}{4\pi}|\mathbf{B}_T|\mathbf{B}_p = \frac{I}{2\pi\alpha}\mathbf{B}_p, \\
\mathbf{S}_E^p &= \frac{\alpha}{4\pi}\mathbf{E}_p\times\mathbf{B}_T + \omega\mathbf{S}_L^p = \frac{I}{2\pi}\left(\frac{\omega}{\alpha}\mathbf{B}_p - \frac{1}{\varpi^2}\mathbf{E}_p\times\mathbf{m}\right).
\end{aligned} \tag{F.161}$$

Thus, at the neutron star surface where $\alpha = \alpha(r_s) \neq 0$,

$$\begin{aligned}
-\mathbf{S}_L\cdot\mathbf{n} \to \frac{dJ}{d\Sigma_s dt} &= -\frac{I}{2\pi\alpha}B_\perp = -\frac{I}{4\pi^2\alpha\varpi}(\nabla\Psi\times e_\phi)\cdot\mathbf{n} \\
-\mathbf{S}_E\cdot\mathbf{n} \to \frac{dM}{d\Sigma_s dt} &= -\frac{I}{2\pi}\left[\frac{\omega}{\alpha}B_\perp - \frac{1}{\varpi}(\mathbf{E}_P\times e_\phi)\cdot\mathbf{n}\right] \\
&= -\frac{I}{2\pi\alpha}\Omega_F B_\perp = \Omega_F\frac{dJ}{d\Sigma_s dt}
\end{aligned} \tag{F.162}$$

where $\mathbf{n}$ denotes the unit vector outer normal to the neutron star surface. Now note that when the spin J of the rotating neutron star and the magnetic field $\mathbf{B}$ are parallel, $B_\perp > 0$, $I > 0$ whereas when J and $\mathbf{B}$ are antiparallel, $B_\perp < 0$, $I < 0$ due to their definitions (16) and (19). Namely, the magnetic flux (and B) is defined to be positive/negative when it directs *upward/downward* while the poloidal current is defined to be positive/negative when it directs *downward/upward* as we noted earlier. Thus one always has $IB_\perp > 0$, and hence from eq.(41) above, we always have

$$-\mathbf{S}_L \cdot \mathbf{n} = -\frac{I}{2\pi\alpha} B_\perp < 0, \qquad \text{(F.163)}$$
$$-\mathbf{S}_E \cdot \mathbf{n} = -\frac{I}{2\pi\alpha} \Omega_F B_\perp < 0.$$

Since the angular momentum and the energy flux going *into* the neutron star surface are all *negative*, this means that the rotating neutron star (i.e. the pulsar) experiences magnetic braking torque, namely spins-down and as a result, always loses part of its rotational energy (at the surface).

9.8 (i) Substituting $\mathbf{E} = \mathbf{E}_p = -(\Omega_F - \omega)/(2\pi\alpha)\nabla\Psi$ into the Maxwell equation $\nabla \times (\alpha \mathbf{E}) = (\mathbf{B} \cdot \nabla\omega)\mathbf{m}$, one can readily realize that

$$(\mathbf{B} \cdot \nabla)\Omega_F = 0 \qquad \text{(F.164)}$$

indicating that Ω_F is constant on magnetic surfaces, i.e. $\Omega_F = \Omega_F(\Psi)$, which represents the generalized Ferraro's isorotation law.
(ii) Combining

- the *freezing-in condition*: $\mathbf{E}_T + \frac{1}{c}(\mathbf{v} \times \mathbf{B})_T = 0$,
- the *particle conservation*: $\nabla \cdot (\alpha\gamma n \mathbf{v}) = 0$,
- the *Maxwell equation*: $\nabla \cdot \mathbf{B} = 0$

one ends up with $\mathbf{u}_p = \gamma \mathbf{v}_p = \eta \left(\mathbf{B}_p/\alpha n\right)$ and hence from

$$\mathbf{u}_T = \gamma \mathbf{v}_T = \eta \left(\frac{1}{\alpha n}\mathbf{B}_T\right) + \gamma \left[\frac{\Omega_F - \omega}{\alpha}\right] \mathbf{e}_\phi \qquad \text{(F.165)}$$

it follows that

$$\mathbf{u} = \gamma \mathbf{v} = \frac{\eta}{\alpha n}\mathbf{B} + \gamma \left[\frac{\Omega_F - \omega}{\alpha}\right] \mathbf{e}_\phi\,, \qquad \text{(F.166)}$$

where the quantity η represents the *particle flow along the magnetic flux* or the *particle-to-magnetic field flux ratio*.
Then plugging $\mathbf{u}$ back into the particle number conservation yields

$$0 = \nabla \cdot (\alpha n \mathbf{u}) = \nabla \cdot (\eta \mathbf{B})$$
$$= \eta(\nabla \cdot \mathbf{B}) + (\mathbf{B} \cdot \nabla)\eta = (\mathbf{B} \cdot \nabla)\eta\,, \qquad \text{(F.167)}$$

which implies that η must be constant on magnetic surfaces as well, i.e. $\eta = \eta(\Psi)$.
(iii)–(iv)
Let ξ^μ be a Killing field associated with an isometry of the background spacetime metric, then $\nabla_\nu(T^{\mu\nu}\xi_\mu) = 0$. Since stationary and axisymmetric spacetimes have

two Killing fields $k^\mu = (\partial/\partial t)^\mu$ and $m^\mu = (\partial/\partial\phi)^\mu$, respectively, the energy flux and angular momentum flux vector

$$P_E^\mu = -T^{\mu\nu}k_\nu\,, \quad P_L^\mu = T^{\mu\nu}m_\nu \tag{F.168}$$

are covariantly conserved. Thus using,

$$T_{\rm p}^{\mu\nu} + T_{\rm em}^{\mu\nu} = n\mu\, u^\mu u^\nu + Pg^{\mu\nu} + \frac{1}{4\pi}\left\{F_\alpha^\mu F^{\nu\alpha} - \frac{1}{4}g^{\mu\nu}F_{\alpha\beta}F^{\alpha\beta}\right\} \tag{F.169}$$

$$u^\mu = (\gamma, \gamma\mathbf{v}) = \left(\gamma, \frac{\eta}{n\alpha}\mathbf{B} + \gamma\left[\frac{\Omega_F - \omega}{\alpha}\right]\mathbf{e}_\phi\right) \tag{F.170}$$

and

$$P_E^A = -T_t^A = nu^A E\,, \quad (A = r, \theta) \tag{F.171}$$

$$P_L^A = T_\phi^A = nu^A L\,, \tag{F.172}$$

one gets two more integrals of motion [72, 97, 98]

$$E = E(\Psi) = \frac{\Omega_F I}{2\pi} + \mu\eta\,(\alpha\gamma + \omega\mathbf{u}_\phi), \tag{F.173}$$

$$L = L(\Psi) = \frac{I}{2\pi} + \mu\eta\, u_\phi$$

together with the total loss of energy and angular momentum given by

$$W_{\rm tot} = \int_0^{\Psi_{max}} E(\Psi)\, d\Psi\,, \tag{F.174}$$

$$K_{\rm tot} = \int_0^{\Psi_{max}} L(\Psi)\, d\Psi\,. \tag{F.175}$$

(v) The entropy conservation $\nabla_\alpha(nsu^\alpha) = 0$ reduces, for stationary axisymmetric case, to

$$\nabla\cdot(\alpha ns\mathbf{u}) = 0\,. \tag{F.176}$$

Thus using

$$\mathbf{u} = \frac{\eta}{\alpha n}\mathbf{B} + \gamma\left[\frac{\Omega_F - \omega}{\alpha}\right]\mathbf{e}_\phi\,, \tag{F.177}$$

one gets

$$\begin{aligned} 0 &= \nabla\cdot(\alpha ns\mathbf{u}) = \nabla\cdot(\eta s\mathbf{B}) \\ &= s\nabla\cdot(\eta\mathbf{B}) + \eta\,(\mathbf{B}\cdot\nabla)s = \eta\,\mathbf{B}\cdot\nabla)s \end{aligned} \tag{F.178}$$

which implies that the entropy per particle s must be constant on magnetic surfaces as well, $s = s(\Psi)$. To summarize, for the stationary axisymmetric case, there are five-integrals of motion (constants on magnetic surfaces)

$$\{\Omega_F(\Psi),\ \eta(\Psi),\ s(\Psi),\ E(\Psi),\ L(\Psi)\}\,. \tag{F.179}$$

We shall now show that once the poloidal magnetic field B_p and the five-integrals of motion given above are known, the toroidal magnetic field B_ϕ and all the other plasma parameters characterizing a plasma flow can be determined. To do so, we solve the two conservation laws and the toroidal component

$$u_\phi = \frac{\eta}{\alpha n}B_\phi + \gamma\left[\frac{\Omega_F-\omega}{\alpha}\right]\varpi = -\frac{2\eta I}{\alpha^2 n\varpi} + \gamma\left[\frac{\Omega_F-\omega}{\alpha}\right]\varpi \tag{F.180}$$

for the Lorentz factor γ, the angular momentum u_ϕ and the poloidal current flux function I to get [72,98]

$$\gamma(\Psi,r) = \frac{E}{\alpha\eta\mu}\frac{\alpha^2(1-\Omega_F L/E) - M^2(1-\omega L/E)}{\alpha^2-(\Omega_F-\omega)^2\varpi^2-M^2} \tag{F.181}$$

$$u_\phi(\Psi,r) = \frac{E}{\varpi\eta\mu}\frac{(1-\Omega_F L/E)(\Omega_F-\omega)\varpi^2 - M^2L/E}{\alpha^2-(\Omega_F-\omega)^2\varpi^2-M^2} \tag{F.182}$$

$$I(\Psi,r) = 2\pi\eta\,\frac{\alpha^2L-(\Omega_F-\omega)\varpi^2(E-\omega L)}{\alpha^2-(\Omega_F-\omega)^2\varpi^2-M^2}\,. \tag{F.183}$$

The quantity

$$M^2 \equiv \frac{4\pi\mu\eta^2}{n} = \frac{\alpha^2u_p^2}{u_A^2} \tag{F.184}$$

is the square of the **Mach number** of the poloidal velocity $u_p = \eta B_p/n\alpha$ with respect to the Alfvén velocity $u_A = B_p/\sqrt{4\pi n\mu}$. The above expressions have critical points, where the denominator vanishes, i.e. at positions along the flow, where

$$\alpha^2(r_A) - (\Omega_F-\omega(r_A))^2\varpi_A^2 = M_A^2\,. \tag{F.185}$$

These are the Alfvén points along the flow. For given rotation, this equation has two solutions, an inner Alfvén point and an outer one. In order to get regular expressions at the Alfvén points, the nominators also have to vanish. This fixes the total angular momentum L

$$M_A^2L/E = \varpi_A^2(\Omega_F-\omega(r_A))(1-\Omega_F L/E)\,. \tag{F.186}$$

In order to determine this Mach number, consider

$$\gamma^2-\mathbf{u}^2 = \gamma^2-\gamma^2\mathbf{v}^2 = \gamma^2(1-\mathbf{v}^2) = 1 \tag{F.187}$$

and into this relation, we substitute the above expressions to get

$$\frac{F_K}{\varpi^2D^2} = \frac{1}{64\pi^4}\frac{M^4(\nabla\Psi)^2}{\varpi^2} + \alpha^2\eta^2\mu^2\,, \tag{F.188}$$

where

$$D = \alpha^2 - (\Omega_F - \omega)^2\varpi^2 - M^2 \tag{F.189}$$

$$\begin{aligned} F_K &= \alpha^2\varpi^2(E - \Omega_F L)^2[\alpha^2 - (\Omega_F - \omega)^2\varpi^2 - 2M^2] \\ &\quad + M^4[\varpi^2(E - \omega L)^2 - \alpha^2 L^2]\,. \end{aligned} \tag{F.190}$$

D is the generalization of the light cylinder function defined for force-free magnetospheres. This is the Bernoulli equation. We bring the wind equation into dimensionless form by scaling radii with the asymptotic light cylinder, $R_L = c/\Omega_F$, $x = \varpi/R_L$,

$$\alpha^2 x^2 \, \frac{F_K(x; M^2, \epsilon)}{D^2(x; M^2)} \left(\frac{E}{\mu}\right)^2 = \alpha^2 x^4 + \frac{B_p^2 x^4}{16\pi^2\mu^2\eta^2}\, M^4\,. \tag{F.191}$$

The parameter $\epsilon = \Omega_F L/E$ is a measure for the inertia of the plasma, with $\epsilon = 1$ in the force–free limit. The last term on the right-hand side can be scaled to the foot point of the magnetic flux surface

$$\Phi_\Psi^{-1}(x) = \frac{B_p\varpi^2}{B_{p,*}\varpi_*^2}\,. \tag{F.192}$$

One of the essential parameters which determine the plasma flow along the flux tube is then given by *Michel's magnetization parameter* σ_* defined as follows [97, 98]

$$\sigma_*(\Psi) = \frac{(B_{p,*}\varpi_*^2)c}{4\pi\mu\eta(\Psi)R_L^2(\Psi)}\,. \tag{F.193}$$

The asymptotic Lorentz factor achieved in the plasma flow along a given flux surface is then essentially determined by the magnetization [98]. Highly relativistic flows are achieved for $\sigma_* \gg 1$.

To summarize, once B_p, $\Omega_F(\Psi)$, $\eta(\Psi)$, $s(\Psi)$, $E(\Psi)$, $L(\Psi)$ are known, the characteristics of the plasma flow, I, γ, u_ϕ, u_p, M^2 can be determined by the above wind equation (F.188). For more details, see [98, 157, 158].

Problems in Chapter 10

10.1 MRI Dispersion Relation

The complete dispersion relation for MRI can be found in [49]. We consider perturbations of the form $\exp(i[\mathbf{k}\cdot\mathbf{x} - \omega t])$. The perturbed MHD equations lead to the following dispersion relation

$$\begin{aligned} &\left[\omega^2 - (\mathbf{k}\cdot\mathbf{V}_A)^2\right]\left[\omega^4 - k^2(c_S^2 + V_A^2)\omega^2 + (\mathbf{k}\cdot\mathbf{V}_A)^2 k^2 c_S^2\right] \\ &\quad - \left[\kappa^2\omega^4 - \omega^2(\kappa^2 k^2(c_S^2 - V_{A\phi}^2) + \left(\mathbf{k}\cdot\mathbf{V}_A)^2\,\frac{d\Omega^2}{d\ln R}\right)\right] \\ &\quad - k^2 c_S^2(\mathbf{k}\cdot\mathbf{V}_A)^2\,\frac{d\Omega^2}{d\ln R} = 0\,. \end{aligned} \tag{F.194}$$

κ is the epicycle frequency defined as

$$\kappa^2 = \frac{d\Omega^2}{d\ln R} + 4\Omega^2 . \tag{F.195}$$

This is a third-order equation in ω^2 which has three solution branches. In the non-rotating case, these solutions are the normal MHD waves, the Alfvén waves and the slow and fast magnetosonic waves. For Keplerian rotation, the slow wave becomes unstable for $\Omega^2 = (\mathbf{k}\cdot\mathbf{V}_A)^2/3$. For this, make a plot of ω^2 vs. Ω^2.

In the Boussinesque approximation, $c_S^2 \to \infty$, the dispersion relation is simplified to a biquadratic equation

$$\omega^4 - \omega^2\left[\kappa^2 + 2(\mathbf{k}\cdot\mathbf{V}_A)^2\right] + (\mathbf{k}\cdot\mathbf{V}_A)^2\left((\mathbf{k}\cdot\mathbf{V}_A)^2 + \frac{d\Omega^2}{d\ln R}\right) = 0 . \tag{F.196}$$

ω^2 will be negative, if

$$(\mathbf{k}\cdot\mathbf{V}_A)^2 < -\frac{d\Omega^2}{d\ln R} . \tag{F.197}$$

Make a plot of the growth rate in units of Keplerian angular velocity as a function of the wavenumber, $\mathbf{k}\cdot\mathbf{V}_A$.

10.2 Ring Diffusion

The calculation is straightforward.

10.3 Relativistic Keplerian Disks

References for a modern treatment of relativistic Keplerian disks can be found in [253].

10.4 Radiative Transfer around Rotating Black Holes

(i) The metric tensor of the Kerr geometry in cylindrical coordinates is given by

$$g_{tt} = -1 + \frac{2M}{R} - \frac{Mz^2}{R^3}\left(1 + \frac{2a^2}{R^2}\right) \tag{F.198}$$

$$g_{t\phi} = -\frac{2aM}{r} + \frac{aMz^2}{r^3}\left(3 + \frac{2a^2}{r^2}\right) \tag{F.199}$$

$$g_{\phi\phi} = r^2 + a^2 + \frac{2Ma^2}{r} - \frac{a^2z^2}{r^2}\left(1 + \frac{5M}{r} + \frac{2Ma^2}{r^3}\right) \tag{F.200}$$

$$g_{RR} = \frac{1}{\mathcal{A}} - \frac{z^2}{r^2\mathcal{A}^2}\left[\frac{M}{r}\left(3 - \frac{4M}{r}\right) - \frac{a^2}{r^2}\left(3 - \frac{6M}{r} + \frac{2a^2}{r^2}\right)\right] \tag{F.201}$$

$$g_{Rz} = \frac{z}{R\mathcal{A}}\left(\frac{2M}{R} - \frac{a^2}{R^2}\right) \tag{F.202}$$

$$g_{zz} = 1 + \frac{z^2}{R^2\mathcal{A}}\left(\frac{2M}{R} - \frac{2Ma^2}{R^3} + \frac{a^4}{R^4}\right) . \tag{F.203}$$

(ii) The dominant part of the radial Euler equation leads to

$$(U^t)^2\,\Gamma^2_{tt} + 2U^tU^\phi\,\Gamma^2_{t\phi} + (U^R)^2\,\Gamma^2_{\phi\phi} = 0\,. \tag{F.204}$$

Together with the normalization condition $U^\mu U_\mu = -1$, this yields the desired results for U^t and U^ϕ.
(iii) The transformation matrices L are explicitly given by

$$L = \begin{pmatrix} -U_t & -U_\phi & 0 & 0 \\ L^1{}_t & L^\phi{}_\phi & 0 & 0 \\ 0 & 0 & 1/\sqrt{\mathcal{A}} & 0 \\ 0 & 0 & 0 & 1 \end{pmatrix} \tag{F.205}$$

and the inverse relation

$$\bar{L} = \begin{pmatrix} U^t & \bar{L}^t{}_\phi & 0 & 0 \\ U^\phi & \bar{L}^\phi{}_\phi & 0 & 0 \\ 0 & 0 & \sqrt{\mathcal{A}} & 0 \\ 0 & 0 & 0 & 1 \end{pmatrix}, \tag{F.206}$$

where

$$\begin{aligned} L^\phi{}_t &= -\sqrt{\tfrac{\mathcal{A}}{\mathcal{B}}}\sqrt{\tfrac{M}{R}} & L^\phi{}_\phi &= R\sqrt{\tfrac{\mathcal{A}}{\mathcal{B}}}\left(1+\tfrac{a}{R}\sqrt{\tfrac{M}{R}}\right) \\ \bar{L}^t{}_\phi &= \tfrac{1}{\sqrt{\mathcal{A}\mathcal{B}}}\left(1+\tfrac{a^2}{R^2}-\tfrac{2a}{R}\sqrt{\tfrac{M}{R}}\right), & \bar{L}^\phi{}_\phi &= \tfrac{1}{R\sqrt{\mathcal{A}\mathcal{B}}}\left(1-\tfrac{2M}{R}+\tfrac{a}{R}\sqrt{\tfrac{M}{R}}\right) \end{aligned} \tag{F.207}$$

(iv) The vector m^i is given by

$$m^i = \nu^2\left[\omega^i{}_{tt} + (\omega^i{}_{tk} + \omega^i{}_{kt})n^k + \omega^i{}_{jk}n^jn^k\right] \tag{F.208}$$

with the expression for transfer equation

$$\begin{aligned} m^i\,\frac{\partial f}{\partial \bar{p}^i} &= m^t\,\frac{\partial f}{\partial \nu} + \left[m^t\sqrt{1-\mu^2} - m^1\sin\chi - m^2\cos\chi\right]\frac{\sqrt{1-\mu^2}}{\mu\nu}\,\frac{\partial f}{\partial \mu} \\ &\quad + \frac{-m^1\cos\chi + m^2\sin\chi}{\nu\sqrt{1-\mu^2}}\,\frac{\partial f}{\partial \chi}\,. \end{aligned} \tag{F.209}$$

(v) The lowest order in the transfer equation has the expression

$$\begin{aligned} &\nu\sqrt{\mathcal{A}}\sqrt{1-\mu^2}\cos\chi\,\frac{\partial f}{\partial R} + \nu\mu\,\frac{\partial f}{\partial z} + \frac{\nu}{r\sqrt{\mathcal{B}}}\left[\sqrt{\frac{M}{r}} + \frac{\mathcal{E}}{\sqrt{\mathcal{A}}}\sqrt{1-\mu^2}\sin\chi\right]\frac{\partial f}{\partial \phi} \\ &+\frac{3\mathcal{A}}{2\mathcal{B}}\sqrt{\frac{M}{r^3}}\,(1-\mu^2)\sin\chi\cos\chi\,\nu^2\frac{\partial f}{\partial \nu} \\ &-\left[\frac{3\mathcal{A}}{2\mathcal{B}}\sqrt{\frac{M}{r^3}}\,(1-\mu^2)\sin\chi + \frac{\mathcal{A}-1}{r\sqrt{\mathcal{A}}}\right]\nu\mu\sqrt{1-\mu^2}\cos\chi\,\frac{\partial f}{\partial \mu} \\ &+\left[\frac{3\mathcal{A}}{2\mathcal{B}}\sqrt{\frac{M}{r^3}}\,\cos^2\chi - \frac{\sin\chi}{r\sqrt{\mathcal{A}}\sqrt{1-\mu^2}}\left(1-\frac{M}{r}-\mu^2\mathcal{F}\right) - 2\sqrt{\frac{M}{r^3}}\right]\nu\frac{\partial f}{\partial \chi} = \bar{Q}\,, \end{aligned} \tag{F.210}$$

where

$$\mathcal{E} = 1 - \frac{2M}{r} + \frac{a}{r}\sqrt{\frac{M}{r}}\,, \quad \mathcal{F} = 1 + \frac{M}{r} - \frac{a^2}{r^2}\,. \tag{F.211}$$

For an axisymmetric radiation field, we have

$$\frac{\partial f}{\partial \phi} = 0\,, \quad \int_0^{2\pi} \sin\chi\, f\, d\chi = 0\,. \tag{F.212}$$

After integration of the transfer equation over χ, we obtain the simple equation

$$\mu \nu^3 \frac{\partial f}{\partial z} = \mu \frac{\partial \bar{I}_\nu}{\partial z} = \nu^2 \bar{Q}\,, \tag{F.213}$$

where $\bar{I}_\nu = \bar{I}_\nu(R, z, \mu)$ is the specific intensity as measured in the local plasma frame LRFM.
(viii) The relevant interactions between plasma and photons near the horizon of a black hole are Bremsstrahlung and Compton scattering, which gives the scattering operator in the plasma frame

$$\begin{aligned} \nu^2 \bar{Q} &= \kappa_{ff}\varrho_0[B_\nu - \bar{I}_\nu] \\ &+ \kappa_T \varrho_0 \frac{\nu}{m_e} \frac{\partial}{\partial \nu}\left[\nu T_e B_\nu \frac{\partial}{\partial \nu}\left(\frac{\bar{I}_\nu}{B_\nu}\right) + \frac{\bar{I}_\nu}{2\nu^2}(\bar{I}_\nu - B_\nu)\right]. \end{aligned} \tag{F.214}$$

κ_{ff} is the Bremsstrahlung opacity and $\kappa_T = 0.4\ \text{cm}^2/\text{g}$ the Thomson opacity. The differential operator describes Compton scattering in the Fokker–Planck approximation [13].

10.6 The solution of this problem is discussed in [36].

Glossary

Accretion disk: Flat disk of matter spiraling down onto the surface of a star or into a black hole. Often, the matter originated on the surface of a companion star in a binary system. Viscosity within the disk generates heat and saps orbital momentum, causing material in the disk to spiral inward, until it impacts in an accretion shock on the central body if the body is a star, or slips toward the event horizon if the central body is a black hole. The most spectacular accretion disks found in nature are those of active galactic nuclei and quasars, which are believed to be supermassive black holes at the center of galaxies. The accretion disk of a black hole is hot enough to emit X-rays just outside of the event horizon. In the modern view, an accretion disk is a quasistationary solution of radiative magnetohydrodynamics, provided the initial configuration has sufficient gas, angular momentum and magnetic fields.

Active galactic nucleus (AGN): The central region of a galaxy that shows unusual energetic activity.

Angular resolution: The ability of a telescope to distinguish two adjacent objects on the sky, or to study the fine details on the surface of some object; often synonymous with "clarity" or "sharpness."

Arcsecond (arcsec): A unit of angular measure of which there are 60 in 1 arcminute (or therefore 3600 in 1 arc degree).

Binary star system: A system which consists of two stars orbiting about their common center-of-mass, held together by their mutual gravitational attraction. Most stars are found in binary star systems.

Black hole: A dense, compact object whose gravitational pull is so strong that, within a certain distance of it, nothing can escape, not even light. Black holes are thought to result from the collapse of certain very massive stars at the ends of their evolution. Current theories predict that all the matter in a black hole is piled up in a single point (or ring, when rotating) at the center, but we do not understand how this central singularity works. To properly understand the black hole center requires a fusion of the theory of gravity with the theory that describes the behavior of matter on the smallest scales, called quantum mechanics. This unifying theory has already been given a name, quantum gravity, but how it works is still unknown.

Blazars: A class of active galaxies that exhibit rapidly variable emission from the radio through gamma-ray band. The radiation is predominantly from jets moving near the speed of light. Blazars are thought to be radio galaxies with their jets oriented toward Earth.

Cataclysmic system: Cataclysmic variables are a class of binary stars containing a white dwarf and a companion star. The companion star is usually a red dwarf, although in some cases it is another white dwarf or a slightly evolved star (subgiant). Several hundreds of cataclysmic variables are known. The stars are so close to each other that gravity of the white dwarf distorts the secondary, and the white dwarf accretes matter from the companion.

Cauchy horizon: A Cauchy horizon is a light-like boundary of the domain of validity of a Cauchy problem (a boundary value problem of the theory of partial differential equations). One side of the horizon contains closed space-like geodesics and the other side contains closed time-like geodesics. The simplest example is the internal horizon of a Reissner–Nordstr"om black hole. It also appears in the Kerr black hole.

CFL condition: The Courant–Friedrichs–Levy condition, usually abbreviated to the CFL condition, says that in any time-marching computer simulation the time-step must be less than the time for some significant action to occur, and preferably considerably less. For example, if we have a computer simulation of a satellite orbiting a planet, the discrete time interval which we use must obviously be less than the orbital period on common sense grounds. For the sake of stability, it must be less than one quarter of the orbital period, and, in practice, one will take a step of about one fortieth of the orbital period. The CFL condition was originally formulated in the context of compressible fluid flows. If we divide the flow volume up into cells, then we need a time-step less than the time taken for a sound wave to cross one of the cells.

Chandrasekhar mass: The upper limit to the mass of a white dwarf, equals $(5.87/\mu^2)M_\odot$, where μ is the mean number of nucleons per electron. For Fe we have $\mu = 56/26$.

Chandra X-ray Observatory (CXO): Formerly called AXAF, Chandra was launched July 23, 1999, and is with XMM–Newton the largest and most sophisticated X-ray observatory to date. NASA's Chandra X-ray Observatory was named in honor of the late Indian–American Nobel laureate, Subrahmanyan Chandrasekhar. The Chandra spacecraft carries a high-resolution mirror, two imaging detectors, and two sets of transmission gratings. Important Chandra features are: an order of magnitude improvement in spatial resolution, and good sensitivity from 0.1 to 10 keV.

Color superconductivity: Color superconductivity is a phenomenon predicted to occur in quark matter if the baryon density is sufficiently high (well above nuclear density) and the temperature is not too high (i.e. below 10^{12} kelvin). Color-superconducting phases are to be contrasted with the normal phase of quark matter, which is just a weakly interacting Fermi liquid of quarks. Unlike an electrical superconductor, color-superconducting quark matter comes in many varieties, each of which is a separate phase of matter. In forming the Cooper pairs, there is a 9×9 color–flavor matrix of possible pairing patterns. The differences between these patterns are very physically significant: different patterns break different symmetries of the underlying theory, leading to different excitation spectra and different transport properties. In theoretical terms, a color-superconducting phase is a state in which the quarks near the Fermi surface become correlated in Cooper pairs, which condense. In phenomenological terms, a color-superconducting phase breaks some of the symmetries of the underlying theory, and has a very different spectrum of excitations and very different transport properties from the normal phase.

Compton Gamma Ray Observatory (CGRO): The Compton Gamma Ray Observatory was the second of NASA's Great Observatories. CGRO, at 17 tonnes, was the heaviest astrophysical payload ever flown at the time of its launch on April 5, 1991 aboard the space shuttle Atlantis. Compton was safely deorbited and re-entered the Earth's atmosphere on June 4, 2000. CGRO had four instruments that covered six decades of the electromagnetic spectrum, from 30 keV to 30 GeV. In order of increasing spectral energy coverage, these instruments were the Burst And Transient Source Experiment (BATSE), the Oriented Scintillation Spectrometer Experiment (OSSE), the Imaging Compton Telescope (COMPTEL), and the Energetic Gamma Ray Experiment Telescope (EGRET).

Compton scattering: The scattering, or collision, of a photon with an electron.

Comptonization: The X-ray power-law component in galactic black hole candidates and AGN is attributed to black-body photons being up-scattered by electrons (that is, the photons gain energy from the electrons via the inverse Compton process), as they traverse a hot plasma with a Maxwellian electron temperature 10–100 keV. Comptonization is saturated, where the photons are in thermal equilibrium with the electrons. Then a cutoff in the spectrum occurs at $\sim 3k_BT_e$, where T_e is the temperature of the hot electrons.

Continuous spectrum: Spectrum in which the radiation is distributed over all frequencies, not just a few specific frequency ranges. A prime example is the black-body radiation emitted by a hot, dense body.

Core: The central region of a planet, star, neutron star, or a galaxy.

Corona: The outermost atmosphere of a star (including the Sun) or of an accretion disk, millions of kilometers in extent, and consisting of highly rarefied gas heated to temperatures of millions of degrees.

Cosmic radiation: Very energetic radiation from outer space which hits the Earth's atmosphere and can still be detected near the surface after various transformations. It consists mostly of highly energetic particles (protons, helium cores, heavy atomic nuclei and leptons) and X-rays and gamma radiation. Only a small fraction of cosmic radiation is produced in the Sun, the rest has its origin in partly still unknown sources inside and outside of the Milky Way.

Cosmological constant: A modification of the equations of general relativity that represents a possible repulsive force in the Universe. The cosmological constant could be due to the energy density of the vacuum.

Cygnus A: This galaxy is the brightest radio source (as indicated by the letter A) in the constellation Cygnus (Swan). The supermassive black hole in its center is a billion times heavier than the Sun. Although the galaxy is relatively distant (300 times further away than the Andromeda Galaxy), it appears to us as the second brightest radio source in the entire sky. This is because the black hole generates tremendous energy as it consumes large amounts of material. Nearby electrons are accelerated in this process, emitting strong radio waves as they spiral outward in magnetic fields.

Cygnus X-1: This is the brightest X-ray source (indicated as X-1) in the constellation Cygnus (Swan). It consists of a bright blue star and a black hole that orbit around each other. The black hole pulls gas off the surface of this star. This gas heats up and shines in X-rays as it falls towards the black hole.

Density: A measure of the compactness of the matter within an object, computed by dividing the mass by the volume of the object.

Eccentricity: A measure of the flatness of an ellipse, equal to the distance between the two foci divided by the length of the major axis.

Eddington luminosity: The limit beyond which the radiation force on matter is greater than the gravitational force. This limit is independent on the radius of the emitting surface. The corresponding luminosity is $L_{\mathrm{Ed}} = 4\pi G M m_p c/\sigma_T$ is proportional to the mass M of the object.

Electron-volt (eV): The energy gained by an electron accelerated by a potential of 1 volt. One electron-volt corresponds to a frequency $\nu = 2.418 \times 10^{14}$ Hz in electromagnetic radiation, or a temperature of 11.606 K.

Ergosphere: The region of a rotating Kerr black hole between the static surface and the event horizon. In this region, everything is forced to rotate in the same sense as the black hole, although you can still escape.

Escape velocity: The speed necessary for an object to escape the gravitational pull of an object. Anything that moves away from the object with more than the escape velocity will never return.

Event horizon: Imaginary spherical surface surrounding a black hole, with radius equal to the Schwarzschild radius, within which no event can be seen heard, or known about by an outside observer.

Excited state: The state of an atom when one of its electrons is in a higher energy orbital than the ground state. Atoms can become excited by absorbing a photon of a specific energy, or by colliding with a nearby atom.

Fluorescence: The absorption of a photon of one energy, or wavelength, and re-emission of one or more photons at lower energies, or longer wavelengths.

Gamma-ray: Region of the electromagnetic spectrum, beyond X-rays, corresponding to radiation of very high frequency and very short wavelength.

Gamma-ray burst (GRB): An outburst that radiates tremendous amounts of energy equal to or greater than a supernova, in the form of gamma-rays and X-rays, with a duration from a few milliseconds to thousands of seconds. GRBs are isotropically distributed on the Sky.

Gamma-Ray Large Area Space Telescope (GLAST): GLAST is a next generation high-energy gamma-ray observatory designed for making observations of celestial gamma-ray sources in the energy band extending from 10 MeV to more than 100 GeV to be launched in 2007. It follows in the footsteps of the CGRO-EGRET experiment, which was operational between 1991 and 1999. The GLAST LAT has a field of view about twice as wide (more than 2.5 steradians), and sensitivity about 50 times that of EGRET at 100 MeV and even more at higher energies.

Globular cluster: Tightly bound, roughly spherical collection of a few hundred thousand of stars spanning about 100 lightyears. Globular clusters are distributed in the haloes around the Milky Way and other galaxies.

Gluons: Term for exchange particles of the strong interaction (derived from glue). There are eight different gluons transmitting the force between the quarks. They are electrically neutral and massless.

Gravitational instability: A condition whereby an object's (inward-pulling) gravitational potential energy exceeds its (outward-pushing) thermal energy, thus causing the object to collapse.

Gravitational lensing: Banding of light from a distant object by a massive foreground object (a star, a galaxy, or a cluster of galaxies).

Gravitational redshift: A prediction of Einstein's general theory of relativity. Photons lose energy as they escape the gravitational field of a compact object. Because a photon's energy is proportional to its frequency, a photon that loses energy suffers a decrease in frequency, or redshift, in wavelength.

Gravitational wave: The gravitational analog of an electromagnetic wave, whereby gravitational radiation is emitted at the speed of light from any mass that undergoes rapid acceleration.

GRS 1915+105: GRS 1915+105 is a microquasar, a galactic object that has been associated with relativistic jets and extremely variable radio, infrared, and X-ray emission. It is thought to be a binary system containing a black hole that is accreting matter from a stellar companion.

Hertzsprung–Russell (HR) diagram: A plot of luminosity vs. temperature for a group of stars that can be used to classify the evolutionary state of stars.

Horizontal branch: Region of the HR diagram where post-main-sequence stars again reach hydrostatic equilibrium. At this point, the star is burning helium in its core, and hydrogen in a shell surrounding the core.

Hybrid (neutron) stars: Neutron stars consisting of normal matter in the outer parts and a quark-matter core. Quark matter is probably in a color-superconducting state (2SC or quark–flavor locked (CFL) phase).

INTEGRAL: INTEGRAL (INTErnational Gamma-Ray Astrophysics Laboratory) is an astronomical satellite for observing the gamma-ray sky. It was selected by the ESA (European Space Agency) science program committee on June 3rd 1993 as a medium size mission. The INTEGRAL satellite was launched on October 17, 2002 by a Russian PROTON launcher. It has a highly eccentric orbit with a revolution period around the Earth of three sidereal days. The perigee is at 10,000 km and the apogee at 152,600 km with an inclination of 51.6 degrees with respect to the equatorial plane. The INTEGRAL science payload consists of two main instruments, the spectrometer SPI and the imager IBIS supplemented by two subsidiary instruments, the X-ray monitor JEM-X and the optical monitoring camera OMC.

Interferometry: Technique in widespread use to dramatically improve the resolution of telescopes, especially radio telescopes. Several radio telescopes observe the object simultaneously, and a computer analyzes how the signals interfere with each other.

Ionization: The process by which ions are produced, typically by collisions of electrons, ions, or photons.

Innermost stable circular orbit (ISCO): This radius marks the location of the innermost stable circular orbit around a black hole. Outside three Schwarzschild radii, all circular orbits are stable, meaning that a small blast on the manoeuvering thrusters by a rocket in circular orbit would not perturb the orbit greatly.

Inverse Compton emission: In physics, Compton scattering or the Compton effect, is the decrease in energy (increase in wavelength) of an X-ray or gamma-ray photon, when it interacts with matter. Inverse Compton scattering indicates the effect, where the photon gains energy (decreasing in wavelength) upon interaction with matter. Inverse Compton scattering is important in astrophysics. In X-ray astronomy, the accretion disk surrounding a black hole is believed to produce a thermal spectrum. The lower energy photons produced from this spectrum are scattered to higher energies by relativistic electrons in the surrounding corona. This is the origin of the power-law component in the X-ray spectra (0.2–100 keV) of accreting black holes. The inverse Compton effect is also important in jets, where relativistic electrons scatter low-frequency photons to gamma-rays.

Jet: A highly directed flow of gas or plasma that comes from such a flow.

Kepler's Laws of motion: Three laws which summarize the motions of the planets about the Sun, or more generally, the motion of one star (neutron star, black hole) around another under the influence of gravity.

Kerr black hole: An exact solution of Einstein's field equations that is the metric outside a spinning event horizon found by Roy Kerr in 1963. It is not the solution for a spinning neutron star.

Killing field: In differential geometry, a Killing vector field is a vector field on a Riemannian manifold that preserves the metric. Killing fields are the infinitesimal generators of isometries; that is, flows generated by Killing fields are continuous isometries of the manifold. Killing fields are named for Wilhelm Killing. A Killing vector field satisfies the Killing equation $L_X g = 0$, where L_X is the Lie derivative along X and g is the Riemannian metric on the manifold.

Kiloelectron-volt (keV): A unit used to describe the energy of X-rays, equal to a thousand electron-volts. One kiloelectron-volt corresponds to a frequency $\nu = 2.418 \times 10^{17}$ Hz in X-rays.

Lagrange point: One of five special points in the plane of two massive bodies orbiting one another, where a third body of negligible mass can remain in equilibrium.

Leptons: One of the two groups of matter particles. There are three pairs of leptons, containing each an electrically charged particle and a neutrino: electron and electron neutrino, muon and muon neutrino, tau and tau neutrino. The leptons are influenced by the electromagnetic and the weak interaction.

LHC: Large Hadron Collider, proton collider at CERN (Geneva), which is built using the old LEP tunnel until 2007.

Light-curve: The variation in brightness of a star with time.

Light deflection: The angle by which a light ray is curved by the gravitational field of a massive body. General relativity gives a value twice as large as that which Newtonian physics would provide, assuming that photons have nonzero mass.

Lighthouse model: The leading explanation for pulsars. A small region of the neutron star, near one of the magnetic poles, emits a steady stream of radiation which sweeps past Earth each time the star rotates. Thus the period of the pulses is just the star's rotation period.

Luminosity: One of the basic properties used to characterize stars. Luminosity is defined as the total energy radiated by a star each second, at all wavelengths.

Magnetosphere: A zone of charged particles trapped by a planet's or star's magnetic field (neutron star or black hole), lying above the atmosphere.

Magnetar: A magnetar is a neutron star with an extremely strong magnetic field, typically a thousand times stronger than in a normal neutron star. Its decay powers the emission of copious amounts of high-energy electromagnetic radiation, particularly X-rays and gamma-rays.

Magnetorotational instability (MRI): Accretion disks are stable to hydrodynamic perturbations, and the fluid flow is expected to be laminar. For there to be turbulence, as required for the standard disk model (α disk), this implies that there is some form of nonlinear hydrodynamic instability, or angular momentum transport is due to some other mechanism. Balbus and Hawley proposed in 1991 a mechanism which involves magnetic fields to generate the turbulence, now called magnetorotational instability (MRI). Magnetohydrodynamics is subtly different from that of hydrodynamics. A weak magnetic field acts like a spring. If there is a weak radial magnetic field in an accretion disk, then two gas volume elements will experience a force acting on them. The inner element will have a force acting to slow it down. This causes it to lose energy and angular momentum and move inwards, where due to orbital mechanics it speeds up. The reverse happens to the outer gas element, which moves outwards and slows down. As a consequence, the magnetic field spring is stretched, transferring angular momentum in the process.

Main sequence: A well-defined band on an HR diagram on which most stars tend to be found, running from the top left of the diagram to the bottom right.

Mass–radius relation: The dependence of the radius of a main-sequence star on its mass. The radius rises roughly in proportion to the mass.

Microquasar: Microquasars are stellar mass black holes, that display characteristics of the supermassive black holes found at the centers of some galaxies. For instance, they have radio jets. In the Spring of 1994, Felix Mirabel from Saclay, France, and Luis Rodriguez, from the National Autonomous University in Mexico City, were observing an X-ray-emitting object called GRS 1915+105 (about 40,000 lightyears away). Their time series of VLA observations showed that a pair of objects ejected from GRS 1915+105 were moving apart at an apparently superluminal speed. This was the first time that superluminal motion had been detected in our own Galaxy.

Millisecond pulsar: A pulsar whose period indicates that the neutron star is rotating nearly 1000 times each second.

Neutrino oscillations: Possible solution to the solar neutrino problem, in which the neutrino has a very tiny mass. In this case, the correct number of neutrinos can be produced in the solar core, but on their way to Earth, some can oscillate, or become transformed into other particles, and thus go undetected.

Neutron star: A dense ball of neutrons that remains after a supernova has destroyed the rest of the star. Typically neutron stars are about 20 km across, and contain more mass than the Sun.

Nonthermal radiation: Radiation released by virtue of a fast-moving charged particle (such as an electron) interacting with a magnetic force field or other particles; this process has nothing to do with heat.

Nova: A star that suddenly increases in brightness, often by a factor of as much as 10,000 then slowly fades back to its original luminosity. A nova is the result of an explosion on the surface of a white dwarf star, caused by matter falling onto its surface from the atmosphere of a binary companion.

Nuclear force: The force that binds protons and neutrons within atomic nuclei, and which is effective only at distances less than about 10^{-13} centimeter.

Nucleon: Building block of atoms, i.e. a proton or a neutron.

Nucleus: Dense, central region of an atom, containing both protons and neutrons, and orbited by one or more electrons.

Opacity: A quantity that measures a material's ability to block electromagnetic radiation. Opacity is the opposite to transparency.

Parallax: The apparent motion of a relatively close object with respect to a more distant background as the location of the observer changes.

Parsec: The distance at which a star must lie in order that its measured parallax due to the Earth's orbit around the Sun is exactly 1 arcsecond, equal to 3.3 lightyears.

Period–luminosity relation: A relation between the pulsation period of a Cepheid variable and its absolute brightness. Measurement of the pulsation period allows the distance of the star to be determined.

Planetary nebula: The ejected envelope of a red giant star, spread over a volume roughly the size of our Solar System, with a hot central star that is in the process of becoming a white dwarf star.

Primordial black holes: A primordial black hole is a hypothetical type of black hole that is formed not by the gravitational collapse of a star, but by the extreme density of matter present during the Universe's early expansion.

Proper motion: The angular movement of a star across the sky, as seen from the Earth, measured in seconds of arc per year. This movement is a result of the star's actual motion through space.

Pulsar: Object that emits radiation in the form of rapid pulses with a characteristic pulse period and duration. Generally used to describe the pulsed radiation from a rotating neutron star.

Quality factor: Quantity characterizing the resonance properties of a resonant system, for example a resonant circuit or a cavity resonator. It depends on the average energy of the system and its dissipative power. The higher the quality is, the more focused is the resonance curve. The bandwidth is correspondingly smaller.

Quantum chromodynamics (QCD): Quantum chromodynamics, the gauge theory describing the color strong interaction.

Quarks: A fractionally charged, basic building block of protons, neutrons, and other elementary particles. There are six different quarks. Similar to the leptons, they form a particle group consisting of three particle pairs: up and down quarks, charm and strange quarks and top and bottom quarks. In nature, quarks can occur in pairs (quark and antiquark, known as mesons) or as a three-piece combination of either quarks or antiquarks.

Quasars: Originally, a distant, highly luminous object that looks like a star. Strong evidence now exists that a quasar is produced by gas falling into a supermassive black hole in the center of a galaxy.

Quasinormal modes: Quasinormal modes (QNM) are the modes of energy dissipation of a perturbed object (neutron star or black hole). In this context, a quasinormal mode is a formal solution of linearized differential equations (such as the linearized equations of general relativity constraining perturbations around a black hole solution) with a complex eigenvalue (or frequency). Black holes have many quasinormal modes (also called ringing modes) that describe the exponential decrease of asymmetry of the black hole in time, as it evolves towards the perfect spherical shape.

Quasiperiodic Oscillations (QPO's): Variations in the intensity of X-radiation from sources that show periodic behavior for short time intervals, and a variety of periods.

Radio galaxy: Type of active galaxy that emits most of its energy in the form of long-wavelength radiation.

Radio lobe: Roundish region of radio-emitting gas, lying well beyond the center of a radio galaxy.

Red-giant branch: The section of the evolutionary track of a star that corresponds to continued heating from rapid hydrogen shell burning, which drives a steady expansion and cooling of the outer envelope of the star. As the star gets larger in radius and its surface temperature cools, it becomes a red giant.

Redshift: Change in the wavelength of light emitted from a source moving away from us. The relative recessional motion causes the wave to have an observed wavelength longer (and hence redder) than it would if it were not moving. The cosmological redshift is caused by the stretching of space as the Universe expands.

Relativity, general theory: The theory of gravity formulated by Einstein that describes how a gravitational field can by replaced by a curvature of spacetime.

Resolution limit: Measure for the smallest intervals a detector can resolve separately. These can be time intervals (time resolution), differences in energy or wavelength (energy resolution) or spatial distances (spatial resolution).

RHIC: The Relativistic Heavy Ion Collider (RHIC) at Brookhaven National Laboratory is a world-class scientific research facility that began operation in 2000, following 10 years of development and construction. RHIC drives two intersecting beams of gold ions head-on, in a subatomic collision. At extremely high energy densities, QCD predicts a new form of matter, consisting of an extended volume of interacting quarks, antiquarks, and gluons. This is the quark–gluon plasma (QGP).

Riemann curvature: In differential geometry, the Riemann curvature tensor is the most standard way to express curvature of Riemannian manifolds, or more generally, any manifold with an affine connection, including torsion. This curvature tensor measures noncommutativity of the covariant derivative. It satisfies several symmetries known as Bianchi identities.

Riemann problem: The Riemann problem is the simplest possible initial value problem for hyperbolic systems. In one spatial dimension, the Riemann (or shock-tube) problem is composed of two uniform states in the infinite domain separated by a discontinuity at the origin. For the Euler equations, the exact solution of the Riemann problem is well known, self-similar, and consists of a combination of three wave types: shocks, rarefaction waves, and contact discontinuities. Apart from being an important test-bench, the Riemann problem is a basic building block for a large class of modern numerical methods, called upwind or Godunov schemes.

Roche limit: Often called the tidal stability limit, the Roche limit gives the distance from a planet at which the tidal force, due to the planet, between adjacent objects exceeds their mutual attraction. Objects within this limit are unlikely to accumulate into larger objects. The rings of Saturn occupy the region within Saturn's Roche limit.

Roche lobe: An imaginary surface around a star. Each star in a binary system can be pictured as being surrounded by a tear-shaped zone of gravitational influence, the Roche lobe. Any material within the Roche lobe of a star can be considered to be part of that star. During evolution, one member of the binary star can expand so that it overflows its own Roche lobe, and begins to transfer matter onto the other star.

Rossi X-Ray Timing Explorer (RXTE): The Rossi X-ray Timing Explorer (RXTE) was launched on December 30, 1995. RXTE features unprecedented time resolution in combination with moderate spectral resolution to explore the variability of X-ray sources. Time-scales from microseconds to months are covered in an instantaneous spectral range from 2 to 250 keV.

Schwarzschild radius: The distance from the center of a nonrotating black hole such that, if all the mass were compressed within that region, the escape velocity would equal the speed of light. Once a stellar remnant collapses within this radius, light cannot escape and the object is no longer visible. See event horizon.

Shock wave: A wave front marked by an abrupt change in pressure caused by an object or material moving faster than the speed of sound. For example, a sonic boom produced by an aircraft going faster than the speed of sound.

Shapiro time delay: The Shapiro time-delay effect, or gravitational time-delay effect, is one of the four classic Solar System tests of general relativity. The time-delay effect was first noticed in 1964 by Irwin I. Shapiro. Radar signals passing near a massive object takes slightly longer to travel to a target and longer to return (as measured by the observer) than it would if the mass of the object were not present. This also affects the propagation of radio signals emitted by a pulsar in orbit around another star. This allows us to measure to the mass of the partner star and the orbital inclination.

Singularity: A point in the Universe where the density of matter and the gravitational field are infinite, such as the center of a black hole.

Spacetime: A synthesis of the three dimensions of space and of a fourth dimension, time; a hallmark of relativity theory.

Spectral class: Classification scheme, based on the strength of stellar spectral lines, which is an indication of the temperature of a star.

Spectroscopic binary: A binary star system which from Earth appears as a single star, but is known to contain more than one star because of the back-and-forth Doppler shifts that are observed as the two stars orbit one another.

Spitzer Space Telescope: NASA's Great Observatory for infrared astronomy was launched in August 2003. Formerly named SIRTF (Space Infrared Telescope Facility), it was renamed in honor of Lyman Spitzer, Jr.

Static limit: The outer boundary of the region around a spinning black hole that is called the ergosphere.

Stellar-mass black hole: A black hole that formed when a massive star died in a supernova explosion and is somewhat more massive than our Sun.

Superconductivity: Property of certain metals, or neutron star matter, at low temperatures. The electrical resistance of the conductor vanishes, so that the electrical current flows without loss. In modern accelerators, often superconducting magnets and high frequency resonators are used which are operated at temperatures near absolute zero. At low temperature, many metals become superconductors. A metal can be viewed as a Fermi liquid of electrons, and below a critical temperature, an attractive phonon-mediated interaction between the electrons near the Fermi surface causes them to pair up and form a condensate of Cooper pairs, which via the Anderson–Higgs mechanism makes the photon massive, leading to the characteristic behavior of a superconductor: infinite conductivity and the exclusion of magnetic fields (Meissner effect).

Superfluidity: Fermionic condensates are a type of superfluid. As the name suggests, a superfluid possesses fluid properties similar to those possessed by ordinary liquids and gases, such as the lack of a definite shape and the ability to flow in response to applied forces. However, superfluids possess some properties that do not appear in ordinary matter. For instance, they can flow at low velocities without dissipating any energy (i.e. zero viscosity). At higher velocities, energy is dissipated by the formation of quantized vortices, which act as holes in the medium where superfluidity breaks down.

Supergravity: In theoretical physics, a supergravity theory is a field theory combining supersymmetry and general relativity. A supergravity theory contains a spin-2 field whose quantum is the graviton. Supersymmetry requires the graviton field to have a superpartner. This field has spin 3/2 and its quantum is the gravitino. Supergravity theories are often said to be the only consistent theories of interacting massless spin 3/2 fields.

Supermassive black hole: A black hole with a mass much greater than the most massive stars (100 solar masses). The central regions of virtually every galaxy are thought to contain a supermassive black hole of a million solar masses or more. Our Milky Way harbors in its center a supermassive black hole (Sag A*) with 3.5 million solar masses.

Supernova: Explosive death of a star, caused by the sudden onset of nuclear burning (type I), or gravitational collapse followed by an enormously energetic shock wave (type II). One of the most energetic events of the Universe, a supernova may temporarily outshine the rest of the galaxy in which it resides. Supernovae of type Ia (exploding white dwarfs) are cosmic standard candles used to measure the expansion law of the Universe.

Supernova remnant: The expanding glowing remains from a supernova explosion. The Cygnus Loop is an example of a shell-type remnant. As the shock wave from the supernova explosion plows through space, it heats and stirs up any interstellar material it encounters, thus producing a big shell of hot material in space. Plerions resemble the Crab Nebula. These SNRs are similar to shell-type remnants, except that they contain a pulsar in the middle that blows out electron–positron winds.

Supersymmetry (SUSY): One of the most promising candidates for a theory which goes beyond the Standard Model. To every particle, a supersymmetric partner is assigned – an exchange particle for every matter particle and vice versa. Until now, none of these supersymmetric partner particles was detected, so that no experimental proof for the theory of supersymmetry exists yet.

Swift: The Swift Gamma-Ray Burst Explorer carries three instruments to enable the most detailed observations of gamma-ray bursts (GRBs) to date. It carries three coaligned instruments known as the BAT, the XRT, and the UVOT. The XRT and UVOT are X-ray and a UV/optical focusing telescopes respectively which produce subarcsecond positions and multiwavelength light-curves for gamma-ray Burst (GRB) afterglows. BAT is a wide field-of-view (FOV) coded-aperture gamma-ray imager that produces arcminute GRB positions onboard within 10 seconds. The spacecraft executes a rapid autonomous slew that points the focusing telescopes at the BAT position in typically 50 seconds.

Synchrotron radiation: Type of nonthermal radiation caused by high-speed charged particles, such as electrons, emitting radiation as they are accelerated in a magnetic field. In accelerator physics, it is produced when electrons or positrons fly through deflecting magnets of ring accelerators or through wigglers or undulators. It is used for analyzing atomic and molecular structures in many natural sciences.

Time dilation: A prediction of the theory of relativity, closely related to the gravitational redshift. To an outside observer, a clock lowered into a strong gravitational field will appear to run slow.

Ultraluminous X-ray source (ULX): An ultraluminous X-ray source (ULX) is an astronomical source of X-rays that is not in the nucleus of a galaxy, and is more luminous than 10^{32} watt, brighter than the Eddington luminosity of a 10 solar-mass black hole. Typically there is about one ULX per galaxy in galaxies which host ULXs, but some galaxies contain many ULXs. The Milky Way does not contain an ULX. A survey of ULXs by Chandra observations shows that there is approximately one ULX per galaxy in galaxies which host ULXs. ULXs are found in all types of galaxies, including elliptical galaxies, but are more ubiquitous in star forming galaxies and in gravitationally interacting galaxies.

Visual binary: A binary star system in which both members are resolvable from Earth.

White dwarf: A star that has exhausted most or all of its nuclear fuel and has collapsed to a very small size (about the Earth's size). These stars are not heavy enough to generate the core temperatures required to fuse carbon in nucleosynthesis reactions. After it has become a red giant during its helium-burning phase, it will shed its outer layers to form a planetary nebula, leaving behind an inert core consisting mostly of carbon and oxygen. The white dwarf is supported only by electron degeneracy pressure. The maximum mass of a white dwarf, beyond which degeneracy pressure can no longer support it, is about 1.4 solar masses depending on its chemical composition.

XMM–Newton: The European Space Agency's large X-ray observatory, launched on December 10, 1999, which is capable of sensitive X-ray spectroscopic observations. XMM–Newton's name comes from the design of its mirrors, the highly nested X-ray Multi-Mirrors. XMM–Newton's highly eccentric orbit (with apogee of 114,000 km away from Earth and a perigee of 7000 km) has been chosen so that its instruments can work outside the radiation belts surrounding the Earth.

X-ray: Region of the electromagnetic spectrum corresponding to radiation of high frequency, corresponding to energies from 0.1 keV to 100 keV, and short wavelengths, far outside the visible spectrum.

X-ray binary: A binary star system in which a normal star is in orbit around a stellar remnant. The remnant accretes material from the normal star and produces X-rays in the process.

X-ray burster: X-ray source that radiates thousands of times more energy than our Sun, in short bursts that last only a few seconds. A neutron star in a binary system accretes matter onto its surface until temperatures reach the level needed for hydrogen fusion to occur. The result is a sudden period of rapid nuclear burning and release of energy.

References

1. M. Camenzind: *General Relativity – The Theory of Space and Time*, Lecture Notes (University Heidelberg 2004), see http://www.lsw.uni-heidelberg.de/users/mcamenzi
2. S.M. Carroll: *Spacetime and Geometry: An Introduction to General Relativity* (Addison-Wesley, New York 2003)
3. S. Chandrasekhar: *Hydrodynamic and Hydrodmagnetic Stability*, Int. Ser. of Monographs on Physics (Oxford Clarendon Press, Oxford 1961)
4. S. Chandrasekhar: *The Mathematical Theory of Black Holes* (Oxford University Press, Oxford 1983)
5. Norman K. Glendenning: *Compact Stars – Nuclear Physics, Particle Physics and General Relativity*, Astronomy and Astrophysics Library, 2nd edn (Springer-Verlag, Berlin, Heidelberg 2000)
6. W.G.H. Lewin, M. van der Klis: *Compact Stellar X-Ray Sources*, Cambridge Astrophysics Series **39** (Cambridge University Press, Cambridge 2006)
7. A.G. Lyne, F.G. Smith: *Pulsar Astronomy* (Cambridge University Press, Cambridge 1998)
8. R.N. Manchester, J.H. Taylor: *Pulsars* (Freeman, New York 1977)
9. F.C. Michel: *Theory of Neutron Star Magnetospheres* (Chicago University Press, Chicago 1991)
10. C. Misner, K. Thorne, J. Wheeler: *Gravitation* (Freeman, San Francisco 1973)
11. M. Nakahara: *Geometry, Topology and Physics*, 2nd edn (IOP, Bristol 2003)
12. C. Rovelli: *Quantum Gravity*, Cambridge Monographs on Mathematical Physics (Cambridge University Press, Cambridge 2004)
13. G.B. Rybicki, A.P. Lightman: *Radiation Processes* (Wiley Interscience, New York 1979)
14. B.F. Schutz: *A First Course in General Relativity* (Cambridge University Press, Cambridge 1986)
15. Stuart L. Shapiro, Saul A. Teukolsky: *Black Holes, White Dwarfs and Neutron Stars: The Physics of Compact Objects* (John Wiley, New York 1983)
16. E.M. Sion, S. Vennes, H.L. Shipman: *White Dwarfs: Cosmological and Galactic Probes*, Astrophysics and Space Science Library **332** (Springer-Verlag, Berlin 2005)
17. H. Stephani: *Relativity – An Introduction to Special and General Relativity*, 3rd edn (Cambridge University Press, Cambridge 2004)
18. N. Straumann: *General Relativity and Relativistic Astrophysics*, 2nd edn (Springer-Verlag, Berlin 2000)
19. F. Weber: *Pulsars as Astrophysical Laboratories for Nuclear and Particle Physics* (IOP, Bristol 1999)
20. S. Weinberg: *Gravitation and Cosmology* (Wiley, New York 1972)

21. M.A. Abramowicz, B. Czerny, J.-P. Lasota, E. Szuszkiewicz: *Slim accretion disks*, ApJ **332**, 646 (1988)
22. M.A. Abramowicz, X. Chen, S. Kato, J.-P. Lasota, O. Regev: *Thermal equilibria of accretion disks*, ApJ **438**, L37 (1995)
23. M.A. Abramowicz, W. Kluzniak, J.P. Lasota: *No observational proof of the black-hole event-horizon*, A&A **396**, L31 (2002); arXiv:astro-ph/0207270
24. F.A. Aharonian, M.A. Atoyan: *Nonthermal radiation of the Crab Nebula*, in Proc. *Neutron Stars and Pulsars: Thirty Years after the Discovery*, ed. N. Shibazaki et al. (Universal Academy Press, Tokoyo 1998), p 439; arXiv:astro-ph/9803091
25. F.A. Aharonian et al.: *The Crab Nebula and pulsar between 500 GeV and 80 TeV: Observations with the HEGRA stereoscopic air Cherenkov*, ApJ **614**, 897 (2004); astro-ph/0407118
26. A. Akmal, V.R. Pandharipande, D.G. Ravenhall: *Equation of state of nucleon matter and neutron star structure*, Phys. Rev. C **58**, 1804 (1998)
27. C. Alcock, E. Farhi, A. Olinto: *Strange stars*, ApJ **310**, 261 (1986)
28. M. Alcubierre, B. Brügmann: *Simple excision of a black hole in 3+1 numerical relativity*, Phys. Rev. D **62**, 14011 (2001)
29. M. Alford: *Color superconducting quark matter*, Ann. Rev. Nucl. Part. Sci. **51**, 131 (2001)
30. M. Alford: *Dense quark matter in nature*, nucl-th/0312007 (2003)
31. M. Alford, S. Reddy: *Compact stars with color superconducting quark matter*, Phys. Rev. D **67**, 74024 (2004)
32. M. Alford, M. Braby, M. Paris, S. Reddy: *Hybrid stars that masquerade as neutron stars*, arXiv:nucl-th/0411016 (2005)
33. A.M. Anile: *Relativistic Fluids and Magnetofluids*, Cambridge University Press (Cambridge 1989)
34. M. Ansorg, A. Kleinwächter, R. Meinel: *Highly accurate calculation of rotating neutron stars*, A&A **381**, L49 (2002)
35. M. Ansorg, A. Kleinwächter, R. Meinel: *Highly accurate calculation of rotating neutron stars: Detailed description of the numerical methods*, A&A **405**, 711 (2003); arXiv:astro-ph/0103173
36. L. Anton, O. Zanotti, J.A. Miralles et al.: *Numerical 3+1 general relativistic magnetohydrodynamics: A local characteristics approach*, ApJ **637**, 296 (2005); arXiv:astro-ph/0506063
37. S. Appl, M. Camenzind: *The structure of relativistic MHD jets: a solution to the nonlinear Grad–Shafranov equation*, A&A **274**, 699 (1993)
38. P.J. Armitage: *Turbulence and angular momentum transport in global accretion disk simulation*, ApJ **501**, L189 (1998)
39. P.J. Armitage, C.S. Reynolds: *The variability of accretion on to Schwarzschild black holes from turbulent magnetized discs*, MNRAS **339**, 1041 (2003)
40. R. Arnowitt, S. Deser, C.W. Misner: *The dynamics of general relativity*, in *Gravitation: An Introduction to Current Research*, ed. L. Witten (John Wiley, New York 1962), p 227
41. J. Arons: *Photon bubbles – Overstability in a magnetized atmosphere*, ApJ **388**, 561 (1992)
42. P. Arras, O. Blaes, N.J. Turner: *Quasi-periodic oscillations from magnetorotational turbulence*, arXiv:astro-ph/0602275
43. Yu.V. Artemova, G.S. Bisnovatyi-Kogan, I.V. Igumenshchev, I.D. Novikov: *Accretion disks with optical depth transition and advection*, Mem. Soc. Astron. Italiana **76**, 84 (2005)

44. A. Ashtekar: *New variables for classical and quantum gravity*, Phys. Rev. Lett. **57**, 2244 (1986)
45. A. Ashtekar: *New Hamiltonian formulation of general relativity*, Phys. Rev. D **36**, 1586 (1987)
46. L. Baiotti, I. Hawke, P. Montero, F. Löffler, L. Rezzolla, N. Stergioulas, T. Font, Ed. Seidel: *Three-dimensional relativistic simulations of rotating neutron star collapse to a Kerr black hole*, Phys. Rev. D **71**, 024035 (2005)
47. S. Balberg, I. Lichtenstadt, G.B. Cook: *Roles of hyperons in neutron stars*, ApJSupp **121**, 515 (1999)
48. S. Balbus, J.F. Hawley: *A powerful local shear instability in weakly magnetized disks. I – Linear analysis. II – Nonlinear evolution*, ApJ **376**, 214 (1991)
49. S. Balbus, J.F. Hawley: *Instability, turbulence, and enhanced transport in accretion disks*, Rev. Mod. Phys. **70**, 1 (1998)
50. S. Balbus: *Enhanced angular momentum transport in accretion disks*, ARA&A **41**, 555 (2003)
51. S. Balbus: *Turbulent energy transport in nonradiative accretion flows*, ApJ **600**, 865 (2004)
52. M. Baldo, I. Bombaci, G.F. Burgio: *Microscopic nuclear equation of state with three-body forces and neutron star structure*, A&A **328**, 274 (1997)
53. D. Balsara: *Total variation diminishing scheme for relativistic magnetohydrodynamics*, ApJSupp **132**, 83 (2001)
54. F. Banyuls, J.A. Font, J.M. Ibanez, J.M. Marti, J.A. Miralles: *Numerical 3+1 general relativistic hydrodynamics: A local characteristic approach*, ApJ **476**, 221 (1997)
55. J.M. Bardeen: *Stability of circular orbits in stationary, axisymmetric space-times*, ApJ **161**, 103 (1970)
56. J.M. Bardeen: *A variational principle for rotating stars in general relativity*, ApJ **162**, 171 (1970)
57. J.M. Bardeen, R.V. Wagoner: *Relativistic disks. I. Uniform rotation*, ApJ **167**, 359 (1971)
58. J. M. Bardeen, B. Carter, S.W. Hawking: *The four laws of black hole mechanics*, Comm. Math. Phys. **31**, 161 (1973)
59. M.A. Barstow, H.E. Bond, J.B. Holberg et al.: *Hubble Space Telescope spectroscopy of the Balmer lines in Sirius B*, MNRAS **362**, 1134 (2005); astro-ph/0506600
60. A.J. Barth, J.E. Greene, L.C. Ho: *Dwarf Seyfert 1 nuclei and the low-mass end of the* $M_{BH} - \sigma$ *relation*, ApJ **619**, L151 (2005)
61. T.w. Baumgarte, S.L. Shapiro: *Evolution of rotating supermassive stars to the onset of collapse*, ApJ **526**, 941 (1999)
62. T.W. Baumgarte, S.L. Shapiro: *General relativistic magnetohydrodynamics for the numerical construction of dynamical spacetimes*, ApJ **585**, 921 (2003)
63. A. Bauswein: *Struktur schnell rotierender Neutronensterne*, Diploma thesis, Technical University Darmstadt 2006
64. G.C. Baym, D. Pethick, P. Sutherland: *The ground state of matter at high densities: Equation of state and stellar models*, ApJ **170**, 299 (1971)
65. G.C. Baym, H. Bethe, C.J. Pethick: *Neutron star matter*, Nucl. Phys. A **175**, 225 (1979)
66. W. Becker, G.G. Pavlov: *The Milky Way – pulsars and isolated neutron stars*, in *The Century of Space Science*, eds. J. Bleeker, J. Geiss, M. Huber (Kluwer Academic Publishers 2002); arXiv:astro-ph/0208356
67. I. Bednarek, R. Manka: *The influence of the strength of hyperon–hyperon interactions on neutron star properties*, arXiv:hep-ph/0506059 (2005)

68. T. Belloni: *Black hole states: Accretion and jet ejection*, astro-ph/0504185 (2005)
69. T. Belloni, M. Mendez, J. Homan: *The distribution of kHz QPO frequencies in bright LMXBs*, A&A **437**, 209 (2005)
70. E. Berti, N. Stergioulas: *Approximate matching of analytic and numerical solutions for rapidly rotating neutron stars*, MNRAS **350**, 1416 (2004)
71. E. Berti, F. Frances, A. Maniopoulou, M. Bruni: *Rotating neutron stars: An invariant comparison of approximate and numerical space-time models*, MNRAS **358**, 923 (2005)
72. V.S. Beskin, I.V. Kuznetsova: *On the Blandford–Znajek mechanism of the energy loss of a rotating black hole*, Il Nuovo Cimento B **115**, 795 (2000)
73. G.S. Bisnovatyi-Kogan, S.I. Blinnikov: *Disk accretion onto a black hole at subcritical luminosity*, A&A **59**, 111 (1977)
74. O. Blaes: *Physics fundamentals of luminous accretion disks around black holes*, in *Accretion discs, jets and high energy phenomena in astrophysics*, ed. V. Beskin, G. Henri, F. Menard et al, Les Houches Summer School **78**, 137 (2004)
75. O.M. Blaes, A. Socrates: *Local dynamical instabilities in magnetized, radiation pressure-supported accretion disks*, ApJ **553**, 987 (2001)
76. O.M. Blaes, A. Socrates: *Local radiative hydrodynamic and magnetohydrodynamic instabilities in optically thick media*, ApJ **596**, 509 (2003)
77. L. Blanchet, T. Damour, B.L. Iyer, C.M. Will, A.G. Wiseman: *Gravitational-radiation damping of compact binary systems to second post-Newtonian order*, Phys. Rev. Lett. **74**, 3515 (1995)
78. L. Blanchet: *Gravitational radiation from post-Newtonian sources and inspiralling compact binaries*, Living Reviews in Relativity **lrr-2002-3** (2002)
79. R.D. Blandford, S.A. Teukolsky: *Arrival-time analysis for a pulsar in a binary system*, ApJ **205**, 580 (1976)
80. R.D. Blandford, R.L. Znajek: *Electromagnetic extraction of energy from Kerr black holes*, MNRAS **179**, 433 (1977)
81. D. Blaschke, D. Voskresensky, H. Grogorian: *Cooling of neutron stars with color superconducting quark cores*, arXiv:hep-ph/0510368 (2005)
82. I. Bombaci, M. Prakash, Ainsworth, J.M. Lattimer: *Physics of neutron star interiors*, Phys. Rep. **280**, 1 (1997)
83. S. Bonazzola, E. Gorgoulhon, M. Salgado, J.A. Marck: *Axisymmetric rotating relativistic bodies: A new numerical approach for exact solutions*, A&A **278**, 421 (1993)
84. S. Bonazzola, E. Gourgoulhon: *A virial identity applied to relativistic stellar models*, Class. Quantum Grav. **11**, 1775 (1994)
85. S. Bonazzola, E. Gourgoulhon, J.A. Marck: *Numerical approach for high precision 3-D relativistic star models*, Phys. Rev. D **58**, 104020 (1998); arXiv:astro-ph/9803086
86. R.H. Boyer, R.W. Lindquist: *Maximal analytic extension of the Kerr metric*, J. Math. Phys. **8**, 265 (1967)
87. S. Brandt, B. Brügmann: *A simple construction of initial data for multiple black holes*, Phys. Rev. Lett. **78**, 3606 (1997)
88. S. Brinkmann: *MHD-instabilities in accretion disks*, Diploma thesis, University Heidelberg 2004
89. S. Brinkmann, M. Camenzind, J. Gracia: *On the global structure of magnetohydrodynamical unstable non-radiative accretion discs*, submitted for publication (2006)
90. M. Brio, C.C. Wu: *An upwind differencing scheme for the equations of ideal magnetohydrodynamics*, J. Comp. Phys. **75**, 400 (1988)
91. G.E. Brown: *High-density equation of state*, Nature **336**, 519 (1988)

92. M. Buballa: *NJL-model analysis of dense quark matter*, Phys. Rep. **407**, 205 (2005)
93. V. Burwitz, F. Haberl, R. Neuhäuser et al.: *The thermal radiation of the isolated neutron star RX J1856.5–3754 observed with Chandra and XMM–Newton*, A&A **399**, 1109 (2003)
94. E.M. Butterworth, and J.R. Ipser: *On the structure and stability of rapidly rotating fluid bodies in general relativity. I – The numerical method for computing structure and its application to uniformly rotating homogeneous bodies*, ApJ. **204**, 200 (1976)
95. A. Cadez, C. Fanton, M. Calvani: *Line emission from accretion discs around black holes: The analytic approach*, New Astron. **3**, 647 (1998)
96. M. Camenzind: *Hydromagnetic flows from rapidly rotating compact objects. I – Cold relativistic flows from rapid rotators*, A&A **162**, 32 (1986)
97. M. Camenzind: *Hydromagnetic flows from rapidly rotating compact objects. II – The relativistic axisymmetric jet equilibrium*, A&A **184**, 341 (1987)
98. M. Camenzind: *Magnetohydrodynamics of rotating black holes*, in: *Relativistic Astrophysics*, ed. H. Riffert, H. Ruder, H.-P. Nollert, F.W. Hehl, p 82 (Vieweg, Braunschweig 1998)
99. M. Camenzind, R. Khanna: *Magnetohydrodynamic processes near rapidly rotating compact objects*, Il Nuovo Cimento B **115**, 815 (2000)
100. M. Camenzind: *The black hole environments*, in *Accretion discs, jets and high energy phenomena in astrophysics*, ed. V. Beskin, G. Henri, F. Menard et al., Les Houches Summer School **78**, 405 (2004)
101. M. Camenzind: *Relativistic outflows from active galactic nuclei*, Mem. Soc. Astron. Italiana **76**, 98 (2005)
102. M. Camenzind: *Cosmic black holes – From stellar to supramssive black holes in galaxies*, Ann. Physik **15**, 60 (2006)
103. M. Camenzind, A. Boucher: *Les noyaux actifs de galaxies*, Lecture Notes in Physics **46**, (Springer-Verlag, Berlin 1997)
104. B.J. Carr: *Primordial black holes – Recent developments*, arXiv:astro-ph/0504034 (2005)
105. B. Carter: *Hamilton–Jacobi and Schrödinger separable solutions of Einstein's equations*, Comm. Math. Phys. **10**, 280 (1968)
106. B. Carter: *The commutation property of a stationary, axisymmetric system*, Comm. Math. Phys. **17**, 233 (1970)
107. B. Carter: *The general theory of mechanical, electromagnetic and thermodynamic properties of black holes*, in: *General Relativity: An Einstein Centenary Survey*, ed. S.W. Hawking, W. Israel, p 294 (Cambridge Univ. Press, Cambridge 1979)
108. J. Casares: *The mass-spectrum of X-Ray binaries*, arXiv:astro-ph/0503071 (2005)
109. C. Catteon, T. Faber, Matt Visser: *Gravastars must have anisotropic pressure*, arXiv:gr-qc/0505137 (2005)
110. P. Cerda-Duran, G. Faye, H. Dimmelmeier, J.A. Font, J.M. Ibanez, E. Mueller, G. Schaefer: *CFC+: Improved dynamics and gravitational waveforms from relativistic core collapse simulations*, A&A **439**, 1033 (2005); arXiv:astro-ph/041261
111. G. Chabrier, P. Brassard, G. Fontaine, D. Saumon: *Cooling sequences and color–magnitude diagrams for cool white dwarfs with hydrogen atmospheres*, ApJ **543**, 216 (2000); arXiv:astro-ph/0006363
112. D. J. Champion, D. R. Lorimer, M. A. McLaughlin, J. M. Cordes, Z. Arzoumanian, J. M. Weisberg, J. H. Taylor: *PSR J1829+2456: A relativistic binary pulsar*, MNRAS **350**, L61 (2004)
113. S. Chandrasekhar: *The maximum mass of ideal white dwarfs*, ApJ **74**, 81 (1931)

114. S. Chandrasekhar: *The equilibrium of distorted polytropes. I. The rotational problem*, MNRAS **93**, 390 (1933)
115. S. Chandrasekhar: *The dynamical instability of gaseous masses approaching the Schwarzschild limit in general relativity*, ApJ **140**, 417 (1964)
116. G. Chapline: *Dark energy stars*, arXiv:astro-ph/0503200 (2005)
117. G. Chapline, E. Hohlfeld, B. Laughlin, D. I. Santiago: *Quantum phase transitions and the breakdown of classical general relativity*, Int. J. Mod. Phys. **A 18**, 3587 (2003); arXiv:gr-qc/0012094
118. G. Chapline, E. Hohlfeld, R. B. Laughlin and D. I. Santiago, Quantum phase transitions and the breakdown of classical general relativity, Int. J. Mod. Phys. A 18 3587 (2003) [arXiv:gr-qc/0012094].
119. A. Chodos et al.: *New extended model of hadrons*, Phys. Rev. D **9**, 3471; *Baryon structure in the bag theory*, Phys. Rev. D **10**, 2599 (1974)
120. http://seesar.lbl.gov/anag/chombo/
121. R. Coker, F. Melia: *Hydrodynamical accretion onto Sagittarius A* from distributed point sources*, ApJ **488**, L149 (1997)
122. J. Contopoulos, D. Kazanas, C. Fendt: *The axisymmetric pulsar magnetosphere*, ApJ **511**, 351 (1999)
123. G.B. Cook, S.L. Shapiro, S.A. Teukolsky: *Spin-up of a rapidly rotating star by angular momentum loss – Effects of general relativity*, ApJ **398**, 203 (1992)
124. G.B. Cook, S.L. Shapiro, S.A. Teukolsky: *Rapidly rotating neutron stars in general relativity. Realistic equations of state*, ApJ **424**, 828 (1994)
125. S. Corbel: *Large scale jets in microquasars*, Memorie della Societa Astronomica It. **76**, 73 (2005)
126. J. Cottam, F. Paerels, M. Mendez: *Gravitationally redshifted absorption lines in the X-ray burst spectra of a neutron star*, Nature **420**, 51 (2003)
127. C.T. Cunningham: *The effects of redshifts and focusing on the spectrum of an accretion disk around a Kerr black hole*, Ap. J. **202**, 788 (1975)
128. T. Damour, N. Deruelle: Ann. Inst. H. Poincare A **44**, 263 (1986)
129. T. Damour, J.H. Taylor: *Strong-field tests of relativistic gravity and binary pulsars*, Phys. Rev. D **45**, 1840 (1992)
130. S.W. Davis, O:M. Blaes, I. Hubeny, N.J. Turner: *Relativistic accretion disk models of high state black hole X-ray binary spectra*, ApJ **621**, 372 (2005)
131. A. Dedner, F. Kemm, D. Kröner et al.: *Hyperbolic divergence cleaning for the MHD equations*, J. Comp. Phys. **175**, 645 (2002)
132. L. Del Zanna, N. Bucciantini, P. Londrillo: *An efficient shock-capturing central-type scheme for multidimensional relativistic flows. II. Magnetohydrodynamics*, A&A **400**, 397 (2003)
133. J.-P. De Villiers, J.F. Hawley: *A numerical method for general relativistic magnetohydrodynamics*, ApJ **589**, 458 (2003)
134. J.-P. De Villiers, J.F. Hawley, J.H. Krolik: *Magnetically driven accretion flows in the kerr metric. I. Models and overall structure*, ApJ **599**, 1238 (2003)
135. J.-P. De Villiers, J.F. Hawley, J.H. Krolik, S. Hirose: *Magnetically driven accretion in the Kerr metric. III. Unbound outflows*, ApJ **620**, 878 (2005)
136. F. Douchin, P. Haensel: *A unified equation of state of dense matter and neutron star structure*, A&A **380**, 151 (2001)
137. H.P. Duerr: *Relativistic effects in nuclear forces*, Phys. Rev. **103**, 469 (1956)
138. M.D. Duez, Y.T. Liu, S.L. Shapiro, B.C. Stephens: *Relativistic magnetohydrodynamics in dynamical spacetimes: numerical methods and tests*, Phys. Rev. D **72**, 024028 (2005); astro-ph/0503420

139. R. Durrer, N. Straumann: *Some Applications of the 3+1 Formalism of General Relativity*, Helv. Phys. Acta **61**, 1027 (1988)
140. I. Dymnikova: *Spherically symmetric space-time with regular de Sitter center*, Int. J. Mod. Phys. D **12**, 1015 (2003)
141. A. Einstein: *Die Grundlage der allgemeinen Relativitätstheorie*, Ann. Phys. **49**, 769 (1916)
142. A. Einstein, Sitzber. Preuss. Akad. Wiss. Berlin 688 (1916) Näherungsweise Integration der Feldgleichungen der Gravitation
143. A. Einstein, Sitzber. Preuss. Akad. Wiss. Berlin 154 (1918) Über Gravitationswellen
144. R. Epstein: *The binary pulsar: Post-Newtonian timing effects*, ApJ **216**, 92 (1977)
145. F.J. Ernst: *A new formulation of the axially symmetric gravitational field problem*, Phys. Rev. **167**, 1175 (1968)
146. F.J. Ernst: *A new formulation of the axially symmetric gravitational field problem II*, Phys. Rev. **168**, 1415 (1968)
147. A.A. Esin, J.E. McClintock, R. Narayan: *Advection-dominated accretion and the spectral states of black hole X-ray binaries: Application to Nova MUSCAE 1991*, ApJ **489**, 865 (1997)
148. A.A. Esin, J.E. McClintock et al.: *Modeling the low state spectrum of the X-ray Nova XTE J1118+480*, ApJ **555**, 483 (2001)
149. C. Evans, J.F. Hawley: *Simulation of magnetohydrodynamic flows – A constrained transport method*, ApJ **332**, 659 (1988)
150. A.C. Fabian, S. Vaughan, K. Nandra et al.: *A long hard look at MCG–6–30–15 with XMM–Newton*, MNRAS **335**, L1 (2002)
151. H. Falcke, F. Melia, E. Agol: *Viewing the shadow of the black hole at the Galactic center*, ApJ **528**, L13 (2000)
152. S.A.E.G. Falle: *Rarefaction shocks, shock errors, and low order of accuracy in ZEUS*, ApJ **577**, L123 (2002)
153. C. Fanton, M. Calvani, F. de Felice, A. Cadez: *Detecting accretion disks in active galactic nuclei*, PASJ **49**, 159 (1997)
154. A.J.Faulkner, M.Kramer, A.G.Lyne et al.: *PSR J1756–2251: a new relativistic double neutron star system*, ApJ **618**, L119 (2004)
155. R. Fender, T.M. Belloni, E. Gallo: *Towards a unified model for black hole X-ray binary jets*, MNRAS **335**, 1105 (2004)
156. C. Fendt: *Stationary models of relativistic magnetohydrodynamic jets*, Proc. 3rd Int. Sakharov Conf. on Physics, **2**, 315 (Scientific World 2003)
157. C. Fendt, F. Memola: *Collimating, relativistic, magnetic jets from rotating disks. The axisymmetric field structure of relativistic jets and the example of the M87 jet*, A&A **365**, 631 (2001)
158. C. Fendt, F. Memola: *Stationary relativistic magnetic jets from black holes*, ApSSS **276**, 297 (2001)
159. J.A. Font: *Numerical hydrodynamics in general relativity*, Living Reviews in Relativity **lrr-2003-4** (2003)
160. R.H. Fowler: *Dense matter*, MNRAS **87**, 114 (1926)
161. J.L. Friedman, L. Parker, J.R. Ipser: *Rapidly rotating neutron star models*, ApJ **304**, 115 (1986)
162. B.L. Friman, O.V. Maxwell: *Neutrino emissivities of neutron stars*, ApJ **232**, 541 (1979)
163. B. Fryxell, K. Olson, P. Ricker et al.: *FLASH: An adaptive mesh hydrodynamics code for modeling astrophysical thermonuclear flashes*, ApJS **131**, 273 (2000)
164. C.F. Gammie: *Photon bubbles in accretion discs*, MNRAS **297**, 929 (1998)

165. C.F. Gammie: *The magnetorotational instability in the Kerr metric*, ApJ **614**, 309 (2004)
166. C.F. Gammie, J.C. McKinney, G. Toth: *HARM: A numerical scheme for general relativistic magnetohydrodynamics*, ApJ **589**, 444 (2003)
167. K. Gebhardt, R. Bender, G. Bower et al.: *A relationship between nuclear black hole mass and velocity dispersion*, ApJ **539**, L13 (2000)
168. D.M. Gelino et al.: *The inclination angle and mass of the black hole in XTE J1118+480*, astro-ph/0601409
169. R. Genzel, R. Schödel, T. Ott et al.: *Near-infrared flares from accreting gas around the supermassive black hole at the Galactic Centre*, Nature **425**, 934 (2003)
170. U.H. Gerlach: *Equation of state at supranuclear densities and the existence of a third family of superdense stars*, Phys. Rev. **172**, 1325 (1968)
171. A.M. Ghez, S.A. Wright, K. Matthews et al.: *Variable infrared emission from the supermassive black hole at the center of the Milky Way*, ApJ **601**, L159 (2003)
172. B. Giacomazzo, L. Rezzolla: *The exact solution of the Riemann problem in relativistic MHD*, J. Fluid Mech. **562**, 223 (2006); gr-qc/0507102
173. A.M. Ghez, S. Salim, S.D. Hornstein et al.: *Stellar orbits around the Galactic Center black hole*, ApJ **620**, 744 (2005)
174. N.K. Glendenning, N.K. 1985, *Neutron stars are giant hypernuclei?*, ApJ **293**, 470 (1985)
175. N.K. Glendenning: *Vacuum polarization effects on nuclear matter and neutron stars*, Nucl. Phys. A **493**, 521 (1989)
176. P. Goldreich, W.H. Julian: *Pulsar electrodynamics*, ApJ **157**, 869 (1969)
177. E. Gourgoulhon: *A 3+1 perspective on null hypersurfaces and isolated horizons*, arXiv:gr-qc/0503113 (2005)
178. J.E. Goldston, E. Quataert, I.V. Igumenshchev: *Synchrotron radiation from radiatively inefficient accretion flow simulations: applications to Sagittarius A**, ApJ **621**, 785 (2005)
179. D. Gondek-Rosinska, E. Gourgoulhon: *Jacobi-like bar mode instability of relativistic rotating bodies*, Phys. Rev. D **66** 044021 (2002)
180. E. Gourgoulhon, S. Bonazzola: *A formulation of the virial theorem in general relativity*, Class. Quantum Grav. **11**, 443 (1994)
181. E. Gourgoulhon, P. Haensel, R. Livine, E. Paluch, S. Bonazzola, J.-A. Marck: *Fast rotation of strange stars*, A&A **349**, 851 (1999)
182. J. Gracia, J. Peitz, Ch. Keller, M. Camenzind, M.: *Evolution of bimodal accretion flows*, MNRAS **344**, 468 (2003)
183. L.J. Greenhill, D.R. Jiang, J.M. Moran et al.: *Detection of a subparsec diameter disk in the nucleus of NGC 4258*, ApJ **440**, 619 (1995)
184. A. Gurevich, V. Beskin, Y. Istomin: *Physics of Pulsar Magnetosphere* (Cambridge University Press, Cambridge 1993)
185. M.E. Gusakov, A.D. Kaminker, D.G. Yakovlev, O.Y. Gnedin: *Cooling of Akmal–Pandharipande–Ravenhall neutron star models*, arXiv:astro-ph/0507560 (2005)
186. P. Haensel, J.L. Zdunik, R. Schaeffer: *Strange quark stars*, A&A **160**, 121 (1986)
187. P. Haensel: *Equation of state of dense matter and maximum mass of neutron stars*, in *Final Stages of Stellar Evolution*, ed. C. Motch, J.-M. Hameury, EAS Publ. Series (EDP Sciences), pp 249-284 (2003)
188. P. Haensel, A.Y. Potekhin: *Analytical representations of unified equations of state of neutron-star matter*, A&A **428**, 191 (2004)
189. N. Häring, H.-W. Rix: *On the black hole mass–bulge mass relation*, ApJ **604**, L89 (2004)

190. T. Hamada, E.E. Salpeter: *Models for zero-temperature stars*, ApJ **134**, 683 (1961)
191. B.M.S. Hansen, J. Liebert: *Cool white dwarfs*, ARA&A **41**, 465 (2003)
192. B.M.S. Hansen et al.: *HST observations of WD cooling sequence in M4*, ApJSup **155**, 551 (2004); arXiv:astro-ph/0401443
193. H.C. Harris, J.A. Munn, M. Kilic et al.: *The white dwarf luminosity function from SDSS imaging data*, arXiv:astro-ph/0510820
194. A. Harten, P.D. Lax, B. van Leer: *On upstream differencing and Godunov-type schemes for hyperbolic conservation laws*, SIAM Review **25**, 35 (1983)
195. J.B. Hartle, Kip S. Thorne: *Slowly rotating relativistic stars. II. Models for neutron stars and supermassive stars*, ApJ **153**, 807 (1968)
196. M. Haugan: *Post-Newtonian arrival-time analysis for a pulsar in a binary system*, Ap. J. **296**, 1 (1985)
197. S. Hawking: *Black hole explosions?* Nature **248**, 30 (1974)
198. S. Hawking: *Black holes and thermodynamics*, Phys. Rev. D **13**, 191 (1976)
199. J.F. Hawley: *Global magnetohydrodynamical simulations of accretion tori*, ApJ **528**, 462 (2000)
200. J.F. Hawley, J.-P. De Villiers: *General relativistic magnetohydrodynamic simulations of black hole accretion disks*, Progr. Theoret. Phys. Supp **155**, 132 (2004)
201. J.R. Herrnstein, L.J. Greenhill, J.M. Moran: *VLBA continuum observations of NGC 4258: Constraints on an advection-dominated accretion flow*, ApJ **497**, L69 (1998)
202. S. Hirose, J.H. Krolik, J.P. De Villiers, J.F. Hawley: *Magnetically driven accretion flows in the Kerr metric. II. Structure of the magnetic field*, ApJ **606**, 1083 (2004)
203. G. t'Hooft: *Dimensional reduction in quantum gravity*, gr-qc/9310026 (1993)
204. I. Hubeny, E. Agol, O. Blaes, J. Krolik: *Non-LTE models and theoretical spectra of accretion disks in active galactic nuclei. III. Integrated spectra for hydrogen–helium disks*, ApJ **533**, 710 (1999)
205. A. Hujeirat, R. Rannacher: *On the efficiency and robustness of implicit methods in computational astrophysics*, NewAR **45**, 425 (2001)
206. A. Hujeirat: *A model for electromagnetic extraction of rotational energy and formation of accretion-powered jets in radio galaxies*, A&A **416**, 423 (2004)
207. A. Hujeirat: *A method for enhancing the stability and robustness of explicit schemes in CFD*, NewA **10**, 173 (2005)
208. A. Hujeirat, M. Camenzind: *Truncated disks – advective tori solutions around BHs. I. The effects of conduction and enhanced Coulomb coupling*, A&A **362**, L41 (2000)
209. A. Hujeirat, M. Camenzind, A. Burkert: *Comptonization and synchrotron emission in 2D accretion flows. I. A new numerical solver for the Kompaneets equation*, A&A **386**, 757 (2002)
210. R. Ibata et al.: *Faint, Moving objects in the Hubble Deep Field: Components of the dark halo?*, ApJ **524**, L95 (1999)
211. S. Ichimaru: *Bimodal behavior of accretion disks: Theory and application to Cygnus X-1 transitions*, ApJ **214**, 840 (1977)
212. I.V. Igumenshchev, R. Narayan, M.A. Abramowicz: *Three-dimensional magnetohydrodynamic simulations of radiatively inefficient accretion flows*, ApJ **592**, 1042 (2003)
213. J.R. Ipser, L. Lindblom: *On the adiabatic pulsations of accretion disks and rotating stars*, ApJ **379**, 285 (1991)
214. T. Islam, S. Balbus: *The dynamics of the magnetoviscous instability*, astro-ph/0504666
215. N. Iwamoto: *Quark beta decay and the cooling of neutron stars*, Phys. Rev. Lett. **44**, 1637 (1980)
216. B.A. Jacoby, A. Hotan, M. Bailes et al.: *The mass of a millisecond pulsar*, arXiv:astro-ph/0507420 (2005)

217. H.-T. Janka: *Neutron star formation and birth properties*, arXiv:astro-ph/0404200
218. M.H. Johnson, E. Teller: *Classical field theory of nuclear forces*, Phys. Rev. **98**, 783 (1955)
219. S. Kato, J. Fukue, S. Mineshige: *Black-hole accretion disks*, in: *Black-Hole Accretion Disks* (Kyoto University Press, Kyoto 1998)
220. R.P. Kerr: *Gravitational field of a spinning mass as an example of algebraically special metrics*, Phys. Rev. Lett. **11**, 237 (1963)
221. R.P. Kerr, A. Schild: *A new Class of Vacuum Solutions of the Einstein Field Equations*, IV Centenario Della Nascita di Galileo Galilei, 1564-1964. Pubblicazioni del Comitato Nazionale per le Manifestazioni Celebrative. Ed. G. Barbera (Firenze), p 222 (1965)
222. R. Khanna, M. Camenzind: *The ω dynamo in accretion disks of rotating black holes*, A&A **307**, 665 (1996); A&A **313**, 108 (1996)
223. R. Khanna: *Der gravitomagnetische Dynamoeffekt in Akkretionsscheiben Schwarzer Löcher*, PhD Thesis, University of Heidelberg 1993
224. R. Khanna: *On the magnetohydrodynamic description of a two-component plasma in the Kerr metric*, MNRAS **294**, 673 (1998)
225. R. Khanna: *Generation of magnetic fields by a gravitomagnetic plasma battery*, MNRAS **295**, L6 (1998)
226. M. Kilic, Ted von Hippel, F. Mullally et al.: *The Mystery deepens: Spitzer observations of cool white dwarfs*, arXiv:astro-ph/0601305
227. S.J. Kleinman, H.C. Harris, D.J. Eisenstein et al.: *A catalog of spectroscopically identified white dwarf stars in the first data release of the Sloan Digital Sky Survey*, ApJ **607**, 426 (2004)
228. H. Komatsu, Y. Eriguchi, I. Hachisu: *Rapidly rotating general relativistic stars. I – Numerical method and its application to uniformly rotating polytropes*, MNRAS **237**, 355 (1989); *Rapidly rotating general relativistic stars. II – Differentially rotating polytropes*, MNRAS **239**, 153 (1989)
229. S.J. Kleinman et al. 2004, *A catalog of spectroscopically identified white dwarf stars from the first data release of the SDSS*, ApJ **607**, 426 (2004); arXiv:astro-ph/0402209
230. S. Koide, K. Shibata, T. Kudoh: *GRMHD simulations of jets from black hole accretion disks*, ApJ **495**, L63 (1998)
231. S. Koide, K. Shibata, T. Kudoh: *Relativistic jet formation from black hole magnetized accretion disks: Method, tests, and applications of a general relativistic magnetohydrodynamic numerical code*, ApJ **522**, 727 (1999)
232. S. Koide, K. Shibata, T. Kudoh, D.L. Meier: *Extraction of black hole magnetic energy by a magnetic field and the formation of relativistic jets*, Science **295**, 1688 (2002)
233. A.V. Koldoba, O.A. Kusnetsov, G. Ustyugova: *An approximate Riemann solver for relativistic MHD*, MNRAS **333**, 932 (2002)
234. A. Komar: *Covariant conservation laws in general relativity*, Phys. Rev. **113**, 934 (1959)
235. H. Komatsu, Y. Eriguchi, I. Hachisu: *Rapidly rotating general relativistic stars. II – Differentially rotating polytropes*, MNRAS **239**, 153 (1989)
236. S. Komissarov: *A Godunov-type scheme for relativistic magnetohydrodynamics*, MNRAS **303**, 343 (1999)
237. S. Komissarov: *On the properties of time-dependent, force-free, degenerate electrodynamics*, MNRAS **336**, 759 (2002)
238. S. Komissarov: *Electrodynamics of black hole magnetospheres*, MNRAS **350**, 407 (2004)
239. S. Komissarov: *General relativistic MHD simulations of monopole magnetospheres of black holes*, MNRAS **350**, 1431 (2004)

240. S. Komissarov: *Observations of the Blandford–Znajek and the MHD Penrose processes in computer simulations of black hole magnetospheres*, MNRAS **359**, 801 (2004); arXiv:astro-ph/0501599
241. S. Komissarov: *Simulation of axisymmetric magnetospheres of neutron stars*, MNRAS **367**, 19 (2006)
242. D. Koester: *White dwarfs: Recent developments*, A&ARev **11**, 33 (2002)
243. D. Koester, G. Chanmugam: *Physics of white dwarf stars*, Progr. Theor. Phys. **53**, 837 (1990)
244. M. Kramer, D.R. Lorimer, A.G. Lyne et al.: *Testing GR with the double pulsar: Recent results*, arXiv:astro-ph/0503386
245. M. Kramer, A.G. Lyne, M. Burgay et al.: *The double pulsar – A new testbed for relativistic gravity*, arXiv:astro-ph/0405179
246. J.H. Krolik, J.F. Hawley, S. Hirose: *Magnetically driven accretion flows in the Kerr metric. IV. Dynamical properties of the inner disk*, ApJ **622**, 1008 (2005)
247. L.D. Landau: *On the theory of stars*, Phys. Zeitschr. Sowjetunion **1**, 285 (1932)
248. J.M. Lattimer, D.F. Swesty: *An effective equation of state for hot dense matter*, Nucl. Phys. A **535**, 331 (1991)
249. J.M. Lattimer, M. Prakash: *Nuclear matter and its role in supernovae, neutron stars and compact object binary mergers*, Phys. Reports **333**, 121 (2000)
250. J.M. Lattimer, M. Prakash: *The physics of neutron stars*, Science **304**, 536 (2004)
251. T. Leismann, L. Anton, M.A. Aloy, E. Müller, J.M. Marti, J.A. Miralles, J.M. Ibanez: *Relativistic MHD simulations of extragalactic jets*, A&A **436**, 503 (2005)
252. C.D. Levermore, G.C. Pomraning: *A flux-limited diffusion theory*, ApJ **248**, 321 (1981)
253. L.-X. Li, E.R. Zimmerman, R. Narayan, J.E. McClintock: *Multi-temperature blackbody spectrum of a thin accretion disk around a Kerr black hole: Model computations and comparison with observations*, ApJS **157**, 335 (2005)
254. E.P.T. Liang, R.H. Price: *Accretion disk coronae and Cygnus X-1*, ApJ **218**, 247 (1977)
255. J. Liebert, P. Bergeron, J.B. Holberg: *The formation rate, mass and luminosity functions of DA white dwarfs from the Palomar Green Survey*, ApJSup **156**, 47 (2005)
256. S. Liu, V. Petrosian, F. Melia: *Electron acceleration around the supermassive black hole at the Galactic Center*, ApJ **611**, L101 (2004)
257. F.S.N. Lobo: *Stable dark energy stars*, Class. Quant. Grav. **23**, 1525 (2006); gr-qc/0508115
258. O. Löhmer, W. Lewandowski, A. Wolszczan, R. Wielebinski: *Shapiro delay in the PSR J1640+2224 binary system*, ApJ **621**, 388 (2005); arXiv:astro-ph/0411742
259. C.P. Lorenz, D.G. Ravenhall, C.J. Pethick: *Neutron star crusts*, Phys. Rev. Lett. **70**, 379 (1993)
260. J.-P. Luminet: *Black holes: A general introduction*, in *Black Holes: Theory and Observation*, eds. F. Hehl, C. Kiefer, R. Metzler, Lecture Notes in Physics, p. 3 (Springer-Verlag, Berlin 1998)
261. A. Lyne, M. Burgay, M. Kramer et al.: *A double-pulsar system: A rare laboratory for relativistic gravity and plasma physics*, Science **303**, 1153 (2004); arXiv:astro-ph/0401086
262. D.A. MacDonald: *Numerical models of force-free black-hole magnetospheres*, MNRAS **211**, 313 (1984)
263. D.A. MacDonald, K.S. Thorne: *Black-hole electrodynamics – An absolute-space/universal-time formulation*, MNRAS **198**, 354 (1982)
264. P. MacNeice, K.M. Olson, C. Mobarry, R. deFainchtein, C. Packer: *PARAMESH: A parallel adaptive mesh refinement community toolkit*, Computer Physics Comm. **126**, 330 (2000)

265. J. Madej et al.: *Mass distribution of DA white dwarfs in the first data release of the SDSS*, A&A **419**, L5 (2004)
266. R.N. Manchester, G.B. Hobbs, A. Teoh, M. Hobbs: *The ATNF Pulsar Catalogue*, AJ **129**, 1993 (2005)
267. V.S. Manko, E.W. Mielke, W. Eckehard, J.D. Sanabria-Gómez: *Exact solution for the exterior field of a rotating neutron star*, Phys. Rev. D **61**, 081501 (2000)
268. V.S. Manko, J.D. Sanabria-Gómez, O.V. Manko: *Nine-parameter electrovac metric involving rational functions*, Phys. Rev. D **62**, 044048 (2000)
269. A. Marscher, S.G. Jorstad, J.L. Gomez et al.: *Observational evidence for the accretion-disk origin of a radio jet in an active galaxy*, Nature **617**, 625 (2002)
270. H.L. Marshall et al.: *A Chandra survey of quasar jets: First results*, ApJSupp **156**, 13 (2005)
271. J.M. Marti, E. Müller: *Numerical hydrodynamics in special relativity*, Living Reviews in Relativity **lrr-2003-6** (2003)
272. A. Martocchia, V. Karas, G. Matt: *Effects of Kerr space-time on spectral features from X-ray illuminated accretion discs*, MNRAS **312**, 817 (2000)
273. T. Maruyama, T. Tatsumi, D.N. Voskresensky, T. Tanigawa, S. Chiba: *Nuclear pasta structures and the charge screening effect*, Phys. Rev. C **72** 015802 (2005)
274. S. D. Mathur: *Where are the states of a black hole?*, arXiv:hep-th/0401115 (2004)
275. R. Matsumoto: *Three-dimensional global MHD simulations of accretion disks advection viscosity, and fluctuations*, Proc. of the Disk-Instability Workshop, 1998, Kyoto, Japan. Ed. by S. Mineshige and J. C. Wheeler. Frontiers Science Series No. 26 (Universal Academy Press, Inc. 1999), p 303
276. O. Maxwell, G.E. Brown, D.K. Campbell, R.F. Dashen, J.T. Manassah: *Beta decay of pion condensates as a cooling mechanism for neutron stars*, ApJ **216**, 77 (1977)
277. P. O. Mazur, E. Mottola: *Weyl cohomology and the effective action for conformal anomalies*, Phys. Rev. D **64**, 104022 (2001)
278. P. O. Mazur, E. Mottola: *Gravitational condensate stars*, arXiv:gr-qc/0109035 (2001)
279. P. O. Mazur, E. Mottola: *Dark energy and condensate stars: Casimir energy in the large*, arXiv:gr-qc/0405111 (2004)
280. P. O. Mazur, E. Mottola: *Gravitational vacuum condensate stars*, Proc. Nat. Acad. Sci. **111**, 9545 (2004); arXiv:gr-qc/0407075
281. J.C. McKinney: *General relativistic magnetohydrodynamic simulations of jet formation and large-scale propagation from black hole accretion systems*, MNRAS **368**, 1561 (2006); astro-ph/0603045
282. T.S. Metcalfe, M.H. Montgomery, A. Kanaan: *Testing white dwarf crystaliization theory with astroseismology of the massive pulsating DA Star BPM 37093*, ApJ **605**, L133 (2004); arXiv:astro-ph/0402046
283. J.E. McClintock, R.A. Remillard: *Black hole binaries*, in *Compact Stellar X-Ray Sources*, eds. W.H.G. Lewin and M. van der Klis (Cambridge Univ. Press, Cambridge 2004); arXiv:astro-ph/0306213
284. I.M. McHardy, I.E. Papadakis, P. Uttley: *Combined long and short time-scale X-ray variability of NGC 4051 with RXTE and XMM–Newton*, MNRAS **348**, 783 (2004)
285. J.C. McKinney: *Total and jet Blandford-Znajek power in presence of accretion disk*, ApJ **630**, L5 (2005); arXiv:astro-ph/0506367
286. J.C. McKinney: *Jet formation in black hole accretion systems I: Theoretical unification model*, arXiv:astro-ph/0506368 (2005)
287. J.C. McKinney: *Jet formation in black hole accretion systems II: Numerical models*, astro-ph/0506369 (2005)

288. J.C. McKinney: *A measurement of the electromagnetic luminosity of a Kerr black hole*, ApJ **611** 977 (2004)
289. F. Melia, R. Coker: *Stellar gas flows into a dark cluster potential at the Galactic Center*, ApJ **511**, 750 (1999)
290. D. Merritt, M. Milosavljevic: *Massive binary black hole evolution*, Living Reviews in Relativity **8**, no. 8; arXiv:astro-ph/0410364 (2004)
291. A. Mignone, G. Bodo: *An HLLC Riemann solver for relativistic flows: I – Hydrodynamics*, MNRAS **364**, 126 (2005)
292. A. Mignone, G. Bodo: *An HLLC Riemann solver for relativistic flows: II – Magnetohydrodynamics*, MNRAS, in press (2006)
293. D. Mihalas, B.W. Mihalas: *Foundations of Radiation Hydrodynamics* (Oxford University Press, Oxford 1984)
294. C. Miller, F.K. Lamb, D. Psaltis: *Sonic-point model of kilohertz quasi-periodic brightness oscillations in low-mass X-ray binaries*, ApJ **508**, 791 (1998)
295. M.C. Miller, E.J.M. Colbert: *Intermediate-mass black holes*, Int. J. Mod. Phys. D **13**, 1 (2004); arXiv:astro-ph/0308402
296. F. Mirabel, L.F. Rodriguez: *A superluminal source in the Galaxy*, Nature **371**, 46 (1994)
297. F. Mirabel, L.F. Rodriguez: *Microquasars in our Galaxy*, Nature **392**, 673 (1998)
298. J. Miralda-Escudè, A. Gould: *A cluster of black holes at the Galactic Center*, ApJ **545**, 847 (2000)
299. R. Moderski, M. Sikora, J.-P. Lasota: *On the spin paradigm and the radio dichotomy of quasars*, MNRAS **301**, 142 (1998)
300. P. Möller, W.D. Myers, W.J. Swiatecki, J. Treiner, J.:*Nuclear mass formula with a finite-range droplet model and a folded-Yukawa single-particle potential*, Atomic Data and Nuclear Data Tables **39**, 225 (1988)
301. S.M. Morsink, L. Stella: *Relativistic precession around rotating neutron stars: Effects due to frame dragging and stellar oblateness*, ApJ **513**, 827 (1999)
302. E. Mottola, P.O. Mazur: *Gravitational condensate stars: An alternative to black holes*, APS, APRI12011M (2002)
303. A. Müller, M. Camenzind: *Relativistic emission lines from accreting black holes. The effect of disk truncation on line profiles*, A&A **413**, 861 (2004)
304. A. Müller: *Black hole astrophysics: Magnetohydrodynamics on the Kerr geometry*, PhD thesis, University of Heidelberg 2004
305. Müller, B.D. Serot: *Relativistic mean-field theory and the high-density nuclear equation of state*, Nucl. Phys. A **606**, 508 (1996)
306. M.P. Muno, E. Pfahl, F.K. Baganoff et al.: *An overabundance of transient X-ray binaries within 1 parsec of the Galactic Center*, ApJ **622**, L113 (2005)
307. R. Narayan, I. Yi: *Advection-dominated accretion: A self-similar solution*, ApJ **428**, L13 (1994)
308. R. Narayan, I. Yi: *Advection-dominated accretion: Underfed black holes and neutron stars*, ApJ **452**, 710 (1995)
309. R. Narayan, R. Mahadevan, J.E. Grindlay, R.G. Popham, C. Gammie: *Advection-dominated accretion model of Sagittarius A*: Evidence for a black hole at the Galactic center*, ApJ **494**, 554 (1998)
310. J.W. Negele, D. Vautherin: *Density-matrix expansion for an effective nuclear Hamiltonian. II*, Phys. Rev. C **11**, 1031 (1975)
311. S.C. Noble, C.F. Gammie, J.C. McKinney, L. Del Zanna: *Primitive variable solvers for conservative general relativistic magnetohydrodynamics*, astro-ph/0512420

312. T. Nozawa, N. Stergioulas, E. Gourgoulhon, Y. Eriguchi: *Construction of highly accurate models of rotating neutron stars – comparison of three different numerical methods*, A&ASuppl **132**, 431 (1998)
313. I. Okamoto, O, Kaburaki: *Thermodynamical and evolutional properties of Kerr black holes*, MNRAS **247**, 244 (1990)
314. I. Okamoto: *The evolution of a black hole's force-free magnetosphere*, MNRAS **254**, 192 (1992)
315. I. Okamoto: *Global asymptotic solutions for magnetohydrodynamic jets and winds*, ApJ **589**, 671 (2003)
316. T. Okuda, V. Teresi, E. Toscano, D. Molteni: *Black hole accretion discs and jets at super-Eddington luminosity*, MNRAS **357**, 295 (2005)
317. J.R. Oppenheimer, G.M. Volkoff: *On massive neutron cores*, Phys. Rev. **55**, 374 (1939)
318. J.R. Oppenheimer, H. Snyder: *On continued gravitational contraction*, Phys. Rev. **56**, 455 (1939)
319. B. Paczynsky, P.J. Wiita: *Thick accretion disks and supercritical luminosities*, A&A **88**, 23 (1980)
320. D.N. Page, K.S. Thorne: *Disk-accretion onto a black hole: I. Time-averaged structure of accretion disk*, ApJ **191**, 499 (1974)
321. D. Page, J.M. Lattimer, M. Prakash, A.W. Steiner: *Minimal cooling of neutron stars: A new paradigm*, ApJSupp **155**, 623 (2004)
322. C. Palenzuela-Luque, C. Bona: *Elements of numerical relativity*, Lecture Notes in Phys. **673** (Springer-Verlag, Berlin 2005)
323. V.R. Pandharipande, D.G. Ravenhall: *Hot nuclear matter*, in Proc. NATO Adv. Research Workshop on nuclear and heavy ion collisions, Les Houches, ed. M. Soyeur et al. (Plenum, New York 1989), p 103
324. J.A. Panei, L.G. Althaus, O.G. Benvenuto: *Mass–radius relations for white dwarf stars of different internal compositions*, A&A **353**, 970 (2000)
325. P. Papadopoulos, J.A. Font: *Relativistic hydrodynamics around black holes and horizon adapted coordinate systems*, Phys. Rev. D **58**, 24005 (1998)
326. P. Papadopoulos, J.A. Font: *Relativistic hydrodynamics on space-like and null surfaces: Formalism and computations of spherically symmetric spacetimes*, Phys. Rev. D **61**, 4015 (1998)
327. J. Peitz, S. Appl: *3+1 Formulation of non-ideal hydrodynamics*, MNRAS **296**, 231 (1998)
328. B.M. Peterson, L. Ferrarese, K.M. Gilbert et al.: *Central masses and broad-line region sizes of active galactic nuclei. II. A homogeneous analysis of a large reverberation-mapping database* ApJ **613**, 682 (2004)
329. Tsvi Piran: *The physics of gamma-ray bursts*, Rev. Mod. Phys. **76**, 1143 (2004)
330. J.A. Pons, J.M. Marti, E. Müller: *The exact solution of the Riemann problem with non-zero tangential velocities in relativistic hydrodynamics*, J. Fluid Mech. **422**, 125 (2000)
331. K. Powell, P.L. Roe, T.J. Linde et al.: *A solution-adaptive upwind scheme for ideal magnetohydrodynamics*, J. Comp. Phys. **154**, 284 (1999)
332. K.H. Prendergast, G.R. Burbidge: *On the nature of some Galactic X-ray sources*, ApJ **151**, L83 (1968)
333. J.L. Provencal, H.L. Shipman, E. Hog, P. Thejll: *Testing the white dwarf mass–radius relation with Hipparcos*, ApJ **494**, 759 (1998)
334. J.L. Provencal, H.L. Shipman, D. Koester, F. Wesemael, P. Bergeron: *Procyon B: Outside the iron box*, ApJ **568**, 324 (2002)

335. B. Punsly, F.V. Coroniti, V. Ferdinand: *Relativistic winds from pulsar and black hole magnetospheres*, ApJ **350**, 518 (1990)
336. B. Punsly, F.V. Coroniti: *Ergosphere-driven winds*, ApJ **354**, 583 (1990)
337. B. Punsly: *Black Hole Gravitohydromagnetics* (Springer-Verlag, Berlin 2001)
338. D.G. Ravenhall, C.J. Pethick: *Matter at large neutron excess and the physics of neutron star crusts*, Ann. Rev. Nucl. Part. Sci. **45**, 429 (1995)
339. S. Reddy: *Novel phases at high density and their roles in the structure and evolution of neutron stars*, Acta Phys. Polon. **B33**, 4101 (2002); arXiv:nucl-th/0211045
340. R.A. Remillard: *X-ray states of black hole binaries in outburst*, in *Interacting Binaries: Accretion, Evolution and Outcomes*, eds. L.A. Antonelli et al.; arXiv:astro-ph/0504126 (2005)
341. C.S. Reynolds, M.A. Nowak: *Fluorescent iron lines as a probe of astrophysical black hole systems*, Phys. Rep. **377**, 389 (2003)
342. H. Riffert, H. Herold: *Relativistic accretion disk structure revisited*, ApJ **450**, 508 (1995)
343. D.H. Rischke: *The quark–gluon plasma in equilibrium*, Progr. Particle Nucl. Phys. **52**, 197 (2004)
344. H. Ritter, U. Kolb: *Catalogue of cataclysmic binaries, low-mass X-ray binaries and related objects*, A&AS **129**, 83 (1998)
345. D.C. Robinson: *Uniqueness of the Kerr black hole*, Phys. Rev. Lett. **34**, 901 (1975)
346. P.L. Roe: *Approximate Riemann solvers, parameter vectors and difference schemes*, J. Comput. Phys. **43**, 357 (1981)
347. P.W.A. Roming, D. Vanden Berk, V. Palshin et al.: *GRB 060313: A new paradigm for short-hard bursts?*, astro-ph/0605005 (2006)
348. S.B. Ruster, V. Werth, M. Buballa, I.A. Shovkovy, D.H. Rischke: *The phase diagram of neutral quark matter: Self-consistent treatment of quark masses*, Phys. Rev. D **72**, 034004 (2005); arXiv:hep-ph/0503184
349. S.B. Ruster, V. Werth, M. Buballa, I.A. Shovkovy, D.H. Rischke: *The phase diagram of neutral quark matter: The effect of neutrino trapping*, Phys. Rev. D **73**, 034025 (2006); arXiv:hep-ph/0509073
350. S.B. Ruster, V. Werth, M. Buballa, I.A. Shovkovy, D.H. Rischke: *Phase diagram of neutral quark matter at moderate densities*, arXiv:nucl-th/0602018
351. D. Ryu, T.W. Jones, A. Frank: *Numerical magnetohydrodynamics in astrophysics: Algorithm and tests for multidimensional flow*, ApJ **452**, 785 (1995)
352. M. Salgado, S. Bonazzola, E. Gourgoulhon, P. Haensel: *High precision rotating netron star models. I. Analysis of neutron star properties*, A&A **291**, 155 (1994)
353. M. Salgado, S. Bonazzola, E. Gourgoulhon, P. Haensel: *High precision rotating neutron star models. II. Large sample of neutron star properties*, A&ASup **108**, 455 (1994)
354. E.E. Salpeter: *Energy and pressure of a zero-temperature plasma*, ApJ **134**, 669 (1961)
355. K. Schertler, P.K. Sahu, C. Greiner, M.H. Thoma: *The influence of medium effects on the gross structure of hybrid stars*, Nucl. Phys. A **637**, 451 (1998)
356. K. Schertler, C. Greiner, J. Schaffner-Bielich, M.H. Thoma: *Quark phases in neutron stars and a third family of compact stars as a signature of phase transitions*, Nucl. Phys. A **677**, 463 (2000)
357. J.D. Schnittman, J.H Krolik, J.F. Hawley: *Light curves from an MHD simulation of a black hole accretion disk*, astro-ph/0606615
358. K. Schöbel, M. Ansorg: *Maximal mass of uniformly rotating homogeneous stars in Einsteinian gravity*, A&A **405**, 405 (2003); arXiv:astro-ph/0301618
359. R. Schödel, T. Ott, R. Genzel, A. Eckart, N. Mouawad, T. Alexander: *Stellar dynamics in the central arcsecond of our Galaxy*, ApJ **596**, 1015 (2003)

360. K. Schwarzschild: Berliner Sitzungsberichte (Phys. Math. Klasse), 189–196, 3. Febr. (Mitt. 13. Jan. 1916) [Einstein himself wrote about this work: *Ihre Arbeit habe ich mit größtem Interesse durchgelesen. Ich hätte nicht erwartet, daß man so einfach die strenge Lösung der Aufgabe formulieren konnte. Die rechnerische Behandlung gefällt mir ausgezeichnet.* Shortly after this publication, Schwarzschild died on May 11, 1916.]
361. L. Segretain, G. Chabrier et al.: *Cooling theory of crystallized white dwarfs*, ApJ **434**, 641 (1994)
362. B.D. Serot, J.D. Walecka: *Properties of finite nuclei in a relativistic quantum field theory*, Phys. Lett. B **87**, 172 (1979)
363. N.J. Shakura, R. Sunyaev: *Black holes in binary systems. Observational appearance*, A&A **24**, 337 (1973)
364. I.I. Shapiro: *Fourth test of general relativity*, Phys. Rev. Letters **13**, 789 (1964)
365. N.J. Shaviv: *The nature of the radiative hydrodynamic instabilities in radiatively supported Thomson atmospheres*, ApJ **549**, 1093 (2001)
366. M. Shibata, T.W. Baumgarte, S.L. Shapiro: *The bar-mode instability in differentially rotating neutron stars: Simulations in full general relativity*, ApJ **542**, 453 (2000)
367. M. Shibata, Yu-ichirou Sekiguchi: *Gravitational waves from axisymmetric rotating stellar core collapse to a neutron star in full general relativity*, Phys. Rev. D **69**, 084024 (2004)
368. I.A. Shovkova: *Two lectures on color superconductivity*, arXiv:nucl-th/0410091 (2004)
369. C.-W. Shu, S. Osher: *Efficient implementation of essentially non-oscillatory shock-capturing schemes*, J. Comp. Phys. **77**, 439 (1988)
370. N.R. Sibgatullin, N.M. Queen: *Oscillations and Waves in Strong Gravitational and Electromagnetic Fields* (Springer-Verlag, Berlin 1991)
371. N.R. Sibgatullin, R.A. Sunyaev: *Disk accretion in gravitational field of a rapidly rotating neutron star with a rotationally induced quadrupole mass moment*, Astron. Letters, **24**, 774 (1998)
372. S. Spindeldreher: *The discontinuous Galerkin method applied to the equations of ideal relativistic hydrodynamics*, PhD thesis, Univeristy of Heidelberg 2002
373. I.H. Stairs, S.E. Thorsett, J.H. Taylor, A. Wolszczan: *Studies of the relativistic binary pulsar PSR B1534+12: I. Timing analysis*, ApJ **616**, 414 (2004)
374. L. Stella, M. Vietri: *kHz quasiperiodic oscillations in low-mass X-Ray binaries as probes of general relativity in the strong-field regime*, Phys. Rev. Lett. **82**, 17 (1999)
375. N. Stergioulas: *The structure and stability of rotating relativistic stars*, PhD thesis, University of Wisconsin-Milwaukee, Milwaukee, USA, 1996
376. N. Stergioulas: *Rotating stars in relativity*, Living Reviews in Relativity **lrr-2003-3** (2003)
377. N. Stergioulas, J.L. Friedman: *Comparing models of rapidly rotating relativistic stars constructed by two numerical methods*, ApJ **444** 306 (1995)
378. J. Stone, D. Mihalas, M.L. Norman: *ZEUS-2D: A radiation magnetohydrodynamics code for astrophysical flows in two space dimensions. III – The radiation hydrodynamic algorithms and tests*, ApJSupp **80**, 819 (1992)
379. T.E. Strohmayer, C.B. Markwardt: *On the frequency evolution of X-ray brightness oscillations during thermonuclear X-ray bursts: Evidence of coherent oscillations*, ApJ **516**, L81 (1999)
380. T.E. Strohmayer, L. Bildsten: *New views of thermonuclear bursts*, arXiv:astro-ph/0301544
381. T.E. Strohmayer: *Future probes of the neutron star equation of state using X-ray bursts*, In: X-ray Timing 2003: Rossi and Beyond. AIP Conf. Proc. **714**, Ed. P. Kaaret, F.K. Lamb, J.H. Swank, Am. Inst. Phys. (2004), p. 245; arXiv:astro-ph/0401465

382. M. Stute, M. Camenzind: *Towards a self-consistent relativistic model of the exterior gravitational field of rapidly rotating neutron stars*, MNRAS **336**, 831 (2002)
383. K. Sumiyoshi, J.Ma. Ibanez, J.V. Romero: *Thermal history and structure of rotating protoneutron stars with relativistic equation of state*, A&ASupp **134**, 39 (1999)
384. L. Susskind: *The world as a hologram*, arXiv:hep-th/9409089 (1994)
385. M. Takahashi: *Transmagnetosonic accretion in a black hole magnetosphere*, ApJ **570**, 264 (2002)
386. Y. Tanaka, K. Nandra, A.C. Fabian et al.: *Gravitationally redshifted emission implying an accretion disk and massive black-hole in the active galaxy MCG:–6–30–15*, Nature **375**, 659 (1995)
387. K. Taniguchi, T.W. Baumgarte, J.A. Faber, S.L. Shapiro: *Black hole-neutron star binaries in general relativity: Effects of neutron star spin*, Phys. Rev. D **72**, 4008 (2005); arXiv:astro-ph/0505450
388. M. Tassoul, G. Fontaine, D.E. Winget: *Evolutionary models for pulsation studies of white dwarfs*, ApJSupp **72**, 335 (1990)
389. J. Taylor, J.M. Weisberg: *Further experimental tests of relativistic gravity using the binary pulsar PSR 1913+16*, ApJ **345**, 434 (1989)
390. A. Timokhin: *High resolution numerical modeling of the force-free pulsar magnetosphere*, AIP Conf. Proc. **801**, 332 (2005); arXiv:astro-ph/0507054 (2005)
391. G. 't Hooft: *The giant leap to the Planck length*, In: Perspectives on High Energy Physics and Cosmology, Eds. A. Gonzalez-Arroyo and C. Lopez (World Scientific, Singapore 1993), pp. 1-9
392. K.S. Thorne, R.H. Price, a. MacDonald: *Black holes: The membrane paradigm* (Yale University Press, Yale 1986)
393. S.E. Thorsett, D. Chakrabarty: *Neutron star masses measurements. I. Radio pulsars*, ApJ **512**, 288 (1999)
394. R.C. Tolman: *Static solution of Einstein's equations for spheres of fluids*, Phys. Rev. **55**, 364 (1939)
395. A. Tomimatsu: *Relativistic dynamos in magnetospheres of rotating compact objects*, ApJ **528**, 972 (2000)
396. E.F. Toro: *Riemann solvers and numerical methods for fluid dynamics*, 2nd Edn (Springer-Verlag, Berlin 1999).
397. S. Torres, E. Garcia-Berro, J. Isern, F. Figueras: *Simulating Gaia performances on white dwarfs*, MNRAS **360**, 1381 (2005)
398. Toth: *The* $\nabla \cdot \mathbf{B} = 0$ *Constraint in shock-capturing magnetohydrodynamics codes*, J. Comp. Phys. **161**, 605 (2000)
399. S. Tremaine, K. Gebhardt, R. Bender et al.: *The Slope of the black hole mass versus velocity dispersion correlation*, ApJ **574**, 740 (2002)
400. J. Trümper, V. Burwitz, F. Haberl, E. Zavlin: *The puzzles of RX J1856.5–3754: Neutron star or quark star?*, Nucl. Phys. B Proc. Suppl. **132**, 560 (2004)
401. N.J. Turner, J.M. Stone: *A module for radiation hydrodynamic calculations with ZEUS-2D using flux-limited diffusion*, ApJSupp **135**, 95 (2001)
402. N.J. Turner, J.M. Stone, J.H. Krolik, T. Sano: *Local three-dimensional simulations of magnetorotational instability in radiation-dominated accretion disks*, ApJ **593**, 992 (2003)
403. N.J. Turner, O.M. Blaes, A. Socrates et al.: *The effects of photon bubble instability in radiation-dominated accretion disks*, ApJ **624**, 267 (2005); arXiv:astro-ph/0501198
404. Y. Uchiyama, C.M. Urry, C.C. Cheung et al.: *Shedding new light on the 3C 273 jet with the Spitzer Space Telescope*, astro-ph/0605530

405. M.H.P.M. van Putten: J. Comp. Phys. **99**, 341 (1993)
406. M.H.P.M. van Putten, A. Levinson: *Theory and astrophysical consequences of a magnetized torus around a rapidly rotating black hole*, ApJ **584**, 937 (2003)
407. E.P. Velikov: Sov. Phys. JETP **36**, 995 (1959)
408. R.V. Wagoner: *Test for the existence of gravitational radiation*, ApJ **196**, 63 (1975)
409. R.M. Wald: *Black hole in a uniform magnetic field*, Phys. Rev. D **10**, 1680 (1974)
410. J.D. Walecka: *A theory of highly condensed matter*, Ann. Phys. **83**, 491 (1974)
411. M. Walker, R. Penrose: *On quadratic first integrals of the geodesic equations for type* {22} *spacetimes*, Comm. Math. Phys. **18**, 265 (1970)
412. D.-X. Wang, W.-H. Lei, Kan Xiao, Ren-Yi Ma: *An analytical model of black hole evolution and gamma ray bursts*, ApJ **580**, 358 (2002); arXiv:astro-ph/0209579
413. G. Watanabe, K. Sato, K. Yasuoka, T. Ebisuzaki: *Phases of hot nuclear matter at subnuclear densities*, Phys. Rev. C **69**, 055805 (2004)
414. G. Watanabe, T. Maruyama, K. Sato, K. Yasuoka, T. Ebisuzaki: *Simulation of transitions between "pasta" phases in dense matter*, Phys. Rev. Lett. **94**, 031101 (2005)
415. J.M. Weisberg, J. Taylor: *Relativistic binary pulsar B1913+16: Thirty years of observations and analysis*, arXiv:astro-ph/0407149 (2004)
416. M. Visser, D.L. Wiltshire: *Stable gravastars – An alternative to black holes?*, Class. Quant. Grav. **21** 1135 (2004); arXiv:gr-qc/0310107
417. F. Weber: *Strange quark matter and compact stars*, arXiv:astro-ph/0407155 (2004)
418. D.T. Wickramasinghe, L. Ferrario: *Magnetism in isolated white dwarf stars*, PASP **112**, 873 (2000)
419. C. Will: *The confrontation between general relativity and experiment*, Living Reviews in Relativity **lrr-2001-4** (2001)
420. J.R. Wilson: *Models of differentially rotating stars*, ApJ **176**, 195 (1972)
421. D.E. Winget, C.J. Hansen, J. Liebert et al.: *An independent method for determining the age of the Universe*, ApJ **315**, 77 (1987)
422. M.A. Wood: *Astero-archaeology: Reading the Galactic history recorded in the white dwarf stars*, PhD thesis, University of Texas at Austin 1990
423. P.R. Woodward, P. Collella: *The Piecewise Parabolic Method (PPM) for gas-dynamical simulations*, J. Comp. Phys. **54**, 115 (1984)
424. D.G. Yakovlev, C.J. Pethick: *Neutron star cooling*, ARA&A **42**, 169 (2004)
425. D.G. Yakovlev, O.Y. Gnedin, M.E. Gusakov et al.: *Neutron star cooling*, Nucl. Phys. A **752**, 590 (2005)
426. M. Yokosawa: *Energy and angular momentum transport in magnetohydrodynamical accretion onto a rotating black hole*, PASJ **45**, 207 (1993)
427. M. Yokosawa: *Structure and dynamics of an accretion disk around a black hole*, PASJ **47**, 605 (1995)
428. M. Yokosawa, T. Inui: *Magnetorotational instability around a rotating black hole*, ApJ **631**, 1051 (2005); arXiv:astro-ph/0503712
429. J. York: *Kinematics and dynamics of general relativity*, in *Sources of Gravitational Radiation*, ed. L.L. Smarr (Cambridge University Press, Cambridge 1979)
430. Feng Yuan, Wei Cui, R. Narayan: *An accretion-jet model for black hole binaries: Interpreting the spectral and timing features of XTE J1118+480*, ApJ **620**, 905 (2005)
431. U. Ziegler: *NIRVANA+: An adaptive mesh refinement code for gas dynamics and MHD*, Comp. Phys. Comm. **109**, 142 (1998)
432. U. Ziegler: *A three-dimensional Cartesian adaptive mesh code for compressible magnetohydrodynamics*, Comp. Phys. Comm. **116**, 65 (1999)

Index

LIBRARY

ASTRONOMY AND ASTROPHYSICS LIBRARY

The Stars By E. L. Schatzman and F. Praderie

Modern Astrometry 2nd Edition
By J. Kovalevsky

The Physics and Dynamics of Planetary Nebulae By G. A. Gurzadyan

Galaxies and Cosmology By F. Combes, P. Boissé, A. Mazure and A. Blanchard

Observational Astrophysics 2nd Edition
By P. Léna, F. Lebrun and F. Mignard

Physics of Planetary Rings Celestial Mechanics of Continuous Media
By A. M. Fridman and N. N. Gorkavyi

Tools of Radio Astronomy 4th Edition, Corr. 2nd printing
By K. Rohlfs and T. L. Wilson

Tools of Radio Astronomy Problems and Solutions 1st Edition, Corr. 2nd printing
By T. L. Wilson and S. Hüttemeister

Astrophysical Formulae 3rd Edition (2 volumes)
Volume I: Radiation, Gas Processes and High Energy Astrophysics
Volume II: Space, Time, Matter and Cosmology
By K. R. Lang

Galaxy Formation By M. S. Longair

Astrophysical Concepts 4th Edition
By M. Harwit

Astrometry of Fundamental Catalogues The Evolution from Optical to Radio Reference Frames
By H. G. Walter and O. J. Sovers

Compact Stars. Nuclear Physics, Particle Physics and General Relativity 2nd Edition
By N. K. Glendenning

The Sun from Space By K. R. Lang

Stellar Physics (2 volumes)
Volume 1: Fundamental Concepts and Stellar Equilibrium
By G. S. Bisnovatyi-Kogan

Stellar Physics (2 volumes)
Volume 2: Stellar Evolution and Stability
By G. S. Bisnovatyi-Kogan

Theory of Orbits (2 volumes)
Volume 1: Integrable Systems and Non-perturbative Methods
Volume 2: Perturbative and Geometrical Methods
By D. Boccaletti and G. Pucacco

Black Hole Gravitohydromagnetics
By B. Punsly

Stellar Structure and Evolution
By R. Kippenhahn and A. Weigert

Gravitational Lenses By P. Schneider, J. Ehlers and E. E. Falco

Reflecting Telescope Optics (2 volumes)
Volume I: Basic Design Theory and its Historical Development. 2nd Edition
Volume II: Manufacture, Testing, Alignment, Modern Techniques
By R. N. Wilson

Interplanetary Dust
By E. Grün, B. Å. S. Gustafson, S. Dermott and H. Fechtig (Eds.)

The Universe in Gamma Rays
By V. Schönfelder

Astrophysics. A New Approach 2nd Edition
By W. Kundt

Cosmic Ray Astrophysics
By R. Schlickeiser

Astrophysics of the Diffuse Universe
By M. A. Dopita and R. S. Sutherland

The Sun An Introduction. 2nd Edition
By M. Stix

Order and Chaos in Dynamical Astronomy
By G. J. Contopoulos

Astronomical Image and Data Analysis 2nd Edition By J.-L. Starck and F. Murtagh

The Early Universe Facts and Fiction 4th Edition By G. Börner

LIBRARY

ASTRONOMY AND ASTROPHYSICS LIBRARY

The Design and Construction of Large Optical Telescopes By P. Y. Bely

The Solar System 4th Edition
By T. Encrenaz, J.-P. Bibring, M. Blanc, M. A. Barucci, F. Roques, Ph. Zarka

General Relativity, Astrophysics, and Cosmology By A. K. Raychaudhuri, S. Banerji, and A. Banerjee

Stellar Interiors Physical Principles, Structure, and Evolution 2nd Edition
By C. J. Hansen, S. D. Kawaler, and V. Trimble

Asymptotic Giant Branch Stars
By H. J. Habing and H. Olofsson

The Interstellar Medium
By J. Lequeux

Methods of Celestial Mechanics (2 volumes)
Volume I: Physical, Mathematical, and Numerical Principles
Volume II: Application to Planetary System, Geodynamics and Satellite Geodesy
By G. Beutler

Solar-Type Activity in Main-Sequence Stars
By R. E. Gershberg

Relativistic Astrophysics and Cosmology
A Primer By P. Hoyng

Magneto-Fluid Dynamics
Fundamentals and Case Studies
By P. Lorrain

Compact Objects in Astrophysics
White Dwarfs, Neutron Stars and Black Holes
By Max Camenzind

Special and General Relativity
With Applications to White Dwarfs, Neutron Stars and Black Holes
By Norman K. Glendenning